CUES FROM THE EXTRACELLULAR SPACE: MATRIX PROTEINS REGULATE MELANOMA INVASION

by

Jelena Grahovac

MS, University of Belgrade, 2007.

Submitted to the Graduate Faculty of

School of Medicine in partial fulfillment

of the requirements for the degree of

Doctor of Philosophy

University of Pittsburgh

2012.

UNIVERSITY OF PITTSBURGH

SCHOOL OF MEDICINE

This dissertation was presented

by

Jelena Grahovac

It was defended on

November 27th 2012.

and approved by

Dorothea Becker, PhD, Professor, Department of Pathology

Jeffrey Hildebrand, PhD, Associate Professor, Department of Biological Sciences

Thomas Smithgall, PhD, Professor, Department of Microbiology and Molecular Genetics

Committee chair: William Saunders, PhD, Associate Professor, Department of Biological Sciences

Dissertation Advisor: Alan Wells, MD DMSc, Professor, Department of Pathology

Cues from the extracellular space: matrix proteins regulate melanoma invasion

Jelena Grahovac, MS

University of Pittsburgh, 2012.

Melanoma is the most aggressive type of skin cancer with increasing incidence rates. To date, there are no effective therapies that can ensure disease free or even progression free survival of melanoma patients. While early stage primary melanoma is curable by surgical resection, survival of patients with metastatic melanoma is measured in months. Therefore it is of utmost importance to decipher molecular events that precede and/or induce the switch towards the invasive melanoma phenotype. In pursue of efficient therapy, attention has to be given not only to the cancer cells themselves but also to the microenvironment that nurtures and promotes malignant behavior. Aggressive melanoma cells drastically remodel their microenvironment. We found that expression of two extracellular matrix (ECM) proteins was significantly altered in melanoma compared to uninvolved patient skin: Tenascin C (TNC) was markedly increased, while small proteoglycan Decorin (DCN) was decreased. We found that invasion of the melanoma cells correlates with TNC expression levels and that cells present TNC asymmetrically at the invasive fronts. We also found that Epidermal Growth Factor-Like (EGFL) repeats of TNC promote melanoma cell invasiveness by activating Rho-associated kinase and increasing cell contractility, thus allowing mesenchymal to amoeboidal switch in mode of migration. Interestingly, TNC and DCN have both been shown to affect signaling through Epidermal Growth Factor receptor (EGFR), but with opposite outcomes on cell proliferation, migration and survival. We adapted skin organ cultures to test the influence of these two proteins

on melanoma invasion and found that DCN can ameliorate TNC induced melanoma invasion. Taken together, our findings imply that ECM composition has a significant role in the regulation of melanoma invasiveness and that even in the presence of increased pro-invasive TNC signaling DCN can be a promising moiety for melanoma therapy.

TABLE OF CONTENTS

LIST OF TABLES

LIST OF FIGURES

PREFACE

This work would not have been possible without the generous help of many people. First, I would like to thank my mentor, Dr Alan Wells for his support and encouragement during my PhD studies. Providing me with the great amount of freedom and just the right amount of guidance helped me grow as a scientist. I would also like to thank my thesis committee members, in particular Dr Dorothea Becker for her insightful expert advice and Dr William Saunders for his thoughtful career advice.

I would like to express gratitude to our collaborators Drs Conrads and Hood, who made important contributions to the work presented in this thesis.

I would also like to thank past and present members of the Wells lab – especially Drs Ludovic Leloup, Qian Wu and Arthur Huen for their friendship and mentoring, Sharanya Kumar and Melanie Rodrigues for all the fun moments in the lab and Diana Whaley for being a lab fairy godmother making sure that everything runs smoothly. I would also like to acknowledge PIMB colleagues and friends - in particular Anna and Reety two great scientists and even better friends.

Finally, I would like to thank my family: mama, tata, Jovana and Milos for the infinite encouragement, love and support.

1.0 INTRODUCTION

More than half a million deaths from cancer are projected to occur in 2012 in United States (Siegel et al., 2012). Metastasis is responsible for 90% of cancer deaths and is the main factor for cancer treatment failure (Hanahan and Weinberg, 2000). Metastasis is a complex, multistage process in which cancer cells exit the primary tumor, survive in the circulation, seed the distant sites and grow. The non-malignant stromal cells and the extracellular matrix in the microenvironment influence each of these stages. Elucidating the means by which the microenvironment facilitates cancer progression may thus contribute to the development of new therapeutics, since targeting both tumor cells and stroma may give greater therapeutic success.

Malignant melanoma is an excellent model for studying molecular changes associated with invasive and metastatic disease, in part due to its sequential step-by-step progression in which molecular changes can be attributed to each step of progression. Easy access to melanocytic lesions and melanoma on the body surface allows the establishment of hundreds of cell lines from different stages of the progression for the purposes of experimental studies, to an extent greater than in the case of any other cancer type (Berking and Herlyn, 2001) .

1.1 MELANOMA

Melanoma is the most aggressive type of skin cancer and its incidence is constantly increasing (Perlis and Herlyn, 2004). It is predicted that in 2012 in the United States, melanoma will be diagnosed in 76250 patients with over 9000 deaths (www.cancer.gov). Melanoma is a significant public health problem and is a great scientific and medical challenge due to its heterogeneity and notorious chemotherapy resistance.

1.1.1 Melanoma progression

Melanoma cells arise from transformed melanocytes, pigmented cells of neuroectodermal origin, that normally reside in the basal layer of the epidermis. In healthy skin the ratio of melanocytes to keratinocytes is approximately 1:5, and melanocyte homeostasis is regulated by keratinocytes by cell-cell contacts mediated by cadherins, through gap junctions and through the secretion of signaling molecules and growth factors (reviewed in (Santiago-Walker et al., 2009). Additionally, melanocytes are kept in place by integrin interaction with the basement membrane. The initial abnormal proliferation of melanocytes that is confined to the epidermis can show varying levels of dysplasia, but if left untreated all melanoma cells have the potential to invade and metastasize. In melanoma, melanocytes undergo E- to N- cadherin switch allowing them to escape keratinocyte control and establish contacts with fibroblasts and endothelial cells in the dermis (Haass et al., 2004) and alter integrin expression which allows their release from the basement membrane (reviewed in (Haass et al., 2005)). The majority of melanomas go through a linear progression: from benign nevi to dysplasia to the radial growth phase (RGP) melanoma that spreads laterally in the epidermis, and further to the vertical growth phase (VGP) melanoma,

which invades into the dermis and has the ability to metastasize, reaching the final step-metastatic melanoma (Figure 1) (Clark et al., 1984).

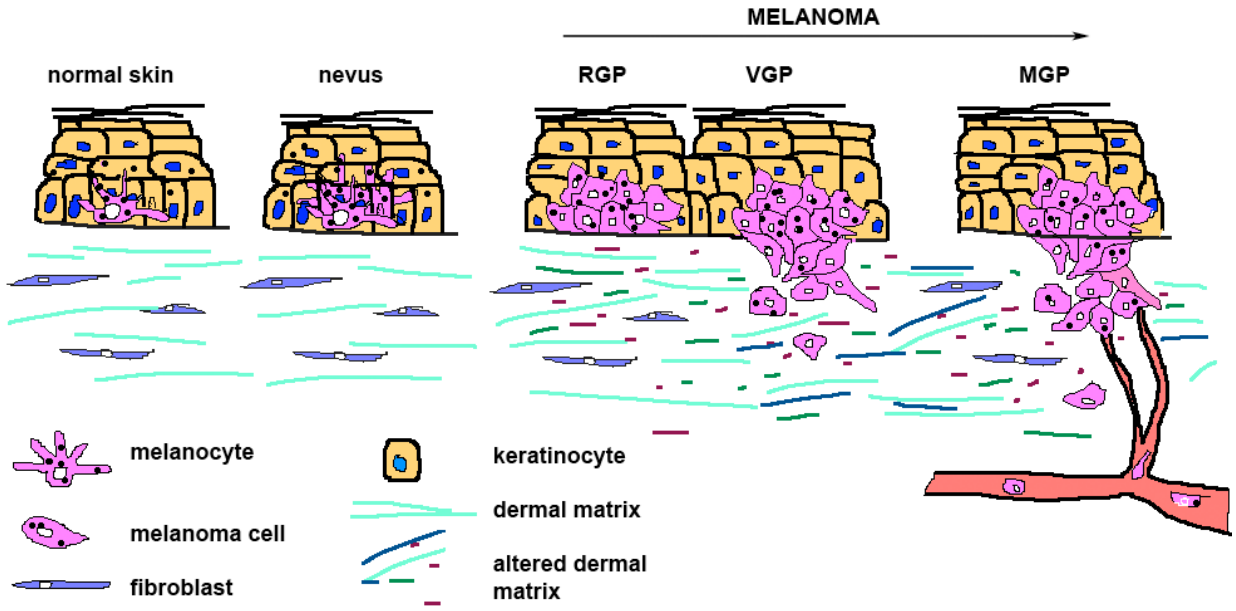

Figure 1. Stages of the melanoma progression.

The adequate surgical resection of RGP melanoma has a high cure rate, but VGP primary melanomas have multiple genetic abnormalities and are able to grow independently of exogenous growth factors, to invade and metastasize. Patients with VGP and MGP melanoma have very poor survival rates. Therefore, it is of crucial importance to elucidate the events that lead to the progression from RGP to VGP melanoma.

To date, there are no good predictive markers for either melanoma progression or the clinical outcome. Melanoma tumors have a very heterogeneous composition, consisting of cells with varying malignant potential, display various antigens and are able to secrete a variety of cytokines and growth factors (Elias et al., 2010a). In addition, melanomas metastasize to

multiple organs and their biological behavior is different from one site to another. Its variability and unpredictability have greatly limited treatment of melanoma, with surgery as the only effective modality of treatment in all types (Elias et al., 2010b).

1.1.2 Current therapy for melanoma

In general, melanoma does not show significant response to chemotherapy. In addition to taxanes and platinum agents the-FDA approved drugs for advanced melanoma are: Dacarbazine – an alkylating and DNA cross-linking agent, Yervoy (Ipilimubab) - a monoclonal antibody targeting T-lymphocyte antigen CTLA-4, Zelboraf (Vemurafenib) - a BRAF inhibitor that blocks V600E mutated BRAF protein and Adesleukin – recombinant analog of interleukin 2 (www.cancer.gov). Two most recently developed drugs, approved in 2011: Yervoy, which helps turn back on the anticancer immune response and Zelboraf, which can be used only in patients carrying the most common mutation in melanoma - V600E BRAF, have unusually severe side effects (including fatal autoimmune reaction and squamous cell carcinoma, respectively) but prolong survival.

Currently, there are no available therapies capable of ensuring a disease-free, or even a progression-free survival of melanoma patients. Targeting a single pathway will not be sufficient to eradicate melanoma. The interaction of melanoma cells with the surrounding stroma strongly influences the transformation and progression processes, and taking into account the complexity of the melanoma microenvironment, should help devise more effective therapeutic regimens. This was recently confirmed by a study in which Dacarbazine treatment was more effective in patients in whom the drug could also induce stromal remodeling in addition to the effects on melanoma tumor cells (Nardin et al., 2011). New treatment strategies have to take into account

the microenvironment, since specific components in the extracellular tumor space provide signals for the invasion and progression of tumor cells and could serve as therapeutic targets.

1.2 TUMOR MICROENVIRONMENT

The cellular microenvironment contributes significantly to normal cellular function as well as to tumor development, growth and spread. The malignant phenotype of tumors is dependent not only on the intrinsic changes in cancer cells but also on the interactions of non-cancer stromal cells, secreted factors and extracellular matrix (ECM) network that together make up the tumor microenvironment. Remodeled tumor microenvironment resembles the changes observed during embryogenesis, including cell plasticity, migration, vasculogenesis and angiogenesis.

Melanoma is composed of melanoma tumor cells and stoma, which includes resident fibroblasts and endothelial cells, infiltrated immune cells, soluble factors and ECM. Aggressive melanoma cells remodel the microenvironment, and in turn, the modified microenvironment has a notable influence on the phenotype both of melanoma cells themselves and of the surrounding stromal cells (Hendrix et al., 2003). Even normal melanocytes can be shifted to invasive behavior by exposure to melanoma-produced ECM (Seftor et al., 2005). In addition, melanoma cells that leave the primary tumor site can induce molecular signals in the microenvironment for other tumor cells to follow, since melanoma cells can express endothelial-associated markers and form tubular structures that mimic vasculogenic networks (Maniotis et al., 1999).

1.2.1 Cells in the tumor stroma

Stromal cells can influence cancer cell behavior by secreting chemokines, cytokines, growth factors, proteases, protease inhibitors and various ECM proteins; and they create a permissive environment for tumorigenesis. The most abundant cell type in solid tumors are fibroblasts (Allen and Louise Jones, 2011) that have a functional role in tumor development since they can promote angiogenesis, proliferation and survival of tumor epithelial cells and can even induce tumorigenesis in non-tumorigenic epithelial cells (Hu and Polyak, 2008a; Olumi et al., 1999). In melanoma, following E- to N-cadherin switch, cancer cells establish communication with fibroblasts through gap junctions (Hsu et al., 2000). Additionally, by producing TGF-β, bFGF and PDGF melanoma cells induce rapid proliferation of fibroblasts, and in turn, fibroblasts produce a series of growth factors that support melanoma growth (Hsu et al., 2002; Li et al., 2003; Li et al., 2009). Melanoma-derived TGF-β activates fibroblasts to produce the matrix with a high expression of collagens, Fibronectin and Tenascin C (Berking et al., 2001), and the invasiveness of melanoma correlates with the ability to stimulate the stromal host fibroblasts (Li et al., 2009). Furthermore, melanoma-associated fibroblasts interfere with natural killer cells' function and thus have an immunosuppressive role (Balsamo et al., 2009).

In addition to the previously postulated six hallmarks of cancer (Hanahan and Weinberg, 2000), inflammation has recently been proposed to be the seventh hallmark (Colotta et al., 2009). Inflammatory cells are recruited to reorganize the tumor stroma and macrophages form a major population in most solid tumors. Macrophage infiltration correlates with the progression of melanoma, and macrophage-derived cytokines induce the production of potent angiogenic factors, such as VEGF and IL-8 by melanoma cells, thus promoting angiogenesis (Torisu et al., 2000). The number of tumor-infiltrating lymphocytes also increases with the melanoma

progression (Hussein et al., 2006). Neutrophils, macrophages and mast cells are the source of matrix metalloproteinase (MMP)-9 in aggressive skin tumors (Coussens et al., 2000) and the production of MMPs by stromal and infiltrating tumor cells greatly contributes to the progression of melanoma by both destruction of the ECM and by modulating the immune response. There is also a possible correlation between the presence of mast cells and the pathogenesis of primary melanoma (Dyduch et al., 2011).

Both cancer-associated fibroblasts (CAFs) and macrophages remodel the existing ECM during the tumor progression by releasing extracellular proteases (Egeblad and Werb, 2002), but CAFs also generate the altered ECM environment by secreting a different profile of ECM proteins compared to their normal counterparts (Allen and Louise Jones, 2011). Cancer subtypes with different clinical outcomes have recently been identified on the basis on the ECM-gene related profiles (Bergamaschi et al., 2008).

1.2.2 Extracellular matrix

In normal physiological conditions extracellular matrix provides the structural support for tissues and organs, for layers of cells in the form of the basement membrane and for individual cells as substrate for migration. It also provides signals for the basic cell functions and serves as a reservoir for biologically active molecules. In vertebrate genomes there are hundreds of genes coding ECM proteins. Some are ancient and present in all Metazoa, like type IV collagens, laminins, Nidogen, Perlecan and collagens XV/XVII which compose the basement membrane, while the novel ones, like tenascins and fibronectins have evolved more recently (reviewed in (Hynes, 2009)). The human matrisome (all the components of the extracellular matrix) accounts for around 4% of the human proteome. In addition to 43 known collagen genes, the human

genome encodes 200 ECM glycoproteins and 35 proteoglycans (Naba et al., 2012). In general, ECM molecules are classified as fiber-forming, such as collagen and elastin, or interfibrillar which are the majority of proteoglycans and glycoproteins (Jarvelainen et al., 2009). ECM proteins are typically large, composed of several protein domains that are specialized for protein interactions and ECM assembly, or for the recruitment of other proteins (such as growth factors) and cells to the ECM (Hynes, 2012). They are often non- and enzymatically linked and are mostly insoluble, which makes their analysis challenging.

After changes in cell-cell adhesion, the remodeling of the ECM plays a critical role in tumor invasion. Both tumor and stromal cells contribute to these changes and tumors of differing metastatic potentials differ in both the tumor- and the stroma-derived components (Naba et al., 2012). In melanoma, production of ECM is drastically altered; there is an increase in the production of collagens, Tenascin C, SPARC and certain laminins and an isoform shift and increase in Fibronectin I expression (Hood et al., 2010; Ilmonen et al., 2004; Ledda et al., 1997; Natali et al., 1995; Pyke et al., 1994). Recent proteomic characterization of the extracellular matrix of human melanoma xenografts in mice has revealed the origin of certain ECM components (Naba et al., 2012): Fibronectin I, Collagen IV and Nidogen in the tumor stroma were secreted by both tumor and stromal compartments equally; Collagen I and III were secreted by both but with greater stromal contribution, which was the case with Tenascin C in more invasive tumors, while in less invasive ones the contribution was equal. Detected Vitronectin, Decorin and Collagen XIV were solely of stromal origin, while the tumor cells secreted certain laminins and latent growth factor binding proteins. Matrix components secreted by the tumor cells varied significantly with their metastatic potential, and the matrisome secreted by stromal compartment changed in response to the potential of tumor cells indicating a profound cross-talk

between tumor and stromal cells. Summary of described melanoma-stromal interactions is depicted in Figure 2.

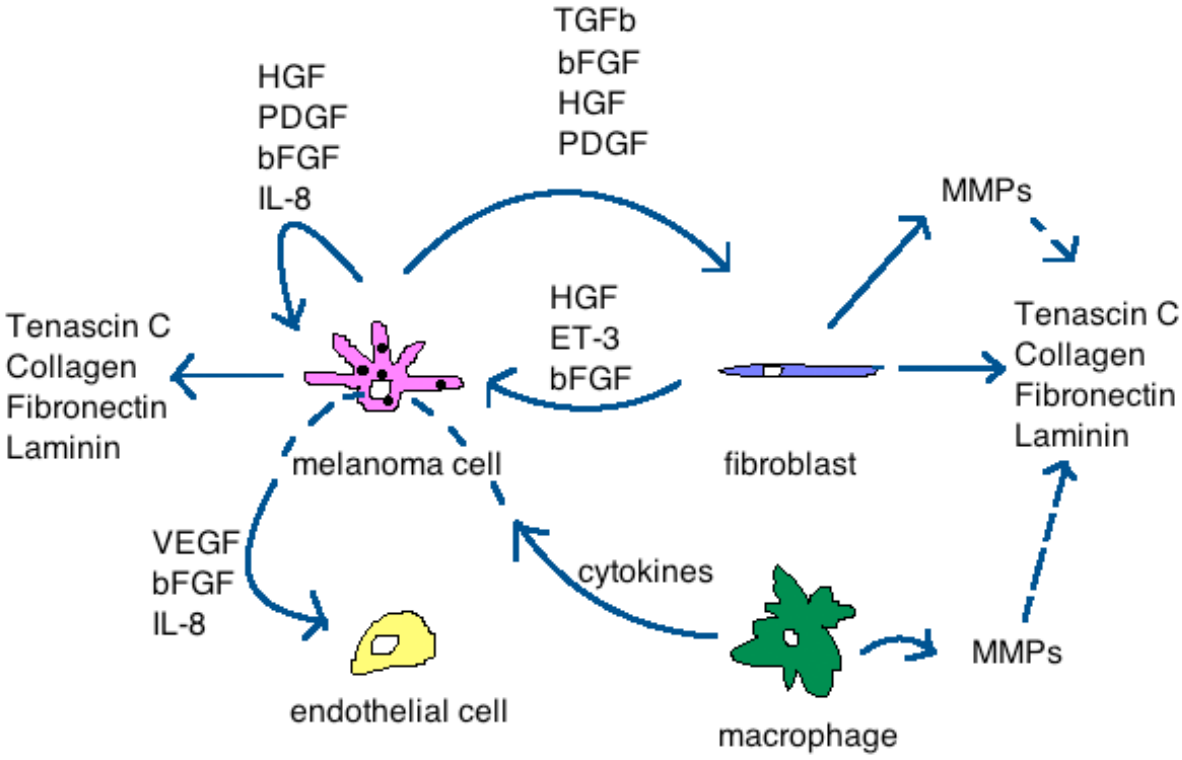

Figure 2. Melanoma-stromal cell interactions through growth factors, cytokines and ECM.

It has been suggested that the progression of tumors to malignancy is controlled by the microenvironment which provides tumor-suppressive signals (Bissell and Hines, 2011); by modifying the ECM composition cancer cells are altering the architecture and homeostasis of the tissue and releasing their malignant potential.

1.3 MATRIKINES

The concept of matrikines has been proposed in order to define protein domains from the ECM which can signal to the surrounding cells (Maquart et al., 1999). Some of these signals can be provided by cryptic sites within the ECM molecules that are revealed only after the structural or conformational alteration (Davis et al., 2000). In the course of tissue injury or tumor invasion, matrix alterations due to ECM denaturation, enzymatic breakdown, mechanical forces or protein multimerization and adsorption, provide a plethora of matrycriptis signals. In recent years, special attention was given to a class of matrikines that are able to signal through growth factor receptors (Tran et al., 2005). These matrikines posses low binding affinity for growth factor receptors but are often present in high valence, which increases the avidity for the receptor and enables efficient signaling. So far, these domains were found in Collagen, Laminin, Decorin and Tenascin C and they enable persistent non-degradable signals (Tran et al., 2004). Interestingly, analysis of melanoma tissue samples and adjacent uninvolved skin of the same patient revealed that the expression of two matrikines Tenascin C and Decorin is opposite, and inversed compared to the expression in the normal human skin (Hood et al., 2010)(Figure 3).

A

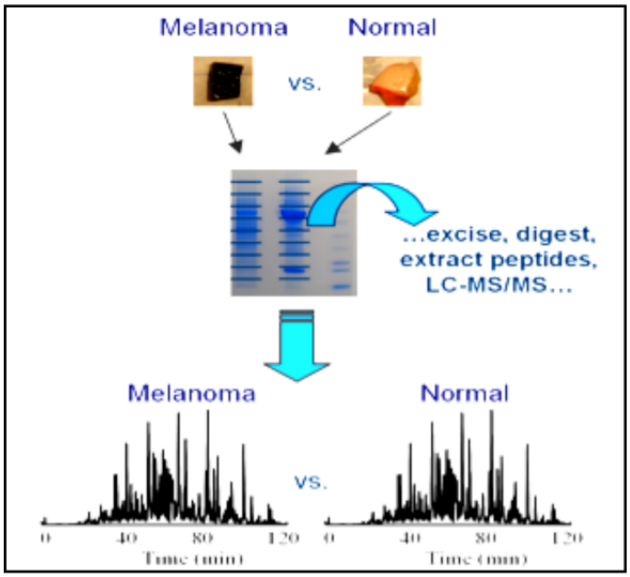

B

ECM protein	Melanoma	Uninvolved skin
Tenascin C	143	0
Fibronectin I	46	20
Collagen I	15	107
Decorin	13	73
Lumican	37	118

Figure 3. Proteomic analysis of human melanoma tissue sample and uninvolved skin of the same patient.

(A) Schematic outline of the proteomic analysis procedure (image courtesy of Drs Thomas Conrads and Brian Hood) (B) Table representing ECM protein counts in melanoma and normal skin. Numbers represent the number of peptides detected out of 10000 analyzed peptides per sample.

1.3.1 Tenascin C

The physiological role of Tenascin C (TNC) lies in establishing of the interactions between the epithelium and the mesenchyme during embryonic development, tissue differentiation and wound repair; therefore expression of TNC is transient and strictly regulated

(Jones and Jones, 2000b). Persistent high levels of TNC are present in various tumor tissues, including brain, bone, prostate, intestine, lung, skin, and breast (Pas et al., 2006). During development TNC is expressed along the pathways of neural crest migration (Mackie et al., 1988), and given that melanocytes are derived from the neural crest, the expression of TNC in melanomas might be a reactivation of a developmental pathway as many of the processes leading to transformation of melanocytes are reminiscent of differentiation stages during development.

Tenascin C is a hexameric glycoprotein composed of 180 to 320 kDa monomers, which are disulfide-linked at their N-termini (Figure 4). Different molecular weights of TNC are the consequence of glycosylation and alternative splicing. Each subunit contains: the N-terminal assembly domain, a domain composed of 14.5 EGF-like repeats, a domain composed of fibronectin type III-like (FNIII) repeats and a fibrinogen-like sequence on the C terminus (Aukhil et al., 1993; Chiquet-Ehrismann and Chiquet, 2003; Erickson and Bourdon, 1989; Jones and Jones, 2000a; Orend, 2005; Orend and Chiquet-Ehrismann, 2006). Modular structure of TNC enables interactions with various binding partners that can have different functions during tissue injury and tumorigenesis. TNC can interact with several other ECM proteins and cell surface receptors thus influencing tissue architecture and cell response.

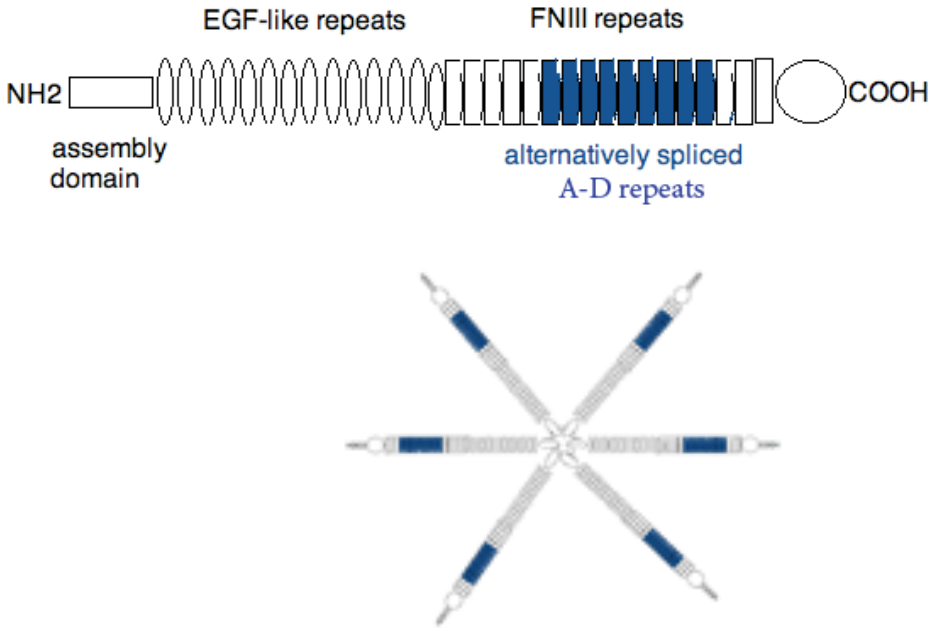

Figure 4. Schematic illustration of TNC monomer and hexamer.

The Fibronectin III (FNIII)-like domain of TNC is the site of interaction with Fibronectin, Heparin, Perlecan, Aggrecan, Versican and Brevican (Midwood and Orend, 2009), and the hexameric structure of TNC may allow cross-linking of ECM molecules and re-organization of the matrix architecture. Cells can interact with the FNIII-like domain of TNC via integrins α2β1, α7β1, α9β1, αVβ1, αVβ3, and αVβ6, which allow cell attachment, and via syndecans-1 and -4, and annexin II which can signal de-adhesion (reviewed in (Midwood and Orend, 2009; Orend and Chiquet-Ehrismann, 2006)). Therefore, the response to TNC differs depending on the receptor repertoire present on the cell surface. TNC can be alternatively spliced within the FNIII-like repeats (designated by letters A to D) and the most represented isoform in tumor tissues is the full length 320 kDa, although different splice variants can co-exist in the same tumor tissue (Pezzolo et al., 2011). It is not clear whether alternatively spliced forms have clearly distinct roles, but the presence of the FNIIIA-D repeats is responsible for some anti-

adhesive and pro-proliferative properties of TNC (Chung et al., 1996; Huang et al., 2001; Murphy-Ullrich et al., 1991). TNC can promote de-adhesion of cells adhered on Fibronectin (FN) (Chiquet-Ehrismann et al., 1988); and this de-adhesion can be signaled by TNC interference with FN binding to Syndecan-4, and preventing the FN induced cell spreading (Huang et al., 2001); or through one of the known receptors for TNC - Annexin II, calcium binding membrane protein, which binds TNC through alternatively spliced A-D fibronectin III-like domain. Only the variants containing the he whole A-D domain can bind and signal de-adhesion via Annexin II (Chung et al., 1996).

Epidermal Growth Factor-like (EGFL) repeats of TNC also have counter-adhesive properties (Prieto et al., 1992; Spring et al., 1989) and have been shown to bind and signal through the Epidermal Growth Factor receptor (EGFR) (Iyer et al., 2007a; Swindle et al., 2001). The affinity of select EGFL repeats for EGFR is in the micromolar range (Swindle et al., 2001) but the matrix-constrained environment that limits diffusion and hexameric presentation of the repeats within the TNC molecule allow high avidity of the binding (Iyer et al., 2007a). Furthermore, the binding of TNC EGFL repeats does not induce receptor internalization, restricting EGFR signaling to the plasma membrane, which preferentially activates the EGFR pro-migratory signaling cascade: the activation of phospholipase C γ involved in lamellipod protrusion formation, and the activation of m-calpain involved in tail retraction during cell migration (Iyer et al., 2008).

Fibrinogen-like globe of TNC binds to $\alpha V\beta 3$ integrin (Yokoyama et al., 2000) and Toll-like receptor 4 (TLR4) and exhibits pro-inflammatory effects by the activation of Toll-like receptors in macrophages and fibroblasts (Midwood et al., 2009).

In summary, TNC is equipped not only to modulate ECM architecture but also to dramatically influence the behavior of cells. TNC expression in tumors can be induced by various inflammatory cytokines and growth factors that are mostly secreted by stromal cells: TNFα, IFNγ, IL-1, -4, -6, -8, -13, EGF and TGFβ, just to name a few (reviewed in (Chiquet-Ehrismann and Chiquet, 2003)). In addition, reactive oxygen species, hypoxia and mechanical stress, which are all present in the tumor tissue, can induce TNC expression (reviewed in (Midwood and Orend, 2009)). TNC can be cleaved by MMPs and serine proteases, and some of these events can reveal cryptic sites. For example, MMP2 cleavage of TNC occurs after the second alternatively spliced FNIII domain (Siri et al., 1995) and reveals a cryptic adhesive site in the FNIII domain that binds to Syndecan-4 and causes β1 integrin activation (Saito et al., 2007). Cleavage sites for MMP2, MMP3, MMP7 and MMP9 are all within the FNIII like domain or the NH2 terminal knob, leaving EGFL repeats intact (Siri et al., 1995). TNC itself induces the expression of MMPs 1, 3, and 9 (Tremble et al., 1994) and activation of MMP2; in addition, TNC deposition is positively regulated by MMP3 and MMP9 (Dang et al., 2004). Consequently, there is a positive feedback loop between induction of MMPs by TNC and its cleavage.

In normal human skin TNC is expressed at low levels in papillary dermis beneath the basal lamina, within the walls of blood vessels and around sweat glands (Lightner et al., 1989) and it comprises only 0.02-0.05% of total protein in papillary dermis. Upon photo damage of the skin TNC can be detected throughout the epidermis, at the epidermal-dermal junction and deep in papillary dermis (Filsell et al., 1999). It is upregulated in wounded skin (Latijnhouwers et al., 1996) being produced by keratinocytes in the early phases of the wound healing (Latijnhouwers et al., 1997) and co-localizes with lymphocyte infiltration in inflamed dermis (Seyger et al.,

1997). TNC peaks at the end of the inflammatory phase of tissue repair and promotes tissue rebuilding, and the levels return to normal after the repair is complete (Betz et al., 1993). The upregulation of TNC in melanoma is an example that supports the hypothesis that "tumors are the wounds that never heal" (Dvorak, 1986) as in the tumor microenvironment constant high levels of TNC are present, produced both by transformed tumor cells and stromal cells (De Wever et al., 2004; Hanamura et al., 1997; Yoshida et al., 1997). *In vitro,* the majority of human melanoma cell lines secrete TNC (Herlyn et al., 1991) and the expression levels of TNC in melanoma cell lines derived from tumors of different stages correlate with the severity of the stage (Figure 14). Thus, an open question remains whether the TNC expressed by the melanoma cells can drive melanoma progression. TNC has been shown to be important for the proliferation of melanoma cells when they are grown as spheres, suggesting its role in the maintenance of tumor initiating cells (Fukunaga-Kalabis et al., 2010). In melanoma tumor tissue, TNC seems to be incorporated in channel-like structures together with Fibronectin and pro-Collagen I (Kaariainen et al., 2006) and it is suggested that these structures can form a continuum between avascular and vascular tumor tissue and can serve as the scaffold for tumor angiogenesis (Midwood et al., 2011). It has also been proposed that cancer cells are the main source of TNC in micrometastases until the stroma takes over and becomes the primary source in larger metastases (Oskarsson et al., 2011). The growth of melanoma tumors in TNC knock-out mice is suppressed compared to the wild type due to the lack of TNC from the stroma, which is needed for VEGF expression and tumor vascularization (Tanaka et al., 2004). It is likely that TNC plays several roles in tumor progression, and that the endogenous TNC synthesized by tumor cells and stroma-derived TNC have both overlapping and distinct roles. The underlying signal transduction pathways responsible for TNC pleiotropic effects are mostly unknown.

1.3.2 Decorin

Decorin (DCN) is the small (40kDa) leucine-rich proteoglycan synthesized chiefly by stromal fibroblasts, endothelial cells under stress and smooth muscle cells (Neill et al., 2012). Decorin contains a protein core and a single chondroitin/dermatan sulfate glycosaminoglycan chain attached to a serine near the N terminus (Chopra et al., 1985) (Figure 5) . It is mostly found in collagen–rich connective tissues (Bianco et al., 1990) where it interacts with high affinity with collagen fibers and is involved in collagen fibrologenesis (Danielson et al., 1997; Keene et al., 2000; Zhang et al., 2006). In addition, DCN can bind to multiple growth factor receptors including EGFR (Iozzo et al., 1999b), Met receptor (Goldoni et al., 2009) and IGF-1R (Iozzo et al., 2011). DCN can also sequester TGFβ family members into the extracellular matrix, as there are two binding sites for TGFβ in the DCN core (Hildebrand et al., 1994).

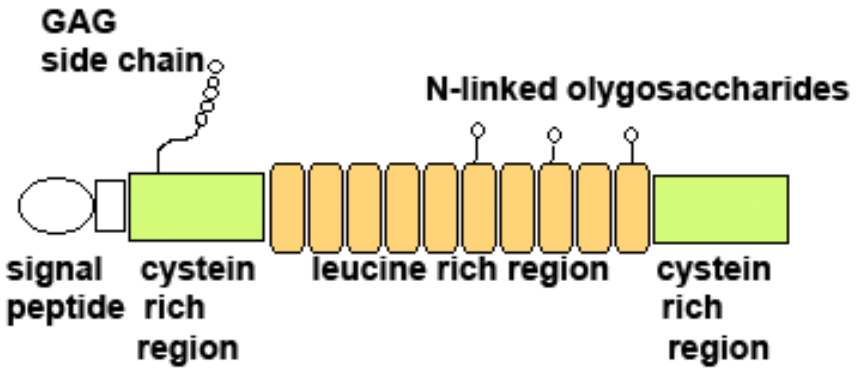

Figure 5. Schematic illustration of Decorin.

The first identified receptor tyrosine kinase to bind Decorin was EGFR (Iozzo et al., 1999b): DCN initially triggers receptor activation, dimerization and internalization, but prolonged exposure induces EGFR down-regulation (Zhu et al., 2005) thus terminating EGFR

signaling. The affinity of DCN is in the nanomolar range (70nM) (Santra et al., 2000; Santra et al., 2002) comparable to the EGF itself, and the binding site of DCN within the EGFR is partially overlapping but distinct from the EGF binding site (Santra et al., 2002). DCN is also an antagonist of the Met receptor (Goldoni et al., 2009) and can inhibit the PDGF receptor (Merline et al., 2011). Therefore, DCN can be considered an endogenous matrix-centric pan-kinase inhibitor (Neill et al., 2012) and along with TGFβ sequestering function which leads to tumor immunosupression and growth retardation, has been proposed to be "a guardian from the matrix" to draw a comparison to "guardian of the genome" p53 (Neill et al., 2012). Notably, the cooperation between Decorin and p53 has already been established (Iozzo et al., 1999a).

In normal human skin Decorin is produced by fibroblasts, with higher expression in deeper dermis compared to the superficial layers (Honardoust et al., 2012). Quiescent fibroblasts are the main source of DCN, as proliferating fibroblasts produce significantly lower levels (Mauviel et al., 1995). The disruption of Decorin leads to abnormal collagen fibril morphology and skin fragility (Danielson et al., 1997). DCN is a vital player in maintaining the overall integrity of the skin by both providing structural organization and indirect signaling (Reed and Iozzo, 2002). In melanoma, Decorin can be found in peritumoral stroma, but not in melanoma cells or dense tumor tissue (Brezillon et al., 2007).

Interestingly, Decorin and Tenascin C, two ECM proteins with opposing roles in tumor progression share two receptors TLR 4 and EGFR. TNC can bind to TLR 4 via its fibrinogen domain (Midwood et al., 2009) and soluble Decorin was also found to bind to TLR 2 and TLR4 on macrophages thus boosting their inflammatory activity and suppressing tumor growth (Merline et al., 2011). The EGFL repeats of TNC and the leucine rich domain of DCN can activate the same receptor – EGFR without sharing structural homology. In addition, TNFα and

TGFβ1 can down-regulate DCN expression (Mauviel et al., 1995), and TGFβ1 is being secreted by melanoma cells and is up-regulating TNC expression (Berking et al., 2001). In melanoma TNC and DCN proteins have inversed expression (Figure 24), which makes it interesting to postulate that one can counteract the other in the melanoma extracellular matrix setting.

1.4 THE ROLE OF THE EXTRACELLULAR MATRIX IN TUMOR CELL ADHESION AND MIGRATION

1.4.1 Cell-matrix adhesion

The adhesion of cells to the extracellular matrix is important for basic cell functions: it is necessary for the cell growth, survival, differentiation and cell migration. On rigid two-dimensional substrates cell adhesion is three-phasic: cells first attach to the substratum, then they spread, and in the last phase they form focal adhesions and stress fibers (Figure 6). The initial attachment is mediated by integrins and their ECM substrates and is weak in strength; next, with the appropriate signals from the ECM the cells increase the surface area of the contact with the substratum and spread through the formation of actin microfilaments. The clustering of integrins and their activation then induces formation of focal adhesions and strengthens the adhesion. This whole process is reversible and upon appropriate intra- or extracellular signals during cell proliferation, motility or morphogenesis, cells can de-adhere to various extents.

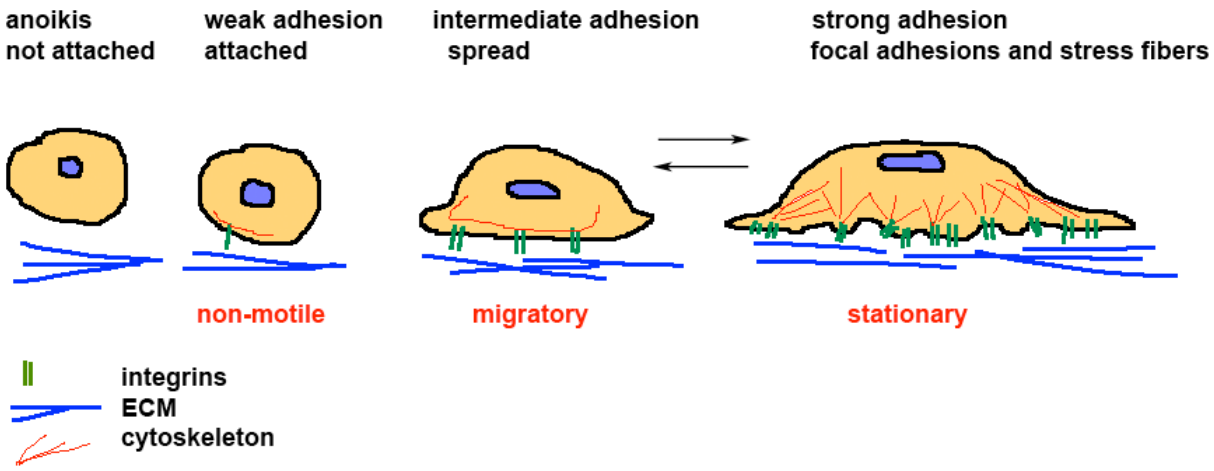

Figure 6. Stages of cell adhesion on two-dimensional substratum.

Much less is known about the process of de-adhesion in which the cell moves to a state of weaker adherence. The state of weaker adherence can be induced by the matricellular proteins Thrombospondin-1 and -2, Tenascin C and SPARC (reviewed in (Murphy-Ullrich, 2001)). These proteins function both in soluble and insoluble states and can promote only initial stages of cell adhesion – attachment and spreading. When presented with other matrix proteins they can antagonize adhesive activities of these other molecules (Adams and Schwartz, 2000; Murphy-Ullrich and Hook, 1989; Wenk et al., 2000) and when added as soluble agents they can disrupt focal adhesion complexes of already spread cells (reviewed in (Orend and Chiquet-Ehrismann, 2000)).

Adhesive proteins can also gain anti-adhesive properties under certain conditions: MMP2 cleavage of Laminin-5 can expose a cryptic anti-adhesive and pro-migratory site in the α2 chain (Giannelli et al., 1997) and the same enzyme can cleave Fibronectin and release its anti-adhesive site that competes with the native Fibronectin (Watanabe et al., 2000). Little is known about the signaling mechanisms that are being activated by the adhesion modulatory ECM proteins, but the

change in cell shape and the reorganization of the actin cytoskeleton are the major common determinants. The major candidate class for the actin cytoskeleton remodeling are integrins, heterodimeric transmembrane receptors, which mediate cell attachment to ECM and link it to the cytoskeleton (Giancotti and Ruoslahti, 1999).

In melanoma, cell matrix interactions shift from Collagen IV and Laminin adhesion in normal melanocytes to Collagen I and Vitronectin in melanoma cells, in addition to the cadherin switch that allows melanoma cell detachment from keratinocytes. Increased and altered expression profiles of integrin combinations that are important for the progression of melanoma are: αVβ3 that binds to Fibronectin, Fibrinogen, Von Wildebrand factor, certain collagens, Thrombospondin-1, Osteopontin, Laminin and Tenascin C; αvβ1 that binds Fibronectin, Vitronectin and Tenascin C and α5β1 that binds Fibronectin ((Albelda et al., 1990; Felding-Habermann et al., 1992; Natali et al., 1997; Natali et al., 1993; Van Belle et al., 1999) and reviewed in (van der Flier and Sonnenberg, 2001)). αVβ3 is especially important for melanoma survival in 3D collagen environment (Montgomery et al., 1994).

1.4.2 Cell migration

The intermediate state of cell adhesion favors motility (DiMilla et al., 1991; DiMilla et al., 1993). Matricellular proteins that promote the intermediate state of adhesion have increased expression at the exact sites of remodeling that require cell migration - during embryogenesis, wound healing, inflammation and tumor invasion. This suggests a role for the matricellular proteins in promoting migration by enabling the intermediate adhesive state. A mathematical model developed by DeMilla, Barbee and Lauffenburger predicts that the maximal motility of cells is achieved when the ratio of the cellular force, achieved through cytoskeletal contractility,

and the adhesive strength, achieved through integrin-matrix interactions, is intermediate (DiMilla et al., 1991). Weak cell adhesion does not generate enough force for the cell movement, and too strong adhesion prevents the releasing of the cell from the ECM (Palecek et al., 1997). Migration requires the coordination of the cell extension, adhesion/de-adhesion and contraction, and is simultaneously regulated by growth factors and the ECM molecules.

In order for cells to move, the existing adhesion sites have to be disassembled and the new ones have to be formed. Current understanding of cell-matrix adhesions and migration is based mostly on *in vitro* studies on rigid 2D surfaces that induce an artificial polarity between lower and upper cell surfaces. *In vivo,* cells are embedded within 3D matrices and focal adhesions differ from classically described *in vitro* adhesions in structure, localization and functions (Cukierman et al., 2001). Both three-dimensionality and the composition of the matrix are contributing to more effective mediation of the adhesion and enhanced migration of cells *in vivo* or in *in vivo*-like 3D matrix compared to mechanically 2D flattened cell matrix, or individually presented matrix components in 2D (Cukierman et al., 2001).

In order to move during tumor invasion *in vivo*, cancer cells must break away from the primary tumor mass and deform and/or degrade the ECM. Contrary to the 2D motility that is based on actin polymerization that propels the cell forward, in 3D environment the force of protrusive actin polymerization drives cells into spindle shaped mesenchymal morphology that can allow cell migration only in the presence of proteases that degrade the surrounding ECM (Sahai and Marshall, 2003; Wolf et al., 2003). A hallmark of tumor cell invasion is upregulation of proteolytic enzymes generated both by migrating cells and the stromal cells (Kessenbrock et al., 2010). Proteolytic mesenchymal migration is a multi step process. The cell polarization and initial protrusion are followed by the attachment of the leading edge to ECM. Next, the cell

surface localized degradation of ECM generates space into which actomyosin contraction will move the advancing cell body deforming both the cell and the ECM. Finally, retraction of the cell rear and turnover of adhesions occur (Friedl and Wolf, 2010; Wolf and Friedl, 2011). However, in 3D context tumor cells can also invade without the requirement for the proteolytic activity and move through ECM without its degradation by acquiring a rounded morphology and using actin contractile force to generate amoeboid bleb-like protrusions that push and squeeze cells through the ECM (Friedl, 2004; Sahai and Marshall, 2003; Wolf et al., 2003; Wyckoff et al., 2006). Migration is possible in the absence of proteolysis if both the porosity of the matrix and the cell body deformability can support it. Molecular and structural characteristics of both tissue microenvironment and cell behavior determine whether cells will migrate collectively or individually in mesenchymal or amoeboid mode. ECM stiffness, fiber orientation, density and gap size provide parameters that modulate cell adhesion and cytoskeletal organization (Friedl and Wolf, 2010). In 3D stiff matrices mesenchymal migratory force generation is β1 integrin-dependent (Wolf et al., 2003) while soft matrices do not reinforce focal adhesion formation and support cell rounding (Ulrich et al., 2009). While mesenchymal migration is dependent on alternative pushing and pulling cycles, amoeboidal migration is equally mechanically complex and combines stronger pushing with less adhesive pulling of the substrate (Friedl and Wolf, 2010). The tuning model proposed by Friedl and co-workers predicts that cell migration is a continuum of states that are determined by several modal parameters that simultaneously control how cell migrates and that their combined magnitudes impact which migrational mode the cell will adopt (Friedl and Wolf, 2010). A central signaling pathway that controls the conversion between mesenchymal and rounded migration is the balance between Rac and Rho signaling (Sahai and Marshall, 2003).

1.4.3 Molecular mechanisms of mesenchymal and amoeboid migration

The Rho family of small GTPases is the key regulator of both cell adhesion and cytoskeleton during cell migration. The most studied members of the family are Cdc42, Rac1 and RhoA. In the mesenchymal mode of migration, formation of actin-rich filopodia and lamellipodia is Cdc42- and Rac1-dependent (Nobes and Hall, 1995; Ridley and Hall, 1992; Ridley et al., 1992). Cdc42 and Rac regulate WASP/WAVE proteins that promote the nucleation of actin filaments and the formation of the leading edge (Miki et al., 1998; Rohatgi et al., 1999). The protruding leading edge is then stabilized by integrin interactions with the ECM and the formation of focal adhesions. Rho and its downstream effector Rho-associate kinase (ROCK) have been shown to be dispensable for the mesenchymal mode of migration (Sahai and Marshall, 2003), where Cdc42 can compensate the loss of Rho/ROCK signaled contractility (Wilkinson et al., 2005). In contrast, the rounded mode of motility is dependent on Rho and ROCK activity (Sahai and Marshall, 2003), where ROCK-dependent myosin light chain (MLC) phosphorylation is crucial for the correct organization of MLC and force generation within the moving cell (Wyckoff et al., 2006). Phosphorylated MLC increases ATPase activity to promote actin-myosin interactions and contractile force generation. The intracellular pressure results in the rupture of the actomyosin cortex and the formation of membrane blebs (Keller and Eggli, 1998). After the formation of the bleb the contractile cortex reassembles (Charras et al., 2006). One major difference between mesenchymal and amoeboid movement is therefore the driving force for the formation of protrusions, which are actin polymerization and cytoplasm inflow, respectively. The silencing of ROCK pathway induces the transition from amoeboidal to mesenchymal invasiveness (Sahai and Marshall, 2003; Sanz-Moreno et al., 2008) and the silencing of Rac induces the opposite shift (Sanz-Moreno et al., 2008; Yamazaki et al., 2009). In addition, active

Rac negatively regulates Rho/ROCK signaling (Sander et al., 1999) and inhibits cell rounding, while active Rho/ROCK limits Rac activity that inhibits cell extension (Sanz-Moreno et al., 2008). Mesenchymal and amoeboid cell phenotypic characteristics and possible signaling controls are summarized in Figure 7.

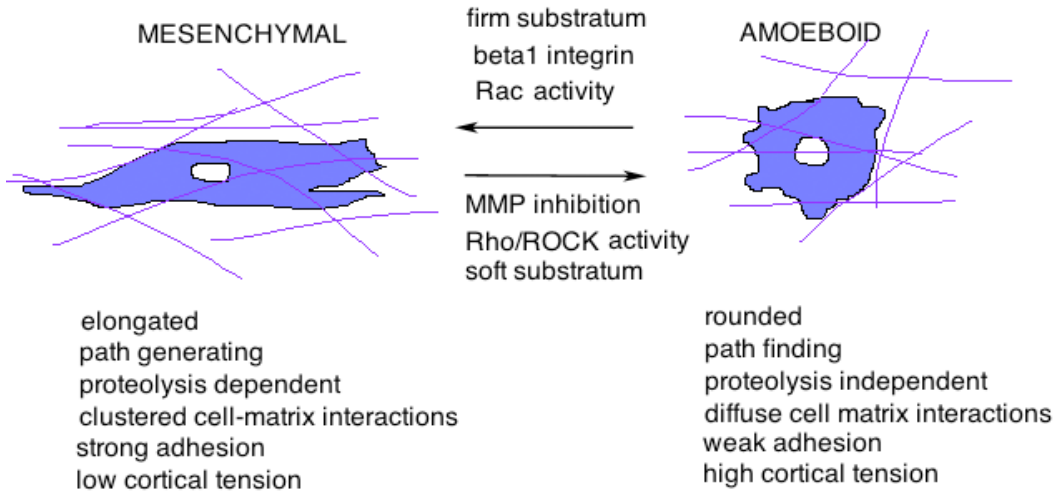

Figure 7. Mesenchymal and amoeboid cell phenotypes.

Rho proteins are often overexpressed in tumors (Fritz et al., 1999) and one of the key events in experimental melanoma metastasis is the upregulation of RhoC (Clark et al., 2000). The inhibition of RhoC or the combined inhibition of RhoA and ROCK1/2 greatly reduce melanoma invasion (Sahai and Marshall, 2003; Wolf et al., 2003). In melanoma, genes involved in the control of cell motility show altered expression levels, but not mutational activation (Gaggioli and Sahai, 2007), as activation of one step but not the others in the migration process would give un-coordinated and inefficient motility. Two modes of migration are interchangeable and arise as a reply to the specifics of the microenvironment (Pankova et al., 2010). So far, apart from the influence of the collagen fiber spatial organization (Provenzano et al., 2008), little is

known about the ECM components that influence the migratory shifts or the cellular receptors that signal them.

1.5 MODELS FOR IN VITRO STUDY OF MELANOMA INVASION

One of the obstacles in developing effective therapeutic approaches for melanoma is the lack of good experimental models that recapitulate the *in vivo* behavior of tumors. Biological properties of 2D cultured melanoma cells only partially resemble those *in situ*. Melanoma development is a result of deregulated signaling between melanocytes, keratinocytes and the stroma, and has to be studied in the context of multicellular 3D environment. As melanocyte regulation by keratinocytes is very intricate, studying melanoma progression requires the organotypic models that would include as many players as possible. The goal is to recreate the characteristics of the tumor in the appropriate microenvironmental context. Rodent models of melanoma have not proven to be successful in recapitulating the early stages of melanoma invasion since melanocytes are localized differently in rodent and human skin and rodents do not develop spontaneous melanoma.

A key feature of signaling from the ECM is the spatial organization of cells within tissues, such that the cell shape, spacing and positioning within the 3D structure are additional factors in cell response to signals. Therefore, it is of importance to study cell migration and invasion in matrices with the models that would most resemble the natural occurrence of these proteins. *In vivo* cells experience the surrounding ECM as a three dimensional network, and this cannot be mimicked in two dimensional cell culture assays.

1.5.1 Skin organ constructs

Skin organ constructs (SOC) are the most advanced *in vitro* models for the study of melanoma-microenvironment interactions and present a link between two-dimensional cultures and *in vivo* models. These cultures are composed of dermal and epidermal equivalents. Dermal equivalents can be made by repopulating *post mortem* acquired de-cellularized human dermis with fibroblasts (Ghosh et al., 1997; Regnier et al., 1986), or by embedding primary fibroblasts into collagen gels and letting them contract and remodel the gel (Bell et al., 1983; Marionnet et al., 2006). Seeding primary keratinocytes on top of dermal equivalents forms epidermis. Gradual withdrawal of EGF from the culture medium induces keratinocyte differentiation. Placing gels on top of rafts and exposing them to air allows keratinization of the epidermis resembling stratum corneum. Keratinocytes can generate normal epidermis irrespective of the species origin of fibroblasts which allows identification of the origin of the components involved in tissue reconstitution (Stark et al., 2004). These organotypic models form the basement membrane and the epidermal-dermal junction is straight in the case of dermal collagen gels (Meier et al., 2000b; Smola et al., 1998), or follows natural ridges in de-cellularized human dermis. Both keratinocytes and fibroblasts contribute to the formation of the basement membrane in SOC and, interestingly, TNC is present during formation of the dermal-epidermal junction (Marionnet et al., 2006). If melanocytes are included in the model, they migrate and position themselves at the basal levels of the epidermis and make contacts to multiple keratinocytes (Valyi-Nagy et al., 1990). Melanoma cells from different stages of progression can be incorporated into SOCs and they reflect the characteristics of the cells *in situ*: RGP cells do not invade into dermis, while VGP and MGP derived cells invade (Meier et al., 2000b). The representative images of SOCs made from contracted collagen gels grown at the air liquid interface are shown in the Figure 8.

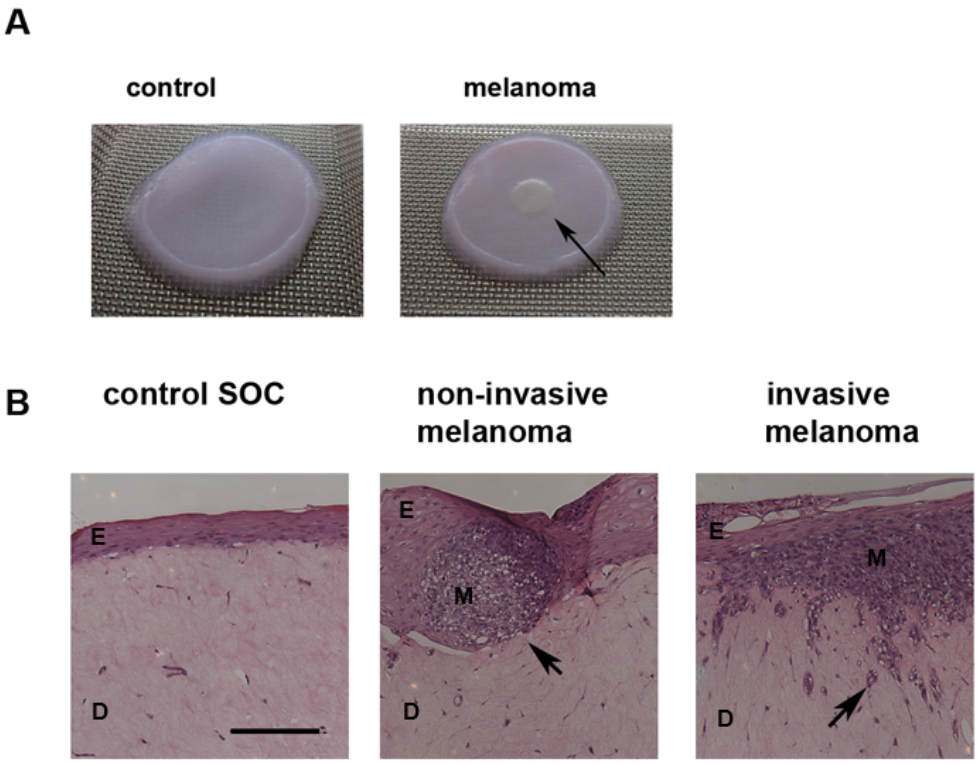

Figure 8. Skin organ constructs.

(A) SOC composed of fibroblast-contracted collagen gel seeded with keratinocytes is shown in the left side panel, and SOC with melanoma cells seeded on top of the epidermis is shown on the right. Arrow points to the mole-like growth of melanoma cells expressing GFP that were initially seeded within a cloning ring on top of the epidermis. (B) H&E staining of SOCs. The arrowheads point to non-invading and invading melanoma tumors, respectively; scale bar 100μm. E-epidermis, D-dermis, M-melanoma.

These cultures are suitable for use of transfected and infected cells and are a useful tool for studying protein function in melanoma progression. Genetic perturbations of melanoma cells sometimes show drastic differences in growth compared to control cells that were otherwise undetectable in 2D culture systems (Hsu et al., 1998; Satyamoorthy et al., 2001). For example,

SOCs were used to show that αVβ3 integrin up-regulation induces conversion from RGP to VGP melanoma and progressive invasion (Hsu et al., 1998). Skin organ reconstructs are healthy for up to a month in culture and biological phenotype of melanoma cells is remarkably stable (Meier et al., 2000b). Quantification of invasion in SOCs can be achieved by taking into account both the depth and the pattern of invasion (Nystrom et al., 2005). In addition, these cultures can be grafted on immunodeficient mice for long-term studies (Javaherian et al., 1998).

1.6 HYPOTHESIS

Given the significant change in the composition of the extracellular matrix in invasive melanomas compared to normal skin counterparts, we reasoned that distinct de-regulated ECM proteins could drive the melanoma cell invasion. We hypothesize that the increased expression of ECM protein Tenascin C by melanoma cells themselves can drive melanoma invasion by increasing migration of cells in 3D environments. We postulate that this pro-invasive effect of TNC would be mapped to the EGFL repeats of TNC, as these were shown to activate the pro-migratory EGFR signaling cascade (Iyer et al., 2008). Furthermore, we hypothesize that another EGFR-binding matrikine, Decorin, could counteract TNC-driven melanoma invasion. In this work we will first test whether skin organ cultures seeded with melanoma cells can recapitulate changes in the ECM found in human melanoma samples and then test the influence of Tenascin C and Decorin on modulating melanoma invasion.

2.0 PROTEOMIC ANALYSIS OF LASER MICRODISSECTED MELANOMA CELLS FROM SKIN ORGAN CULTURES

Brian L. Hood *[1,3], Jelena Grahovac *[2], Melanie S. Flint[1, 3], Mai Sun[1, 3], Nuno Charro[3], Dorothea Becker[2], Alan Wells[2, 4] and Thomas P Conrads[1, 2]

Departments of [1]Pharmacology & Chemical Biology and [2]Pathology, and the [3]Mass Spectrometry Platform, Cancer Biomarkers Facility, University of Pittsburgh Cancer Institute, University of Pittsburgh, and [4]Pittsburgh VA HealthCare System

* These authors contributed equally to this work

This work was published in the Journal of Proteome Research, 2010.

2.1 ABSTRACT

Gaining insights into the molecular events that govern the progression from melanoma *in situ* to advanced melanoma, and understanding how the local microenvironment at the melanoma site influences this progression, are two clinically pivotal aspects that to date are largely unexplored. In an effort to identify key regulators of the crosstalk between melanoma cells and the melanoma-skin microenvironment, primary and metastatic human melanoma cells were seeded into skin organ cultures (SOCs), and grown for two weeks. Melanoma cells were recovered from SOCs by laser microdissection and whole-cell tryptic digests analyzed by nanoflow liquid chromatography-tandem mass spectrometry with an LTQ-Orbitrap. The differential protein abundances were calculated by spectral counting, the results of which provides evidence that cell-matrix and cell-adhesion molecules that are upregulated in the presence of these melanoma cells recapitulate proteomic data obtained from comparative analysis of human biopsies of invasive melanoma and a tissue sample of adjacent, non-involved skin. This concordance demonstrates the value of SOCs for conducting proteomic investigations of the melanoma microenvironment.

2.2 INTRODUCTION

Despite increasing efforts aimed at melanoma prevention and, equally important, early detection, the worldwide incidence of melanoma continues to rise. As there are no effective treatment regimens for patients with advanced melanoma, the molecular basis of melanoma progression is likely to hold the key to clinical treatment. Melanoma progression is a pathologically well-defined process and when surgically resected with a wide and deep margin, the prognosis for patients with melanoma *in situ* is favorable. While melanoma *in situ* is confined to the epidermis, primary melanoma in the vertical growth phase (VGP) has invaded deep into the dermis and, unlike melanoma *in situ* but like melanoma in the metastatic growth phase (MGP), VGP melanoma proliferates aggressively.

Over the past few years, high-throughput studies such as serial analysis of gene expression (SAGE), whole-genome microarray expression profiling and integrative analysis by microarray-based comparative genomic hybridization (array-CGH) have led to the identification of genes that previously were not known to be expressed in advanced melanomas, and/or were found to be upregulated with progression from early to advanced-stage melanoma. More recently, mass spectrometry (MS)-based proteomics has been used to identify proteins that are differentially expressed in VGP versus MGP melanomas (Baruthio et al., 2008), or to detect melanoma in its early stage of development (Caron et al., 2009; Forgber et al., 2009; Paulitschke et al., 2009). Unlike in the case of breast cancer, however, where various high-throughput molecular approaches have generated significant information detailing the interactions among epithelial and stromal cells that play supporting roles in tumorigenesis (Hu and Polyak, 2008b), little information is yet available regarding the contributions of the local microenvironment to melanoma invasion and progression.

The epidermis is a multilayered structure, which is separated by an intact basement membrane from mesenchymal support cells. The stem cell-like basal keratinocytes undergo asymmetric replications with a multi-cell vertical differentiation resulting in enucleation and formation of a keratinized barrier. Neuroectoderm-derived melanocytes migrate into and reside in the epidermis where they are in contact with and communicate through E-cadherin and connexin junctions with keratinocytes. As part of the invasion process, melanoma cells must transit an E-cadherin-bridged epithelial milieu, attach to and breach the laminin/fibronectin-rich basement membrane and penetrate the dermis to reach conduits for dissemination, such as the host vasculature (Fig. 9A).

Detailed insights are lacking regarding how the local microenvironment affects or alters molecular features of melanoma cells that may be required to drive invasion and progression, arising from the absence of suitable skin models that mimic invasive growth. Indeed, rodent skin does not recapitulate the structural microenvironment of human skin and other animal models, such as porcine, do not present naturally occurring melanomas. *Ex vivo* human skin organ cultures (SOCs; Fig. 9B) have been used to investigate various human skin conditions including wound healing and have been used in a limited fashion in melanoma research (Eves et al., 2003; Eves et al., 2000; Herlyn et al., 2001; Meier et al., 2000a; Neil et al., 2000). Skin organ cultures are derived from excess pathological specimens obtained during cosmetic surgery or post bariatric weight loss, or can be generated *ex vivo* from human skin components (Margulis et al., 2005).

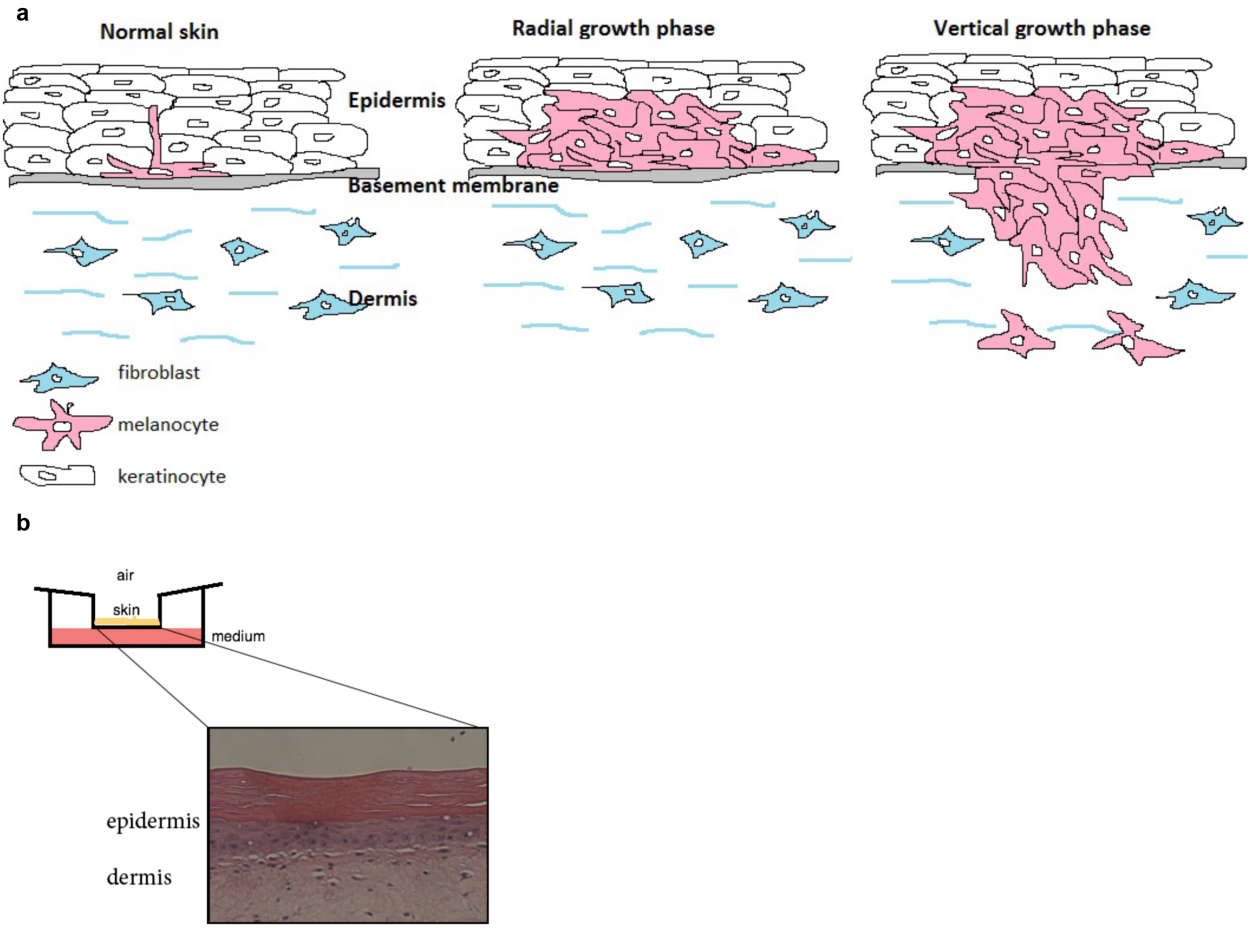

Figure 9. Melanoma model.

(A) Stages of melanoma progression in skin. Melanocytes reside in the epidermal/dermal junction. Early stage radial growth phase melanoma cells descend into the papillary dermis and spread laterally. Invasion deep into the dermis characterizes melanomas in the vertical growth phase. (B) Skin organ culture (SOC). SOCs are maintained at the air-liquid interface. (Inset) Hematoxylin and eosin stained section collected on day 12 of culture.

In the present study, we demonstrate that seeding VGP and MGP melanoma cells into SOCs leads to formation of melanoma nodules after approximately 12 days. Laser micro-dissection was utilized to acquire the melanoma tumor nodule from these tissue sections, as well as samples from collagen-injected and non-injected SOCs, which were analyzed by nano-flow liquid chromatography-tandem mass spectrometry (LC-MS/MS). An analysis of differential protein abundances by spectral counting was conducted, and demonstrates that the proteomic profiles very closely resemble that obtained from a differential proteomic analysis of human melanoma and an adjacent skin biopsy free of melanoma. These data suggest that melanoma-seeded SOCs represent a unique model system for investigating the molecular events in the microenvironment that promote melanoma invasion and progression.

2.3 RESULTS AND DISSCUSION

The impact of the microenvironment on the expression of proteins that govern invasion and progression of melanoma is one of the fundamental, but yet largely unresolved questions regarding this malignancy. To gain a better understanding of the underlying molecular events involved in this process, the study presented here served to determine whether an *in vitro* skin organ culture system can recapitulate protein abundance differences between melanoma cells and surrounding skin of melanoma and adjacent non-involved skin tissue samples as identified by a differential proteomic analysis. The SOCs were injected with either VGP (WM983A) or MGP (WM1158) melanoma cell lines, or collagen alone to serve as a control. These two melanoma cell lines are widely utilized and were selected solely to compare melanoma growth to normal (e.g. non-involved) skin in this SOC model and not to provide a detailed comparison of VGP

versus MGP. Approximately 10,000 cells were collected by laser micro-dissection from these FFPE SOC sections (Fig. 10A). The micro-dissected cells were processed using an "MS-friendly" heat-induced, enzyme-mediated (HI/EM) antigen retrieval method, followed by trypsin digestion (Fig. 10B). Peptide digests were analyzed by LC-MS/MS; Figure 10C shows a representative base peak chromatogram of a digest from approximately 5,000 cells on column from the micro-dissected FFPE VGP melanoma SOC section. This analysis afforded the identification of upwards of several hundred proteins per sample at a false discovery rate of approximately 2%, with all samples processed in duplicate.

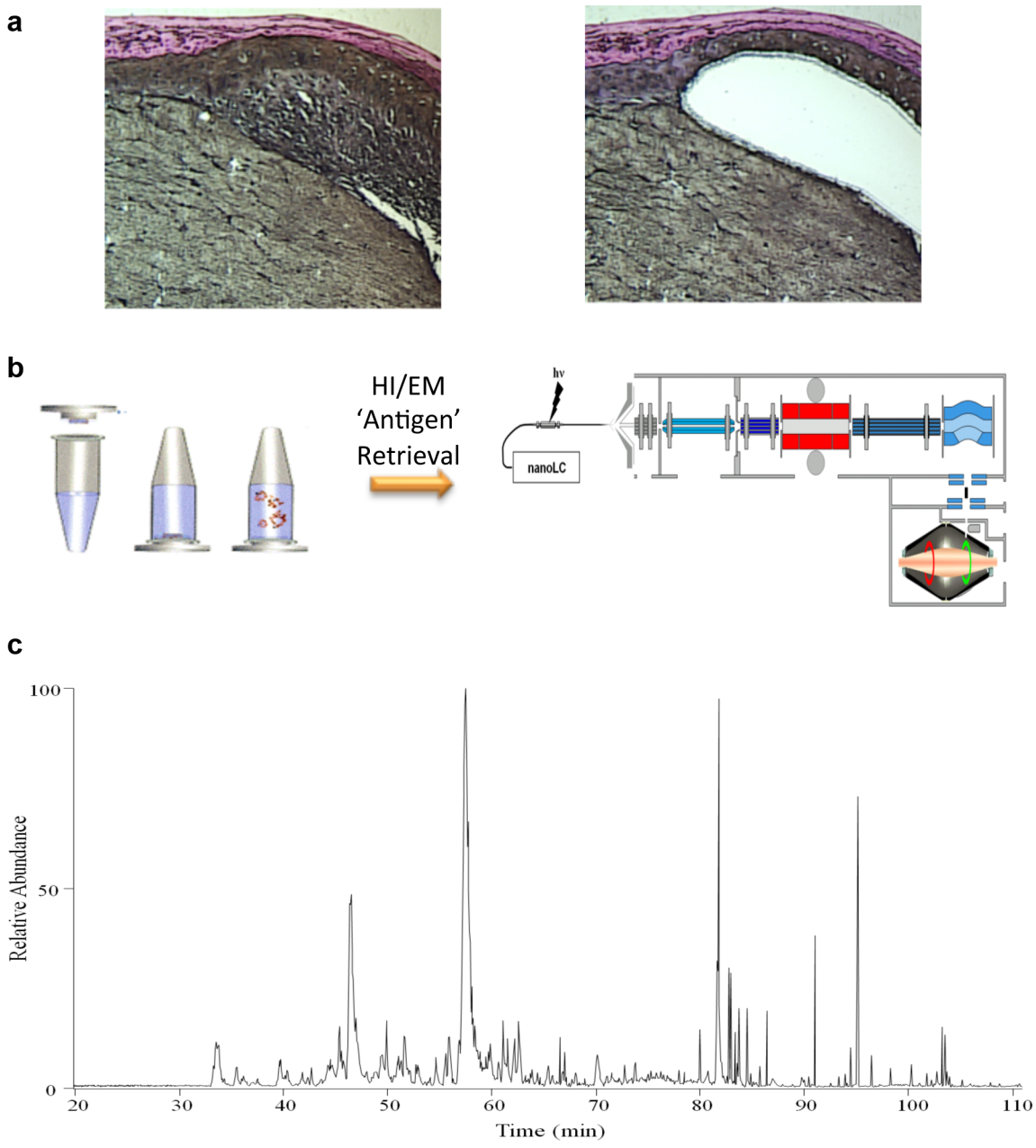

Figure 10. Mass spectrometry-based proteomic analysis of melanoma and skin organ cultures.

(A) Hematoxylin and eosin staining of formalin-fixed, paraffin-embedded (FFPE) skin organ culture (SOC) sections injected with approximately 10 000 VGP melanoma cells (WM983A) before (left panel) and after (right panel) laser microdissection. (B) Laser microdissected FFPE

tissue samples were processed using a heat-induced, enzyme-mediated digestion protocol for LC-MS/MS analysis. (C) Base peak chromatogram of approximately 5000 VGP melanoma cells obtained by laser micro-dissection from the FFPE SOC tissue sections.

Differences in protein abundance between the various SOC-derived samples were derived by spectral counting, where it was found that proteins such as Tenascin C (TNC) and Fibronectin, which have been described in the literature to play a role in melanoma cell invasion (Fukunaga-Kalabis et al., 2008; Kaariainen et al., 2006), were identified by high spectral count in the MGP melanoma SOC sections, and at lower levels in the VGP melanoma SOC sections (Table 1).

Table 1. Spectral count data for selected extracellular matrix and cytoskeletal proteins identified in melanoma-injected or control SOCs and from melanoma and normal human skin tissue

Protein	Function	Skin organ cultures				Biopsy	
		WM1158	WM983A	collagen	ctrl	melanoma	normal
Tenascin C	Matrix	19	7	1	0	143	0
Fibronectin	Adhesion/Matrix	11	6	0	0	46	20
Collagen 1	Matrix	17	8	6	10	15	107
α-Actinin-4	Adhesion/Cytoskeleton	2	1	0	0	76	22
Thrombospondin-1	Adhesion/Matrix	2	2	0	0	4	1
Plectin	Adhesion/Cytoskeleton	17	1	0	1	153	15
Transgelin 2	Adhesion/Cytoskeleton	6	0	0	0	14	18
Cytokeratin 5	Adhesion/Cytoskeleton	69	9	30	31	43	9
Cytokeratin 14	Adhesion/Cytoskeleton	56	1	22	13	25	14

Cytokeratin 6A	Adhesion/Cytoskeleton	41	6	26	30	17	0
Cytokeratin 16	Adhesion/Cytoskeleton	17	0	7	5	11	0
Cytokeratin 17	Adhesion/Cytoskeleton	22	0	5	4	1	0

These proteins were either not identified or were identified at very low abundance in the collagen and non-injected SOC controls. Increases in the abundance of TNC have been documented in MGP melanomas, and it has been suggested that relatively low levels of TNC expression may be associated with a lower risk for metastasis (Ilmonen et al., 2004). Like TNC, Fibronectin is another protein implicated in melanoma invasion. Specifically, it has been reported that these two proteins stimulate the invasive features of primary melanoma cells in 3D collagen matrices, and that TNC, Fibronectin and pro-collagen I form specific channel structures for melanoma invasion (Kaariainen et al., 2006). Tenascin C and Fibronectin are produced not only by fibroblasts, but also by endothelial cells and keratinocytes (Jones and Jones, 2000a). However, it is not yet fully established to what extent these proteins are also produced by VGP and/or MGP melanoma cells. The data presented here document that melanocytes, propagated *in vitro*, do not produce detectable levels of TNC (Fig. 11) and only low levels of Fibronectin (data not shown). In contrast, both MGP and VGP melanoma cells express substantial amounts of these matrix proteins. These matrix components are not only secreted but also incorporated into an insoluble matrix surrounding the cells, likely giving rise to the apparent difference in the relative levels of TNC transcript versus protein abundances measured in this study. The important point regarding this finding is that these melanoma cells produce these matrix components which are known to drive cell migration and tumor invasion (Iyer et al., 2007b).

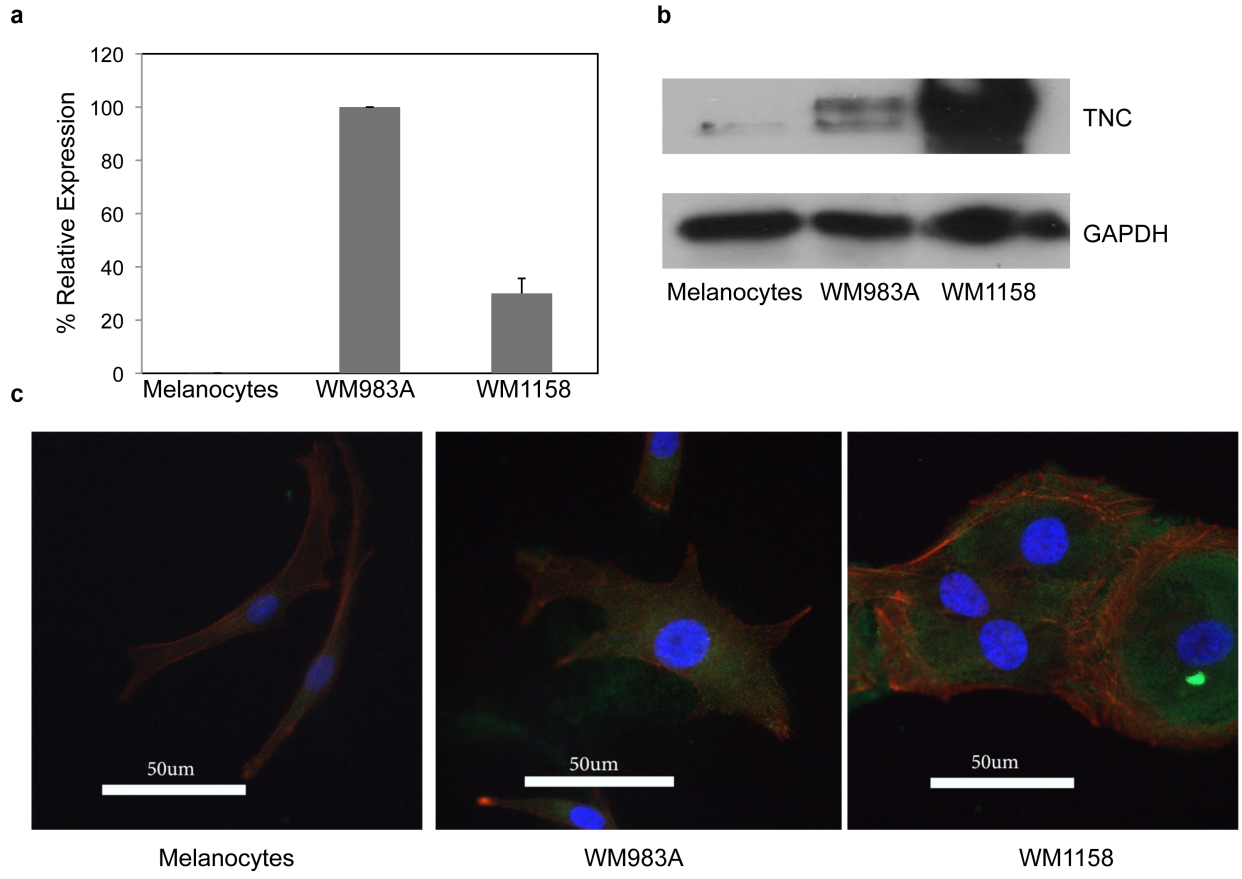

Figure 11. Expression of Tenascin C in melanoma cells.

(A) Quantitative RT-PCR analysis of the expression of Tenascin C (TNC) mRNA in WM983A (VGP) and WM1158 (MGP) melanoma cells compared to human melanocytes, propagated in vitro. The data are expressed as the mean (standard deviation from three independent experiments. (B) Immunoblot analysis depicting the level of TNC in the VGP and MGP melanoma cell lines and melanocytes. (C) Immunofluorescence analysis of melanocytes and VGP and MGP melanoma cell lines, probed with antibody to TNC (pseudocolored green) and actin (pseudocolored red). The cells were counterstained with fluorescent DAPI (pseudocolored blue).

α-Actinin-4 (ACN4) is another protein identified as differentially abundant between the SOC melanoma samples and controls. Furthermore, as depicted in Figure 12, this protein is clearly present at higher levels in melanoma cells compared to melanocytes, both at the level of the transcript and protein. α-Actinin-4 is an actin cytoskeleton filament bundling protein and plays crucial roles in cell migration and cytokinesis (Sjoblom et al., 2008). In addition, growth factor signaling is important for dynamic control of ACN4/actin filament interactions, which in turn regulates cell adhesion during substratum attachment and nuclear segregation during mitosis (Shao et al., 2009).

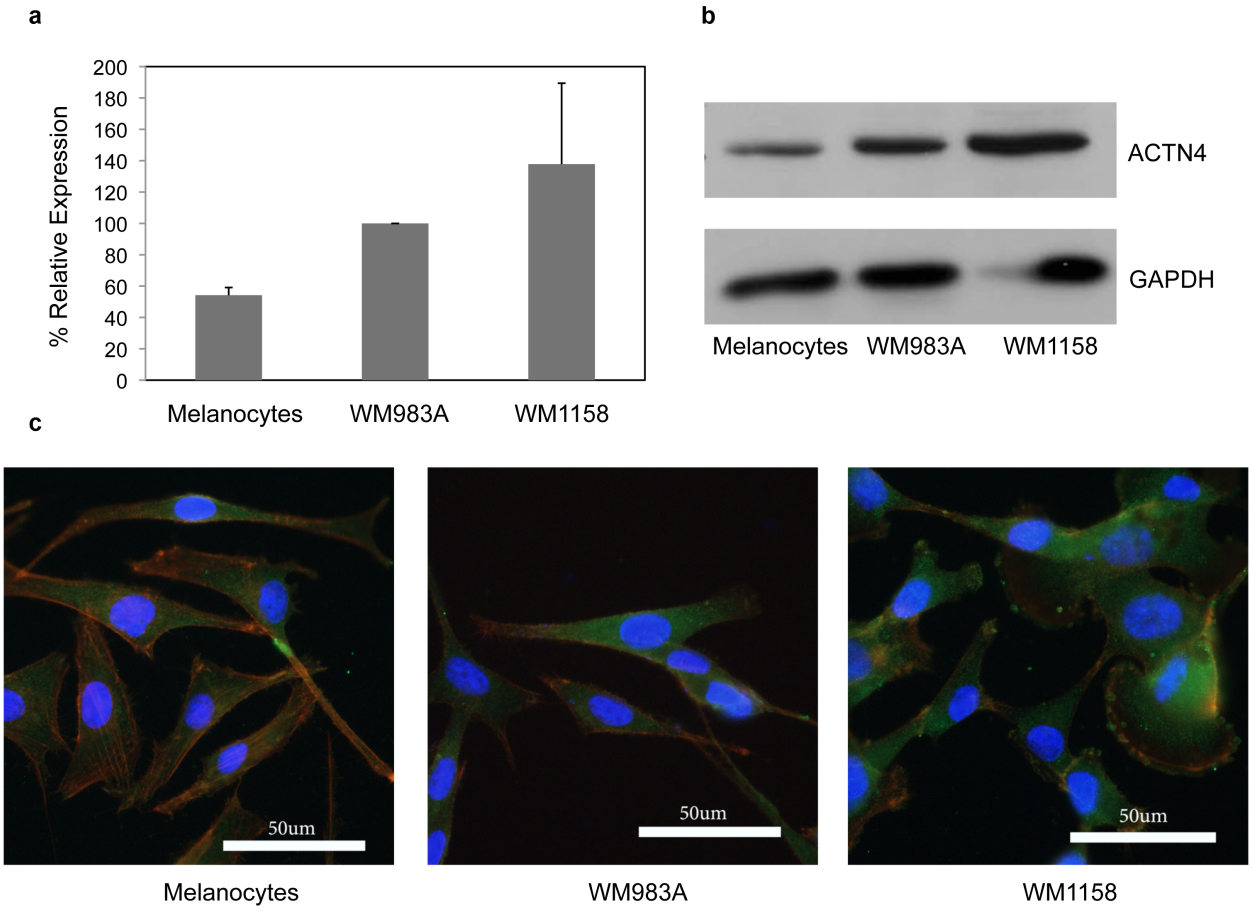

Figure 12. Alpha-actinin-4 expression in melanoma cells.

(A) Quantitative RT-PCR analysis of α-actinin-4 (ACN4) expression in the WM983A (VGP) and

WM1158 (MGP) melanoma cell lines and in melanocytes. The data are expressed as the mean (standard deviation from three independent experiments. (B) Immunoblot analysis of ACN4 expression in the VGP and MGP melanoma cell lines and in melanocytes. (C) Immunofluorescence analysis of melanocytes and VGP and MGP melanoma cell lines, probed with antibody to ACN4 (pseudocolored green) and actin (pseudocolored red). The cells were counterstained with fluorescent DAPI (pseudocolored blue).

The increased expression of both TNC and ACN4 was verified by immunohistochemistry (IHC) in WM983A injected SOCs in the region of the tumor lesion as compared to the collagen-injected controls (Fig. 13). As expected, TNC appears to be localized to the extracellular space (Fig. 13A) whereas ACN4 expression is primarily observed to be intracellular (Fig. 13C). While low levels of TNC can be observed in the collagen-injected SOC, this observation likely arises from the fact that these skin cultures are immature and composed of neonatal fibroblasts and keratinocytes, both of which produce TNC.

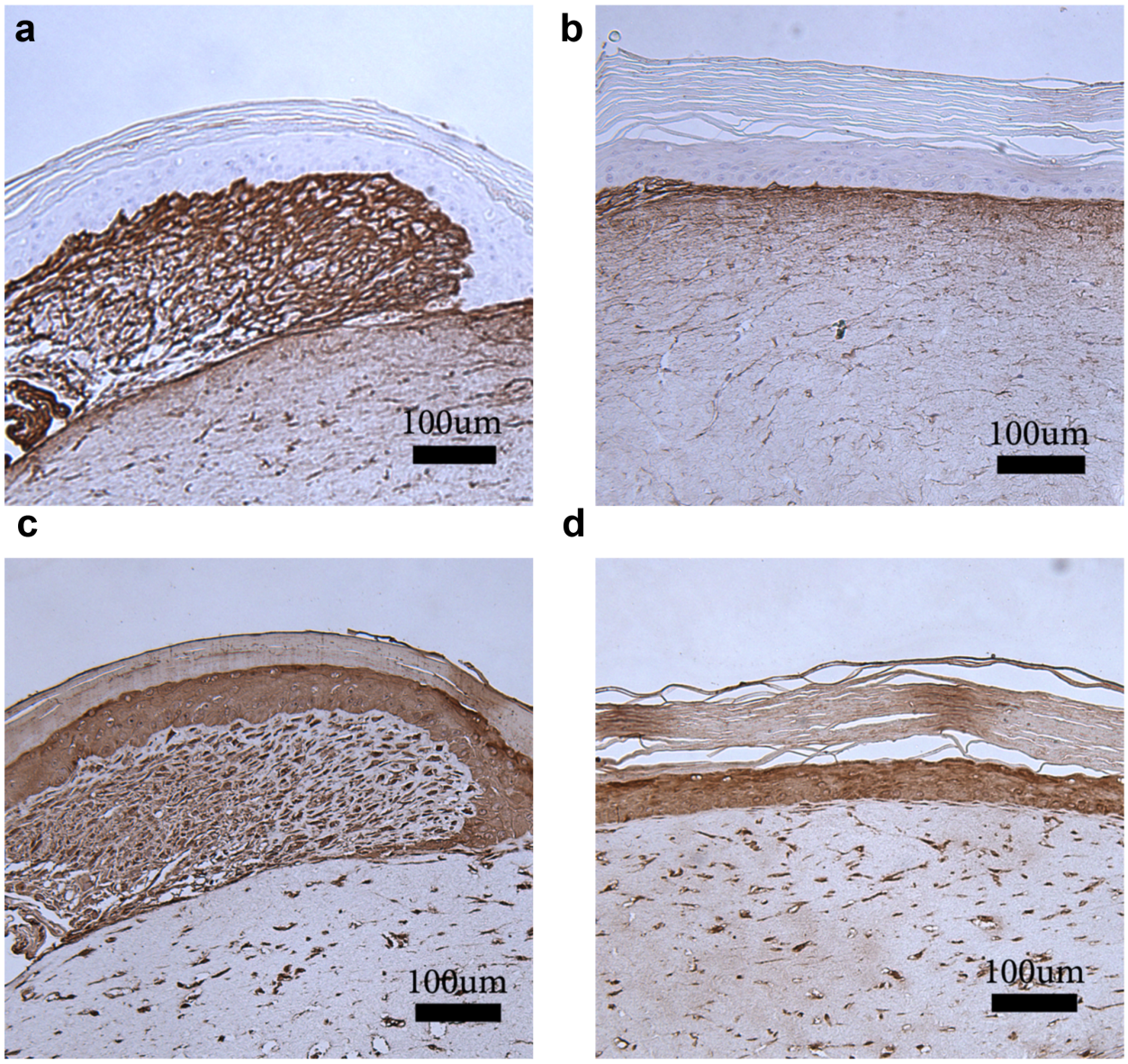

Figure 13. Immunohistochemical analysis of Tenascin C and α-actinin-4 in SOCs.

Immunohistochemical analysis of the expression of Tenascin C (TNC) (A and B) and α-actinin-4 (ACN4) (C and D) in SOCs injected with WM983A melanoma cells (A and C) compared to collagen injection controls (B and D).

Thrombospondin-1 (TSP-1) was identified with an elevated abundance in both the MGP and VGP SOC sections compared to the controls. TSP-1 is a secreted protein that plays a role in

tissue remodeling, is upregulated in response to injury and inflammation (Bornstein, 2001) and has been detected at elevated levels in sera of patients with advanced melanoma (Bornstein, 2009; Rofstad and Graff, 2001; Sid et al., 2004). Plectin was also substantially more abundant in the MGP melanoma cells than in the VGP melanoma cells. Plectin, a structural protein found in nearly every cell type, interacts with numerous cytoskeletal components and has a role in the interactions of intracellular junctions and contributes to tissue integrity (Svitkina et al., 1996; Wiche, 1989). Plectin has been shown to be upregulated in pancreatic and colon cancer (Bausch et al., 2009; Lee et al., 2004), but there are no reports that cite this protein as being expressed in advanced melanomas. Similar to Tenascin C and Fibronectin, Plectin was identified with an increased relative abundance in the melanoma tissue sample as compared to that of the normal skin sample.

Alpha-enolase and pyruvate kinase M2 were identified with elevated abundances in the MGP SOC section relative to the other SOC samples. Increased levels of α-enolase have been previously associated with tumor cell migration and metastasis (Liu and Shih, 2007) and have been shown to be elevated in several metastatic melanoma cell lines (Nawarak et al., 2009; Rodeck et al., 1991). This increased expression level of α-enolase and pyruvate kinase M2 may reflect the apparent increased utilization of glycolysis for ATP generation in tumor cells as suggested by Warburg (Warburg et al., 1970).

There are a number of notable proteins identified in the present study that merit further investigation. Of these, transgelin 2, a homolog of transgelin and member of a family of actin-binding proteins that is proposed to be involved in cytoskeletal cross-linking and polymerization, was identified in greater relative abundance in the MGP SOC tissue section as compared to the other samples. There are several reports citing an upregulation of transgelins in gastric (Huang et

al., 2008) and colorectal (Zhang et al., 2009) cancers. Transgelin has been shown to be involved with ERK-related signal transduction, however, the function of transgelin in cancer development and progression remains to be elucidated. The cytokeratin (CK) pairs 5/14 and 6/16 and 17 were observed with decreased abundances in the VGP SOC section. It is well known that cytokeratins play a significant role in the organization and integrity of cellular structure and are indicators for differentiation state and metastatic nature of tumor cells. A previous study established diminished expression levels of CK 5/14 and 6/16 and 17 in metastatic melanoma (Riker et al., 2008). The present analyses also reveal an apparent increase in the abundance of pulmonary surfactant protein D in the VGP SOC section. While its role in melanoma has not been fully explored, the gene encoding this protein has been shown to be induced in a variety of metastatic pulmonary and non-small cell lung cancers, and is detectable in a variety of others, such as gastric, pancreas and prostate (Betz et al., 1995).

2.4 CONCLUSIONS

The findings of these proteomic analyses establish the feasibility of using SOCs for evaluating the tumor microenvironment and the changes in the molecular events that drive invasion and progression of melanoma. Melanoma cell lines, representing VGP and MGP melanoma, injected into SOCs demonstrate the ability to perform a differential proteomic analysis using a spectral count approach and generation of proteomic profiles which very closely resemble those obtained from an analysis of differential protein abundances from melanoma and normal skin biopsy tissues. Indeed, several known melanoma-related proteins, such as Tenascin C and Fibronectin, were identified at different relative abundances in the SOCs, which directly

correspond to the abundance differences observed in the analysis of the tissue biopsy samples. These data suggest that melanoma-seeded SOCs represent a unique model system to gain further insight regarding proteins that support melanoma cell invasion and the crosstalk between melanoma cells and the skin microenvironment.

2.5 MATERIALS AND METHODS

2.5.1 Cell cultures and tissue samples

Normal human epidermal melanocytes (FC-0019, Lifeline Cell Technology, Walkersville, MD) were maintained in DermaLife Basal Medium with LifeFactors (LM-0027, Lifeline Cell Technology). The VGP (WM983A) and MGP (WM1158) human melanoma cell lines were propagated *in vitro* as described (Becker et al., 1989). De-identified, post-diagnosis, excess pathological specimens, representing an advanced melanoma and an adjacent skin biopsy with no clinical signs of melanoma, resected from a patient, were obtained in compliance with a University of Pittsburgh Cancer Institute (UPCI) and University of Pittsburgh Institutional Review Board (IRB)-approved protocol.

2.5.2 Antibodies and reagents

An anti-human/mouse Tenascin C monoclonal antibody (MAB2138) was purchased from R&D Systems (Minneapolis, MN), and mouse anti-α-actinin-4 antibody (sc-49333) was from Santa Cruz Biotechnology, Inc. (Santa Cruz, CA). Antibodies were used at a 1:200 dilution for

immunoblotting and immunocitochemistry. For immunohistochemistry stainings, anti-human Tensacin C mouse monoclonal antibody (ab6393) and anti-human/mouse α-actinin 4 antibody (ab32816, Abcam, Cambridge, MA) were used at the final concentration of 2 μg/ml.

2.5.3 Skin organ cultures

Skin organ culture experiments were performed on human Epiderm full-thickness 400 (EFT-400) 3D skin-like structures obtained from MatTek Corporation (Ashland, MA). These constructs contain human-derived dermal fibroblasts and epidermal keratinocytes and utilize bovine collagen as the base for the dermal matrix. Cultures were maintained at the air-liquid interface and supplied every other day with maintenance medium (EFT-400-MM, MatTek). Cultures were injected intra-epidermaly with 10,000 melanoma cells (either WM983A or WM1158) resuspended in 3 μg/mL rat tail collagen (R&D Systems). Collagen-injection and non-injected SOCs served as controls. On day 13 after injection, tissues were divided in half with a razor; one half was formalin-fixed and paraffin-embedded, and the other half was embedded in OCT and frozen in liquid nitrogen. This time point was chosen based on previous reports as sufficient time for growth of tumor-like structures within the SOC (Eves et al., 2000; Meier et al., 2000a). Furthermore, the SOC maintain structural integrity for throughout this time period but begin to degenerate upon further culture. Cells from defined regions were acquired by laser micro-dissection (Leica LMD 6000, Leica Microsystems, Inc., Bannockburn, IL) and collected in 40 μL of purified H_2O in RNAase/DNAse-free microcentrifuge tubes.

2.5.4 FFPE sample preparation

Samples were brought to 100 mM NH_4HCO_3, pH 8.4, 60% acetonitrile and incubated in a thermal cycler at 100 °C for 1 h, and thereafter at 65 °C for an additional 2 h. Samples were cooled to ambient temperature, followed by addition of 100 ng of modified porcine sequencing grade trypsin (Promega) and incubated for 16 h at 37 °C. Samples were vacuum-dried and desalted using PepClean desalting columns (Pierce) according to the manufacturer's protocol. Eluted peptides were vacuum-dried and stored at -80 °C.

2.5.5 Human melanoma biopsy sample preparation

Cryopreserved melanoma and human skin samples were placed in a Petri dish containing phosphate-buffered saline (PBS) on wet ice and cut into small pieces with a scalpel. Tissues were transferred to microcentrifuge tubes, homogenized for 10 s, snap-frozen in liquid nitrogen and brought to ambient temperature. Tissue lysates were sonicated for 15 sec (50 Hz) and supernatant was collected by centrifugation (2000 x *g*, 10 min). Fifty μg of each protein lysate was resolved by 1D SDS-PAGE and each lane was cut into ten equivalent slices that were digested in-gel according to established protocols.(Wilm et al., 1996) Briefly, gel bands were destained in 50% acetonitrile in 50 mM NH_4HCO_3, pH 8.4 and vacuum-dried. Trypsin (20 μg/mL in 25 mM NH_4HCO_3, pH 8.4) was added and samples were incubated on wet ice for 45 min. The supernatant was removed and gel bands were covered with 25 mM NH_4HCO_3, pH 8.4 and incubated at 37 °C overnight. Tryptic peptides were extracted with 70% acetonitrile, 5% formic acid, lyophilized to dryness and resuspended in 0.1% trifluoroacetic acid (TFA) prior to LC-MS/MS analysis.

2.5.6 Mass spectrometry analyses

Skin organ culture tryptic digests were analyzed in duplicate by nanoflow reversed-phase liquid chromatography (LC)-MS/MS using a nanoflow LC (Dionex Ultimate 3000, Dionex Corporation, Sunnyvale, CA) coupled online to a linear ion trap MS (LTQ-XL, ThermoFisher Scientific, San Jose, CA). Human biopsy tissue tryptic digests were similarly analyzed on an LTQ-Orbitrap MS (ThermoFisher). Separations were performed using 75 μm i.d. x 360 o.d. x 15 cm long fused silica capillary columns (Polymicro Technologies, Phoenix, AZ) slurry packed in house with 5 μm, 300 Å pore size C-18 silica-bonded stationary phase (Jupiter, Phenomenex, Torrance, CA).

Following sample injection onto a C-18 trap column (Dionex), the column was washed for 3 min with mobile phase A (2% acetonitrile, 0.1% formic acid) at a flow rate of 30 μL/min. Peptides from the SOC tissue sections were eluted using a linear gradient of 0.33% mobile phase B (0.1% formic acid in acetonitrile)/minute for 130 min, then to 95% B in an additional 15 min, all at a constant flow rate of 200 nL/min. In the case of the melanoma and skin tissue samples, peptides were eluted using a linear gradient of 1% mobile phase B/minute for 40 min, then to 95% B in an additional 10 min, all at a constant flow rate of 200 nL/min. Column washing was performed at 95% B for 15 min for all analyses, after which the column was re-equilibrated in mobile phase A prior to subsequent injections.

For the SOC analyses, the MS was operated in data-dependent MS/MS mode in which each full MS scan was followed by seven MS/MS scans performed in the linear ion trap (LIT) where the seven most abundant peptide molecular ions were selected for collision-induced dissociation (CID), using a normalized collision energy of 35%. The human melanoma and normal skin tissue digests were analyzed using a high resolution (R=60,000 at *m/z* 400) full MS

scan conducted in the Orbitrap followed by tandem MS of the top five molecular ions in the LIT as described above. Data were collected over a broad precursor ion selection scan range of *m/z* 375-1800 for the SOC analysis and *m/*z 350-1800 for the analysis of the human tissue samples. Dynamic exclusion was enabled for both MS analyses to minimize redundant selection of peptides previously selected for CID.

2.5.7 Bioinformatic analysis

Tandem mass spectra were searched against the UniProt human protein database (11/09 release) from the European Bioinformatics Institute (http://www.ebi.ac.uk/integr8), using SEQUEST (ThermoFisher Scientific). Additionally, peptides were searched for methionine oxidation with a mass addition of 15.9949 Da. Peptides were considered legitimately identified if they met specific charge state and proteolytic cleavage-dependent cross correlation scores of 1.9 for $[M+H]^{1+}$, 2.2 for $[M+2H]^{2+}$ and 3.5 for $[M+3H]^{3+}$, and a minimum delta correlation of 0.08. A false peptide discovery rate of approximately 2% was determined by searching the primary tandem MS data using the same criteria against a decoy database wherein the protein sequences are reversed (Elias and Gygi, 2007). Results were further filtered using software developed in-house, and differences in protein abundance between the samples were derived by summing the total CID events that resulted in a positively identified peptide for a given protein accession across all samples (spectral counting) (Liu et al., 2004). The spectral count data were normalized for each protein accession by calculating the percent contribution of the spectral count values for each protein accession against the total number of peptides identified within a given sample (Patel et al., 2008).

2.5.8 Real-time PCR

Total mRNA from the melanocytes and melanoma cell lines was isolated using an RNAeasy Mini Kit (Qiagen, Valencia, CA), and 1 μg of mRNA was reverse-transcribed into the corresponding first-strand cDNA with the Quantitect Transcription Kit (Qiagen). PCR reactions were performed on a MX3000P Real-Time PCR instrument (Stratagene, Agilent Technologies, Santa Clara, CA), using 1 μl of first-strand cDNA per reaction with Brilliant SYBR Green QPCR Master Mix (Stratagene). Primers (Integrated DNA Technologies, Coralville, IA) are listed in the Table 2:

Table 2. Primers used in real time PCR

cDNA	Sequence of primers
Tenascin C	
Forward	5'-GAGGTCAACAAAGTGGAGGCA-3'
Reverse	5'-GAGAGATTGAAGCTCTCGGGAG-3'
α-Actinin-4	
Forward	5'-CATATCAGGGGAGCGGTT-3'
Reverse	5'-GCAATAAAGTCCAGCGCT-3'
GAPDH	
Forward	5'-GAGTCAACGGATTTGGTCGT-3'
Reverse	5'-TTCATTTTGGAGGGATCTCG-3'

All experiments were performed in triplicate, fold-abundance changes in transcript levels were quantified by the ΔCt method and target gene expression was normalized to GAPDH. The VGP melanoma cell line, WM983A, was used as a reference.

2.5.9 Immunoblotting and Immunostaining

Cell lysates were obtained by snap-freezing, thawing, and vortexing in lysis buffer (50 mM Hepes, pH 7.9, 0.4 M KCl, 0.5 mM EDTA, 0.1% NP-40, 10% glycerol) supplemented with 1 mM sodium orthovanadate, 50 mM sodium fluoride and protease inhibitor cocktail set V (Calbiochem, EMD Chemicals, Gibbstown, NJ). Protein concentrations were determined by the BCA assay (Pierce, Rockford, IL), and 100 μg of total protein per sample was resolved by 1D SDS-PAGE. Samples were transferred to PVDF membranes (Millipore, Billerica, MA), blocked with 5% milk in PBST and incubated with primary antibody overnight at 4 °C. Secondary antibody was added for 1 h at ambient temperature and blots were detected with SuperSignal West Pico Chemiluminescent Substrate (Pierce).

Normal human melanocytes, and likewise melanoma cells, were seeded on glass coverslips and fixed with 2% formaldehyde for 30 min at ambient temperature. After washing with PBS, cells were treated for 5 min with 0.2% Triton-X on wet ice and blocked with 5% goat serum for 30 min at ambient temperature. Incubation with anti-tenascin-C diluted in 1% goat serum was performed for 2 h at ambient temperature. After washing extensively with PBS, secondary goat anti-mouse 488-Alexa Fluor antibody (Molecular Probes, Invitrogen) was added for 1 h. Actin fibers were stained with rhodamin phalloidin (Invitrogen) for 40 min at ambient temperature and nuclei were stained with DAPI. Slides were mounted and images were acquired with a 60X objective using an Olympus BX-40 microscope.

2.5.10 Immunohistochemistry in SOCs

5μm sections of paraffin embedded specimens were cut, transferred to poly-L-lysine coated slides and deparaffinized 2 hours at 58°C. Slides were then dewaxed in xylene, rehydrated in series of desending grades of alchocol and washed with deionized water. Antigens were retrieved for 15 min in 1% pepsin in 10mM HCl for TNC staining or heat induced for 20min in citrate biffer pH6 (Dako, Carpinteria, CA) for ACN-4 staining. Endogenous peroxidase was blocked with 3% H_2O_2, and sections were then incubated in 5% goat serum to decrease background staining. Sections were incubated with primary antibodies for 2h in humified chamber in 37°C incubator, washed and incubated with biotinilated secondary goat anti-mouse antibody (Jackson ImmunoResearch, West Grove, PA) at 1:250 dillution. Vectastatin ABC kit (PK-6100) and DAB peroxidase kit (SK-4100) were both form Vector Laboratories (Burlingame, CA). Slides were counter stained with Meyer's hematoxylin (Vector Laboratories), dehydrated and mounted with Permount solution (Fisher Scientific, Pittsburgh, PA). Images were acquired with a 10X objective using Olympus BX-40 microscope and SPOT imaging software (Sterling Heights, MI).

2.6 SUPPORTING INFORMATION

The complete list of peptides/proteins, identified in the various SOC sections and the melanoma and skin tissue samples are listed in Appendix A (Global protein and peptide results for the skin organ construct FFPE tissue samples (Tabs 1 and 2 respectively) and biopsy tissue

sample (Tabs 3 and 4 respectively) analyses. Xcorr, Sequest cross correlation score; DeltaCn, Sequest delta correlation score.).

2.7 ACKNOWLEDGMENTS

The David Scaife Foundation (TPC) supported this work, in-kind contributions from the Pittsburgh VA HealthCare System (AW) and a grant from the National Institutes of Health (DB). The authors would like to thank Dr Zhou Wang for the use of the laser microscope, Diane George for technical assistance and the helpful advice from the two anonymous reviewers.

3.0 MELANOMA CELL INVASIVENES IS PROMOTED AT LEAST IN PART BY THE EPIDEMAL GROWTH FACTOR-LIKE REPEATS OF TENASCIN C

Jelena Grahovac, Dorothea Becker and Alan Wells

Department of Pathology, University of Pittsburgh and Pittsburgh VAMC, Pittsburgh PA, 15217 USA

This work was published in the Journal of Investigative Dermatology, 2012.

3.1 ABSTRACT

Tenascin C (TNC), overexpressed in invasive growths, has been implicated in progression of melanoma but the source and function of this molecule are not well defined. We found TNC expression at the front of invading melanoma cells, and that adding TNC to matrices enhances individual melanoma cell migration. As TNC is a multidomain protein, we examined the role of the TNC EGF-like repeats (EGFL) as these activate motogenic signaling cascades. We overexpressed a TNC fragment containing the assembly and EGFL domains of TNC (TNCEGFL). TNCEGFL-expressing melanoma cells had lower speed and persistence in 2D migration assays due to a shift in the adhesion-contractility balance, as expression of TNCEGFL delayed melanoma cell attachment and spreading. The less adhesive phenotype was due, in part, to increased ROCK signaling concomitant with MLC2 and MYPT phosphorylation. Inhibition of ROCK activity, which drives transcellular contractility, restored adhesion of TNCEGFL expressing melanoma cells and increased their migration in 2D. In contrast to the diminished migration in 2D, TNCEGFL-expressing melanoma cells had higher invasive potential in Matrigel invasion assays, with cells expressing TNCEGFL having amoeboid morphology. Our findings suggest that melanoma-derived TNC EGFL play a role in melanoma invasion by modulating ROCK signaling and cell migration.

3.2 INTRODUCTION

Melanoma, which continues to increase in frequency, has a very low response rate to current therapies, with the tumor invading through a collagen-rich dermis to disseminate to ectopic sites. The transition from melanoma *in situ* and radial growth phase (RGP) to the vertical growth phase (VGP) melanoma is poorly understood. The invasive aspects of tumor progression represent complex molecular events, which involve recognition and remodeling of extracellular matrix (ECM), changes in intracellular signaling and reorganization of the cytoskeleton, allowing for enhanced motility of tumor cells (Friedl and Gilmour, 2009; Wells, 2000). While there are numerous changes in both the melanoma cells and the dermis during this progression, one striking feature is the re-expression of Tenascin C (TNC) (Hood et al., 2010; Ilmonen et al., 2004; Kaariainen et al., 2006). TNC is an extracellular matrix protein linked to development and tissue regeneration along with tumor invasion (Jones and Jones, 2000b; Midwood et al., 2011). TNC is barely detectable in normal skin, but present in substantial amounts in advanced melanoma particularly at the invasive fronts and lack of detectable TNC in primary melanoma lesions has been shown to correlate with a lower risk of developing metastases (Kaariainen et al., 2006). In the tumor microenvironment, TNC is produced by both transformed tumor cells and stromal cells (De Wever et al., 2004; Hanamura et al., 1997; Yoshida et al., 1997) and *in vitro,* the majority of human melanoma cell lines secrete TNC (Herlyn et al., 1991). Thus, an open question remains of whether the TNC expressed by the melanoma cells can drive tumor cell invasion.

TNC is a hexameric protein composed of 180 to 320 kDa monomers, which are disulfide linked at the N-termini. Each subunit contains: a globular N-terminal assembly domain, a

domain composed of 14.5 Epidermal Growth Factor-like (EGFL) repeats, a domain composed of fibronectin type III-like (FNIII) repeats, and a fibrinogen-like sequence on the C terminus (Aukhil et al., 1993), and each domain has a potentially distinct role (Jones and Jones, 2000b). Tenascin C has been shown to modulate many of the processes involved in cell migration and invasion (reviewed in (Orend, 2005; Orend and Chiquet-Ehrismann, 2006). The majority of cancer cell lines fail to attach on TNC coated surfaces (Huang et al., 2001), with some exceptions where TNC is adhesive (Paron et al., 2011), while endothelial cells attach and spread on TNC (Sriramarao et al., 1993). In addition, soluble and substratum-adsorbed TNC have distinct effects on cell adhesion and proliferation (Orend and Chiquet-Ehrismann, 2000). These seemingly discrepant findings are in part traceable to the different signaling propensities of the multiple domains of TNC being impacted by the presence of other matrix components and the potentially differential effects of signals in two- versus three-dimensions.

We have previously reported that distinct EGFL repeats of TNC bind and signal through the EGF receptor in a novel manner as ultra low affinity/high avidity ligands (Iyer et al., 2007a; Swindle et al., 2001). The 'staccato' nature of the individual EGFL repeat binding to the receptor results in an anti-adhesive phenotype that must be balanced by the adhesive matrix proteins or even the fibronectin-like repeats of TNC. In the presence of adequate pro-adhesive moieties, these EGFL repeats restrict signaling to the plasma membrane and preferentially activate a motogenic signaling cascade (Iyer et al., 2008). As little is known about TNC matrikine role in melanoma we tested the role of EGFL repeats in melanoma motility and invasion. Herein we report that TNC promotes melanoma cell invasion and that this activity can be localized to the EGFL repeats.

3.3 RESULTS

3.3.1 Advanced melanoma cell lines express TNC and increase migration in response to exogenous TNC

In melanoma, TNC is present at high concentrations in the dermal matrix having increased from negligible levels in normal dermis (Hood et al., 2010; Kaariainen et al., 2006; Tuominen and Kallioinen, 1994). We examined TNC expression in human melanoma tissue microarray with the antibody specific for the EGFL repeats of Tenascin C (ab6393) and observed that it's expression increases with melanoma progression (Figure 14A). To test whether melanoma cell derived TNC could be involved in dissemination we first examined expression levels in three melanoma cell lines derived from different stages. The WM35 cells derived from superficial spreading melanoma (RGP/VGP) expressed little if any TNC, similar to human melanocytes (Hood et al., 2010), while VGP WM983A cells and metastatic growth phase (MGP) cells derived from the same patient WM983B expressed high levels of TNC (Figure 14B). This TNC was incorporated into the cell-generated matrix in the extracellular space and, of greater interest, the melanoma-derived TNC was being secreted asymmetrically at the front of the invading melanoma cells, as observed by confocal microscopy during the invasion of a Matrigel matrix (Figure 14C and D). In fact, we found that invasiveness of the three melanoma cell lines directly correlated to the TNC expression levels (R^2=0.83) (Figure 14E). These data strongly suggest a role for TNC, derived from the melanoma itself as driving transmigration.

As motility is a predictive aspect of tumor invasion (Kassis et al., 2001; Wells, 2000) and consistent with reports of TNC being motogenic (Chung et al., 1996; Iyer et al., 2008; Nishio et al., 2005; Paron et al., 2011; Swindle et al., 2001), melanoma cell lines expressing higher levels

of TNC migrated faster in live cell tracking experiments and had greater directional persistence, as measured by cell track straightness (Figure 14F, white bars). That the increase in cell speed was due to the TNC incorporated into the substratum was shown by adding TNC to the Collagen-I coating on tissue culture dishes; this further increased melanoma migration of all three cell lines tested (Figure 14F, gray bars). Additionally, there was high correlation (R^2=0.99) between levels of TNC being expressed by melanoma cells, but not with exogenously added TNC, and cell track straightness. Cell track straightness is a measure of directionality of cell movement and is a ratio between displacement of a cell and the track length for a set period of time implying a directional component to the endogenously expressed TNC. These data suggest that both endogenously produced and exogenously presented TNC contribute to melanoma migration, but that the cells asymmetrically place the endogenously produced TNC to promote directional translocation.

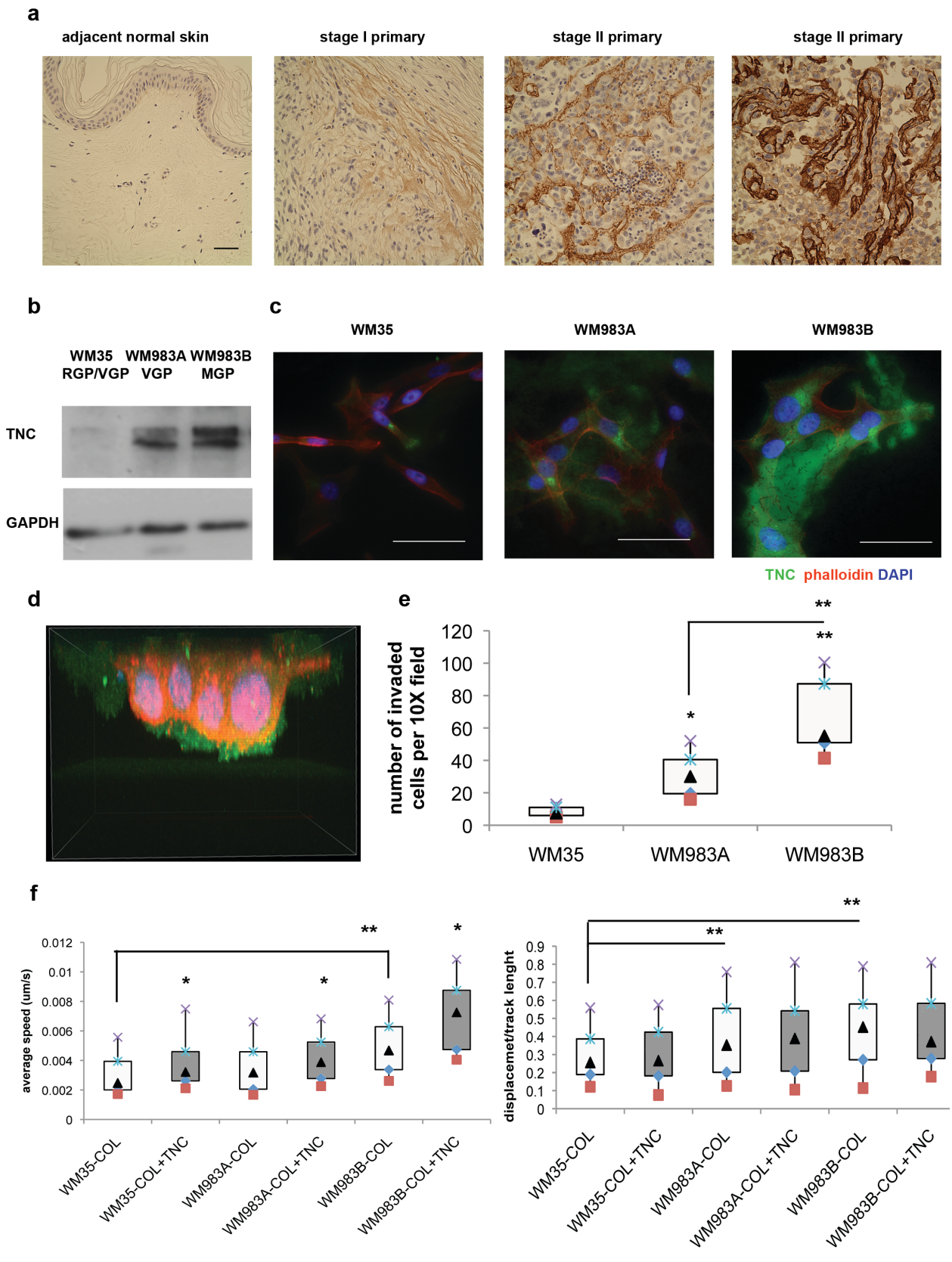
a
adjacent normal skin
stage I primary
stage II primary
stage II primary
b
WM35 RGP/VGP
WM983A VGP
WM983B MGP
TNC
GAPDH
c
WM35
WM983A
WM983B
TNC phalloidin DAPI
d
e
number of invaded cells per 10X field
120
100
80
60
40
20
0
WM35
WM983A
WM983B
f
average speed (um/s)
0.012
0.01
0.008
0.006
0.004
0.002
0
displacemet/track lenght
0.9
0.8
0.7
0.6
0.5
0.4
0.3
0.2
0.1
0
WM35-COL
WM35-COL+TNC
WM983A-COL
WM983A-COL+TNC
WM983B-COL
WM983B-COL+TNC

Figure 14. Expression of TNC in human melanoma samples and cell lines and its influence on melanoma cell invasion and migration.

*(A) TMA (tissue micro-array) stained with the antibody recognizing EGFL repeats of TNC (ab6393) (brown) and counterstained with hematoxylin. Scale bar 50μm. Shown are representative primary tumor samples. (B) Immunoblot and (C) immunostaining analyses show increased TNC protein expression and extracellular deposition in VGP and MGP phase melanoma cell lines compared to a cell line derived from superficially spreading melanoma. Scale bars are 50μm. Images are representative of at least three independent experiments. (D) During invasion in Matrigel, TNC is deposited at the fronts of WM983A cells. The size of the 3D model is: width 83μm, height 85μm, depth 63μm. (E) Melanoma cell lines expressing higher amounts of TNC invade to a greater extent in Matrigel invasion assays (R^2=0.83). Shown is the mean ± SD of three experiments. (F) Melanoma cell speed (left panel) increases on surfaces coated with Collagen I -Tenascin C mixture compared to Collagen I alone, while cell track straightness (displacement divided by total track length, right panel) correlates with the levels of endogenous TNC expression (R^2=0.99) but does not change upon exogenous addition of TNC. Box and whisker plots summarize average from three independent experiments, N > 50 tracks per treatment in repeated experiments. *p < 0.05, ** p < 0.01 (box encompasses 25-75%, with bars 10 (square)-90 (X)%, median is the triangle).*

3.3.2 TNCEGFL expression impairs migration of melanoma cells in 2D

TNC is distinguished from most of the other Tenascin family members by the inclusion and/or extent of the EGF-like repeat region. We have reported that at least some of these EGFL repeats function as cryptic growth factors that preferentially promote motility (Iyer et al., 2007a;

Swindle et al., 2001). As multivalent concatamers of EGF-like repeats are difficult to synthesize and pose challenges to incorporating into matrices, we over-expressed the Tenascin C EGF-like repeats transcript in the WM983A cell line (WM983A-TNCEGFL), a cell line already expressing substantial amounts of endogenous full length TNC, but responding to additional exogenous TNC (Figure 14). A vertical growth phase melanoma cell line was chosen as a model system as an intermediate phenotype of the cell lines tested regarding motility in 2D and 3D assays, so that changes in both directions can be observed. The TNCEGFL monomer ran in PAGE analyses at the predicted size of 69kDa and, as assessed under non-reducing conditions, assembled in polymers with the endogenous full length TNC (Figure 15A). Staining with antibody that recognized the EGFL repeats (MAB2138, R&D Systems) revealed that TNCEGFL formed punctuated extracellular network, compared to WM983A cells transfected with an empty vector (WM983A-EV), which formed prominent fibrilar TNC mesh, supporting the role of TNC FN repeats in organization of TNC extracellular network (Ramos et al., 1998) (Figures 15B, lower panel and 18B). Interestingly, while WM983A-EV cells arranged themselves in a distributed mesh, the WM983A-TNCEGFL cells aligned to form cords (Figure 15B, upper panel).

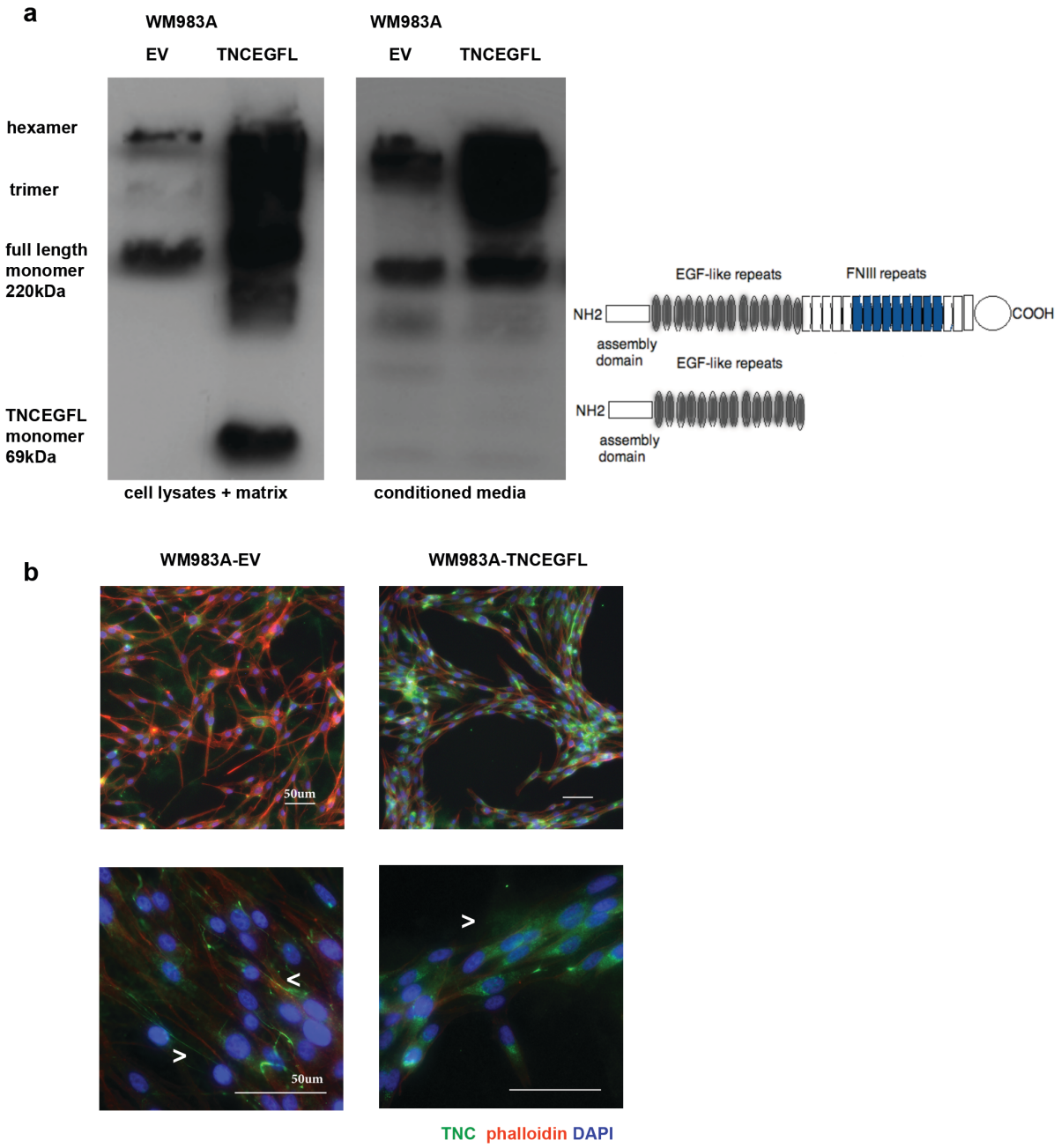

Figure 15. Expression of TNCEGFL in WM983A cell line.

(A) Immunoblotting of TNC under non-reducing conditions with the antibody recognizing EGFL repeats (R&D Systems): whole cell lysates and matrix are shown in the left and conditioned

melanoma media are in the right. Graphic depiction of the full length TNC and TNCEGFL construct is provided. (B) Immunostaining of TNC: endogenous TNC forms fibrilar mesh in the ECM while TNCEGFL is punctuate (lower panel 60X, arrow heads point to the TNC fibers and punctae, respectively), WM983A-TNCEGFL forms organized cords compared to unorganized WM983A-EV cell distribution (upper panel 20X). Scale bars 50μm.

Of interest, and unexpectedly, WM983A-TNCEGFL cells migrated significantly slower in a 2D wound healing assay that measures directional collective 2D migration (Figure 16A) and presented individually at a significantly reduced average speed in live cell tracking experiments (3.9 nm/s) compared to WM983A-EV cells (4.5 nm/s) (Figure 16B). Moreover, cell track straightness was significantly reduced (Figure 16B right panel) in WM983A-TNCEGFL cells, suggesting that the loss in cell movement directionality in 2D is contributing to decrease in collective cell migration. The phenotype was confirmed in WM35 cell line, which expresses little if any endogenous TNC. Upon transient expression of either full length TNC or TNCEGFL average cell speed and cell track straightness significantly decreased in 2D live cell tracking experiments with the TNCEGFL cells migrating the slowest (Figure 17). This confirms the

findings with the over-expression of TNC constructs in the invasive melanoma cells.

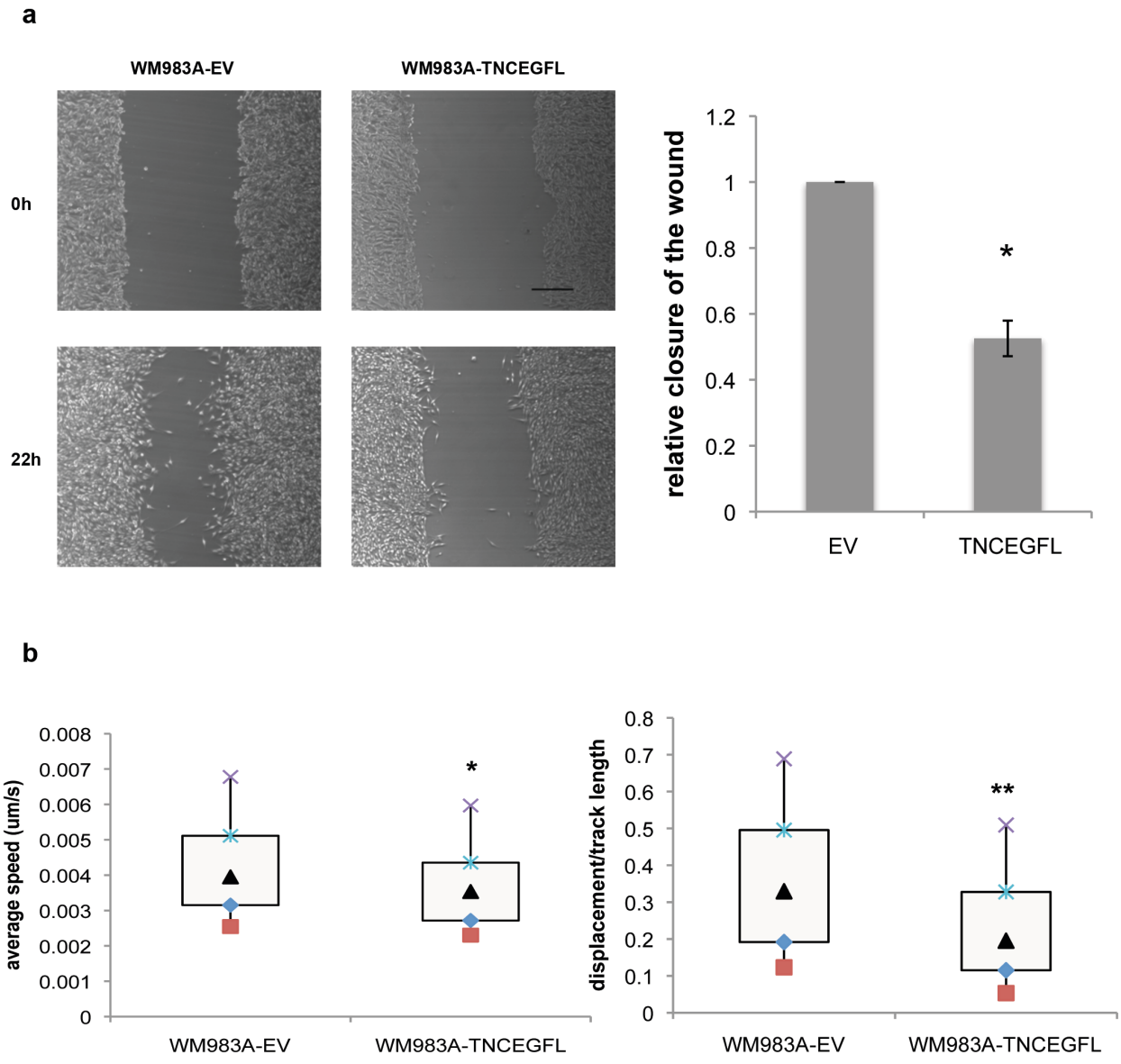

Figure 16. WM983A-TNCEGFL cells present impaired 2D cell migration.

(A) WM983A-TNCEGFL cells migrate significantly slower in wound healing assays. Scale bar 200µm. The graph shows mean ± SEM of three experiments each in triplicate. (B) Individual cell speed and track straightness of WM983A-TNCEGFL cells are significantly

*decreased compared to WM983A-EV cells. N > 50 tracks per phenotype (box encompasses 25-75%, with bars 10%-90%, median is the triangle). * p < 0.05, ** p < 0.01.*

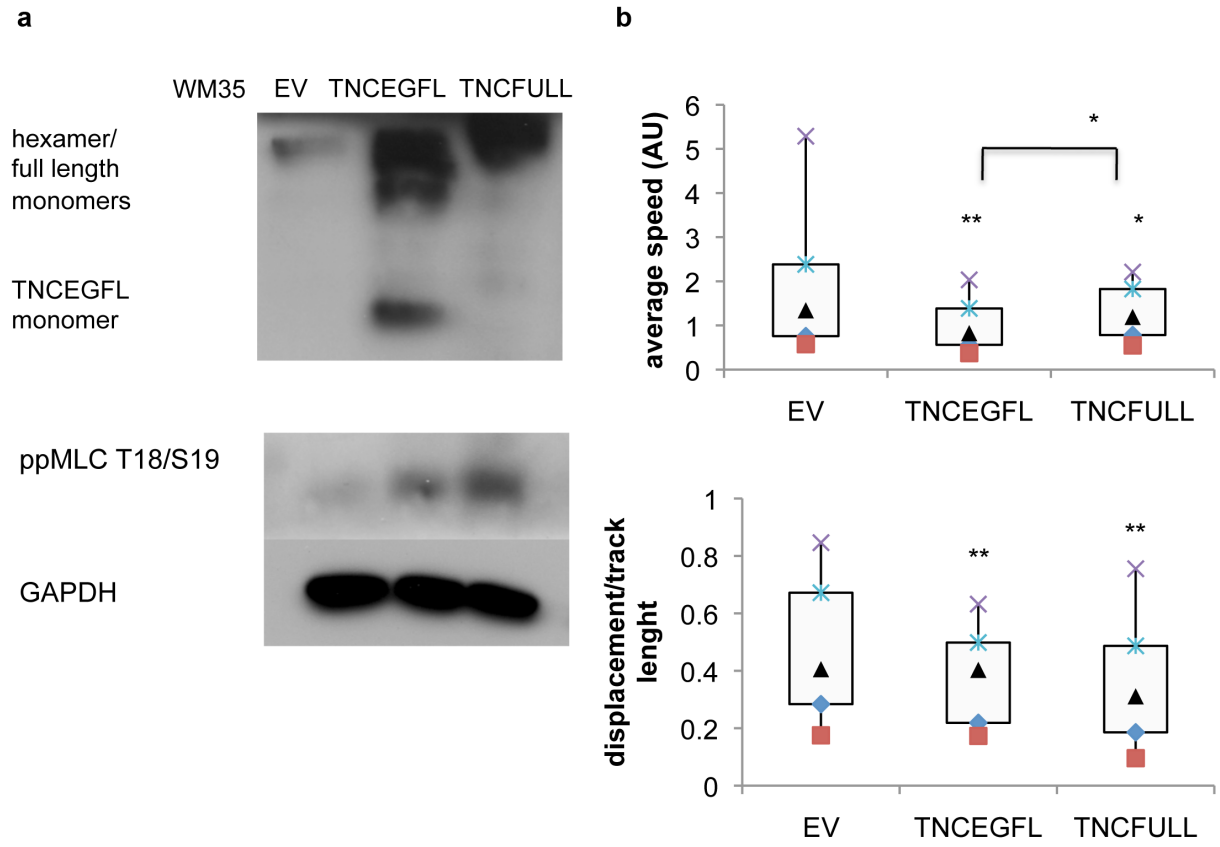

Figure 17. Expression of TNCFULL or TNCEGFL impairs WM35 cell migration.

(A) Immunoblotting of TNC under non-reducing conditions with the antibody recognizing EGFL repeats (R&D Systems) and ppMLC: whole cell lysates and matrix at the end of live cell tracking experiment; increased ppMLC in cells transfected with TNC constructs. Intensities of protein bands were determined by integrating optical density over the band area

*using Image J software, normalized to the GAPDH levels and divided by the lane 1. (B) Individual cell speed and track straightness of WM35 cells transfected with TNCFULL or TNCEGFL are significantly decreased compared to WM35-EV cells. N > 50 tracks per phenotype. * $p < 0.05$, ** $p < 0.01$. TNCEGFL expressing cells have more severe phenotype than TNCFULL.*

3.3.3 TNCEGFL expression impairs melanoma cell attachment

Migration speed in 2D results from a balance in adhesion and contractility in a biphasic manner (DiMilla et al., 1991; DiMilla et al., 1993; Lauffenburger and Horwitz, 1996). Decrease in adhesiveness could alter the cell speed in increasing or decreasing manner, depending on the initial adhesiveness to substratum. Examining this aspect, we found that TNCEGFL expressing cells were slower to adhere to and spread on substrata (Figure 18A). In cell spreading assays, TNCEGFL expressing cells started spreading with a 4h lag compared to cells expressing an empty pcDNA3.1 vector (Figure 18A). Furthermore, attachment of WM983A cells was inversely correlated to the amount of TNCEGFL repeats being expressed (Figures 18A and B). While over-expression of the full length of TNC (TNCFULL) did not impair cell attachment, expression of the EGFL repeats suppressed attachment in dose dependent manner. This phenotype was intrinsic as the difference in cell spreading and migration between WM983A-TNCEGFL and WM983A-EV persisted on plastic culture dishes or Fibronectin-1 coated surfaces (Figure 19). The difference in adhesiveness was not likely due to altered attachment proteins as the integrin profile of the TNCEGFL-expressing cell line remained the same as the one transfected with an empty vector, as determined by PCR Array (SABiosciences, PAHS-013A) (Table 3) nor was this an artifact of cell death as 48 hours post plating there were equal

cell numbers (Figure 18B). The reduced adhesion and spreading were due to an anti-adhesive phenotype of the EGFL repeats, as quantified in inverted centrifugation assays. Adherent WM983A-TNCEGFL cells detached to a greater extent when subjected to centrifugal force than WM983A-EV cells (Figure 18C).

Table 3. Integrin profiles of WM983A-EV and WM983A-TNCEGFL cell lines determined by PCR array

gene symbol	WM983A-TNCEGFL Ct	WM983A-EV Ct	fold change
ITGA1	25.60	26.23	1.34
ITGA2	28.35	29.09	1.45
ITGA3	25.85	25.87	0.88
ITGA4	21.79	22.03	1.03
ITGA5	25.92	25.40	0.61
ITGA6	20.59	20.59	0.87
ITGA7	30.17	30.58	1.16
ITGA8	35.00	35.00	0.87
ITGAL	34.60	34.81	1.01
ITGAM	32.18	35.00	6.14
ITGAV	22.20	21.86	0.67
ITGB1	20.05	20.14	0.93
ITGB2	33.03	35.00	3.41
ITGB3	25.83	26.14	1.08

ITGB4	34.74	34.18	0.59
ITGB5	25.15	25.95	1.51
HPRT1	22.04	21.83	
RPL13A	19.21	18.89	
GAPDH	17.24	16.99	
ACTB	14.33	15.34	

* The grey shaded genes' average threshold cycle is relatively high (> 30), meaning that its relative expression level is quite low and thus quantitation is difficult, in both control and test samples, and thus, fold changes while in two seemingly significant, are likely biologically irrelevant. All other changes for mRNA that are present at readily measurable levels are not statistically significant.

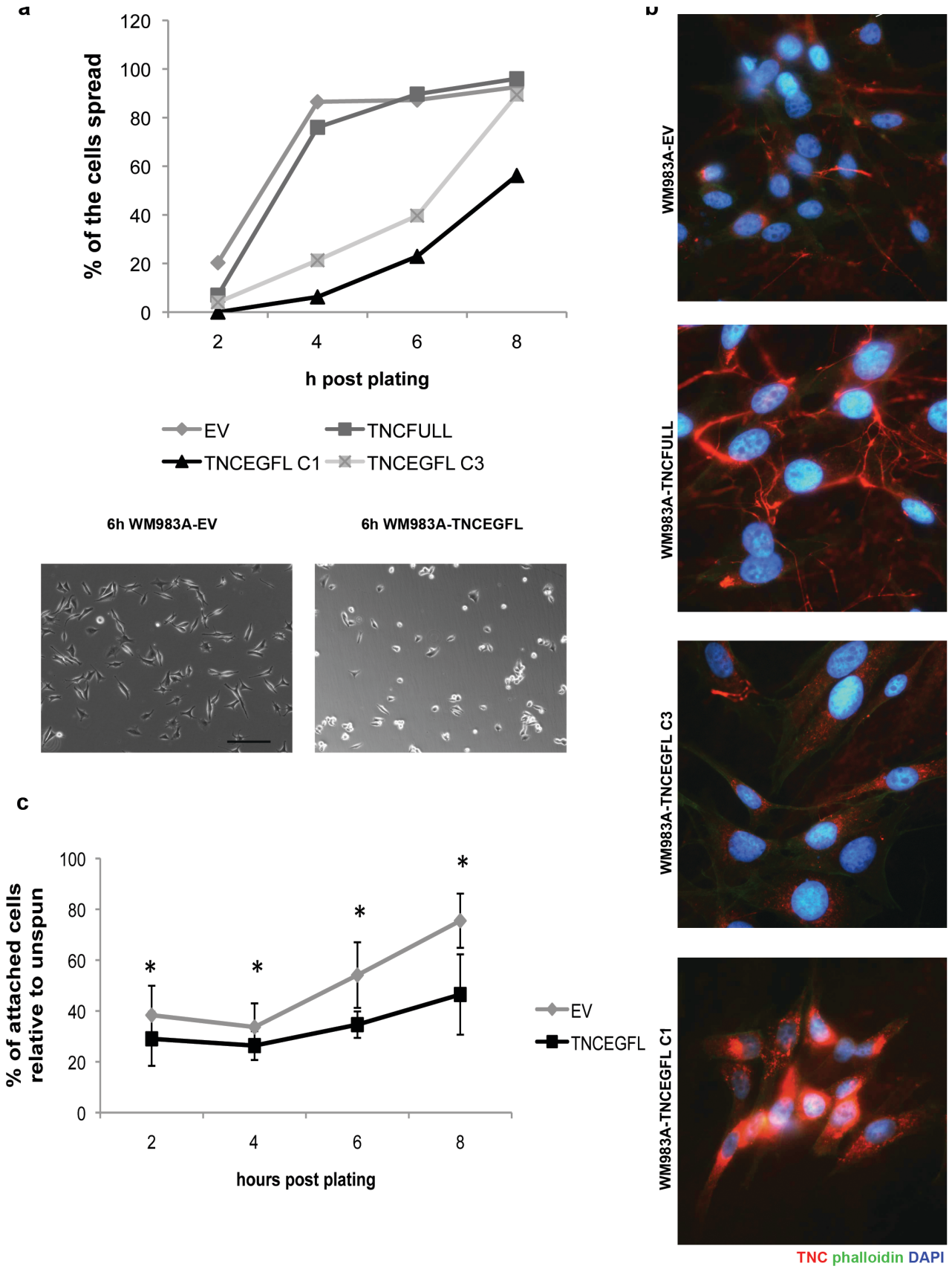

Figure 18. WM983A-TNCEGFL cells present impaired cell spreading and attachment that is TNCEGFL dose dependant.

*(A) Cells were imaged at the indicated times after seeding by phase contrast microscopy and scored for the percentage of spread cells (upper panel). Lower panel shows the difference in cell spreading at 6h. Shown are representative of three experiments. Scale bar 100μm. (B) Immunostaining of TNC in two clones of WM983A-TNCEGFL (C1 and C3) and the full length TNC (TNCFULL) construct. (C) WM983A-TNCEGFL detached to a greater extent in inverted centrifugation assays. Shown is an average ± SEM of three experiments, each in triplicate. * $p < 0.05$.*

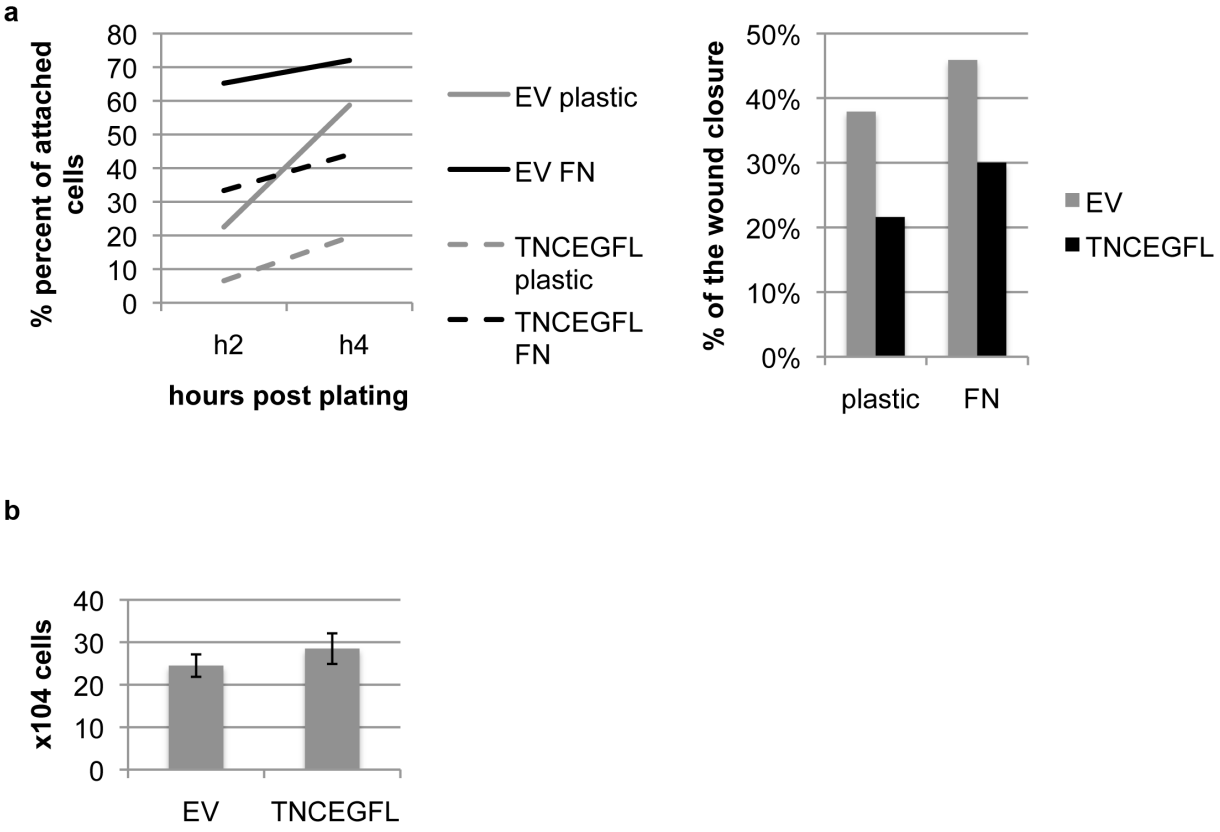

Figure 19. TNCEGFL expressing cells have anti adhesive phenotype that persists on Fibronectin coated surfaces and have unchanged proliferation rates compared to WM983A-EV cells.

(A) Quantification of cell attachment assay (left panel) and wound healing assay (right panel) on 2μg/cm^2 fibronectin coated surface. (B) Number of WM983A-EV and WM983A-TNCEGFL cells 48h post plating determined with trypan blue dye exclusion.

3.3.4 Expression of TNCEGFL activates ROCK signaling

The critical aspect of both cell migration and attachment/spreading is the ratio of adhesion to transcellular contractility (Lauffenburger and Horwitz, 1996). As integrin profiles were similar and the phenotype persisted across different substrata, we focused on contractility that creates tension within the cell and determines the round cell shape (reviewed in (Sanz-Moreno and Marshall, 2010)), mainly the Rho-associated kinase (ROCK) and myosin light chain 2 (MLC2). ROCK inhibitor Y27632 dramatically improved adhesion and spreading of WM983A-TNCEGFL cells when added at the time of plating (Figure 20A). 2D migration of WM983A-TNCEGFL cells was slightly but statistically significantly increased when 5μM Y27632 was added at the time of introducing "the wound", compared to the WM983A-EV (Figure 20B). This is in accordance with findings that inhibition of ROCK in the absence of three-dimensional environment enhances cell movement (Sahai and Marshall, 2003) as it allows generation of protrusions and adhesion of the leading edge.

Activated ROCK affects the state of MLC2 phosphorylation by direct phosphorylation of MLC2 and by phosphorylation and inhibition of MLC phosphatase (Amano et al., 2000). Phosphorylation of MLC2 on Ser-19 is only partially dependent on ROCK whereas diphosphorylation on both Thr-18 and Ser-19 and myosin phosphatase phosphorylation (which is inhibitory to this contractility antagonist) on Thr-853 are ROCK dependent (Ren et al., 2004). It has been shown that upon cell detachment Rho-ROCK signal transduction is disrupted (Ren et

al., 2004). Therefore, we examined the phosphorylation status of these molecules in trypsinized (detached) and replated WM983A-EV and WM983A-TNCEGFL cells during the time course of 8 hours (Figure 20C). We observed that after detachment phosphorylation levels drop and during the course of attachment WM983A-EV cells gradually increase diphosphorylation of MLC2 (ppMLC2) while TNCEGFL expressing cells have constant higher levels of ppMLC2. Monophosphorylation on Ser-19, as expected, did not differ in WM983A-TNCEGFL cells compared to WM983A-EV. Increased diphosphorylation of MLC2 may induce premature contraction and decreased spreading, the phenotype that we observe in TNCEGFL expressing cells. Additionally, in TNCEGFL expressing cells phosphorylation of Thr-853 MYPT, myosin-binding subunit of myosin phosphatase, that inhibits its phosphatase activity, was increased compared to WM983A-EV. Furthermore, transient expression of TNCFULL or TNCEGFL in WM35 cells increased basal levels of ppMLC (Figure 17A) As adhesion provides physical support for contraction and effective migration on rigid substrates, our results imply that overly activated ROCK and its effectors in TNCEGFL expressing cells lead to impaired cell attachment and movement in 2D.

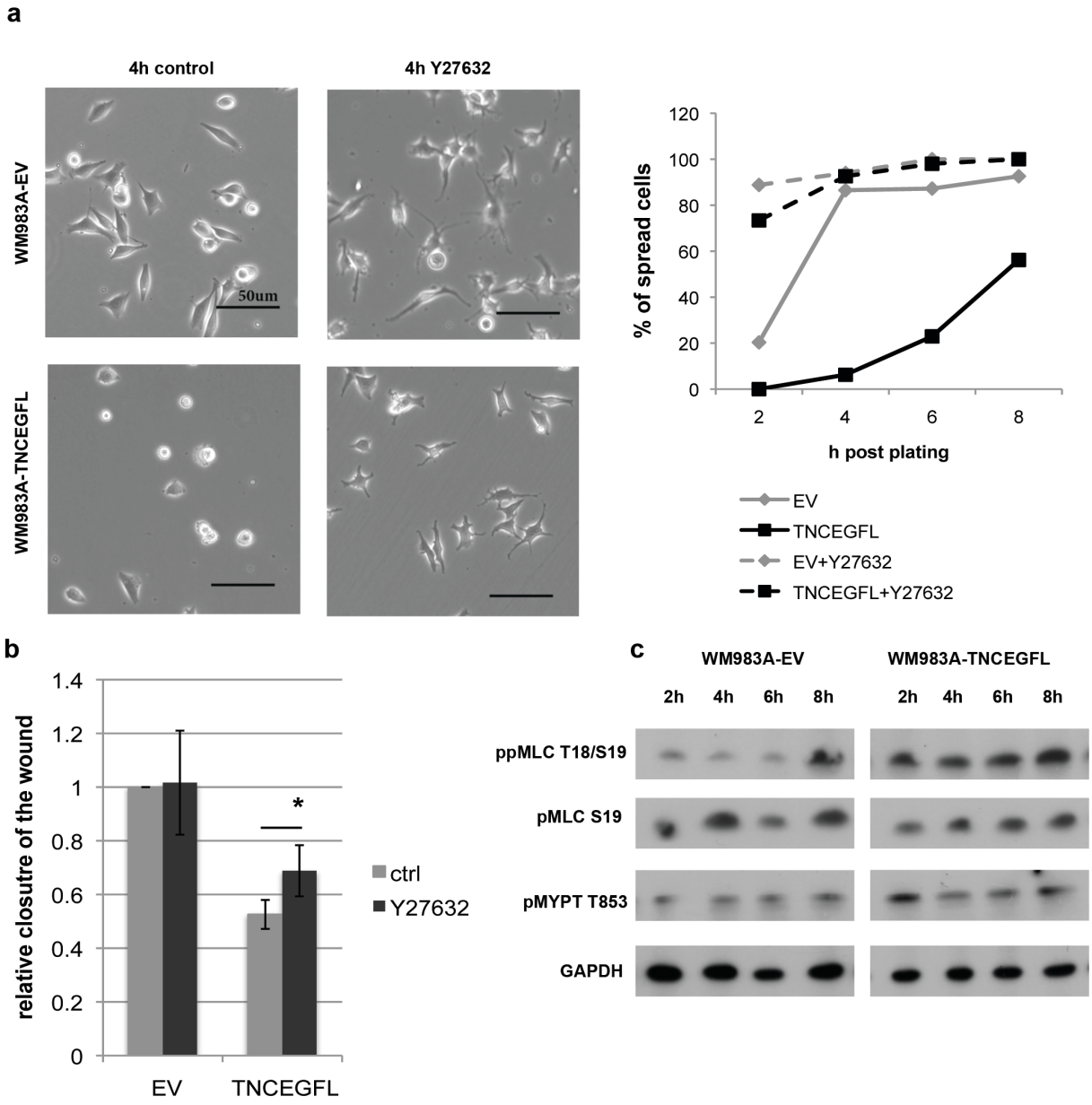

Figure 20. Expression of TNCEGFL activates ROCK signaling.

*(A) Effects of ROCK inhibitor Y27632 on WM983A cell spreading (shown at 4h post plating (left panel) and quantification (right panel)) and migration (B). Shown is mean ± SEM of three experiments each in triplicate, * p > 0.05. Scale bars 50μm. (C) Phosphorylation of the*

downstream ROCK effectors MLC2 and MYPT in WM983A-TNCEGFL cells during the course of attachment compared to WM983A-EV. Intensities of protein bands determined by integrating optical density over the band area using Image J software, normalized to the GAPDH levels showed increases between 1.5 to 2.0 fold across all three repeats for WM983A-TNCEGFL ppMLC and pMYPT levels compared to WM983A-EV across time points.

3.3.5 TNCEGFL expressing melanoma cells have increased invasion potential

The foregoing presents a cell that is less attached to the substrata, and likely exhibits greater shape plasticity, and thus may preferentially move through a 3D matrix (Friedl et al., 1998; Wolf et al., 2003). To address the question of the role of TNCEGFL in 3D migration and invasion we performed Matrigel invasion experiments. WM983A-TNCEGFL cells had rounded morphology in Matrigel, as observed by confocal microscopy, and the phenotype could be reverted to the elongated mesenchymal type in the presence the ROCK inhibitor (Figure 21A). In addition, WM983A-TNCEGFL cells invaded to a greater extent than WM983A-EV cells (Figure 21B). Confocal imaging of individual invading cells in 3D revealed that WM983A-TNCEGFL cells had rounded blebbing morphology with high diphosphorylated MLC present in the invading blebs, compared to WM983A-EV cells which had a mesenchymal morphology with filamentous protrusions (Figure 21C). Increased invasion potential was not due to increased gelatinase activity as the activities of MMP2 and MMP9 did not change (Figure 22). Our findings are in line with the notion that round melanoma cells are able to squeeze through gaps in ECM more readily (Gaggioli and Sahai, 2007) as a result of strengthening of the Rho/ROCK signaling

pathway as one of the mechanisms leading to mesenchymal to amoeboid migration transition (reviewed in (Friedl, 2004)).

Finally, we tested the ability of WM983A-EV and WM983A-TNCEGFL cells to invade into the collagen-rich dermis of all-human skin organ cultures, a model that better captures melanoma invasion in the human skin. While WM983A-EV cells disrupted formation of stratified epidermis, they did not invade into dermis in the 20-day period. On the contrary, WM983A-TNCEGFL cells were able to penetrate in the dermis compartment of skin organ cultures (Figure 21D).

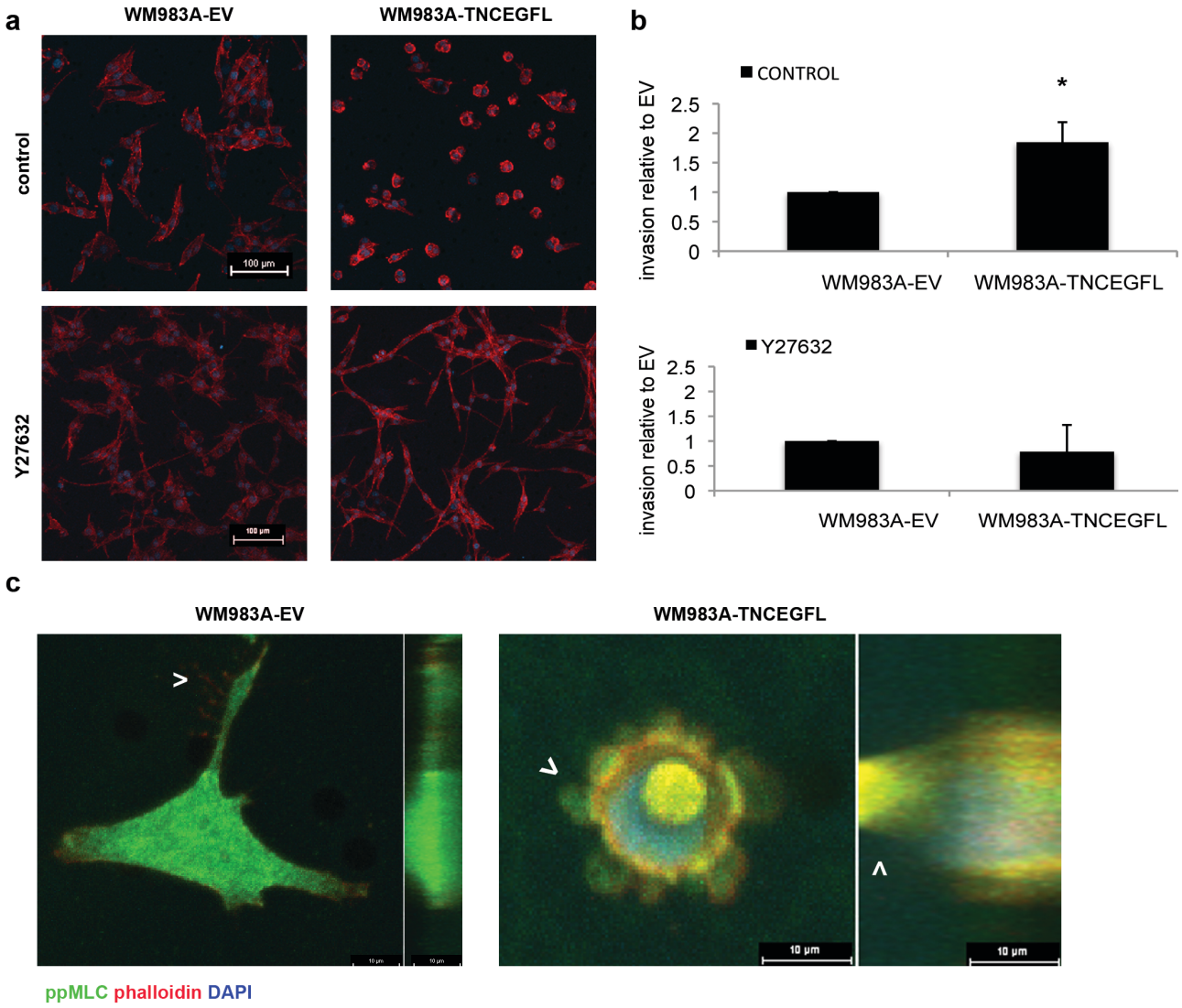
a
WM983A-EV
WM983A-TNCEGFL
control
Y27632
100 µm
b
CONTROL
*
invasion relative to EV
2.5
2
1.5
1
0.5
0
WM983A-EV
WM983A-TNCEGFL
Y27632
c
WM983A-EV
WM983A-TNCEGFL
10 µm
ppMLC phalloidin DAPI
d
control skin organ culture
WM983A-EV
WM983A-TNCEGFL
E
M
D

Figure 21. TNCEGFL expressing cells have rounded morphology in 3D and present higher invasion potential.

*(A) Morphology of WM983A-EV and WM983A-TNCEGFL cells seeded in Matrigel in the absence or presence of Y27632 inhibitor. Scale bars 100μm. (B) Extent of invasion into Matrigel after 48h, in the absence or presence of Y27632 inhibitor, results are shown relative to the WM983A-EV invasion, average ± SD n=3, * $p < 0.05$. (C) Confocal stacks of individual WM983A-EV and WM983A-TNCEGFL invading cells in 3D Matrigel, immunostained for diphosphorylated MLC (Cell Signaling). Arrowheads point to actin protrusions and blebs, respectively. The left hand part of each image is the Z stack in the transverse plane through the cell, whereas the right hand part is the coronal section with the depth to the left. Scale bars 10μm. (D) Representative images of H&E stained skin organ cultures seeded without or with WM983A-EV and WM983A-TNCEGFL melanoma cells after 20 days of culture. Arrow points to invading WM983A-TNCEGFL cells. Scale bar 100μm. E-epidermis, D-dermis, M-melanoma. These results are representative of three independent experiments.*

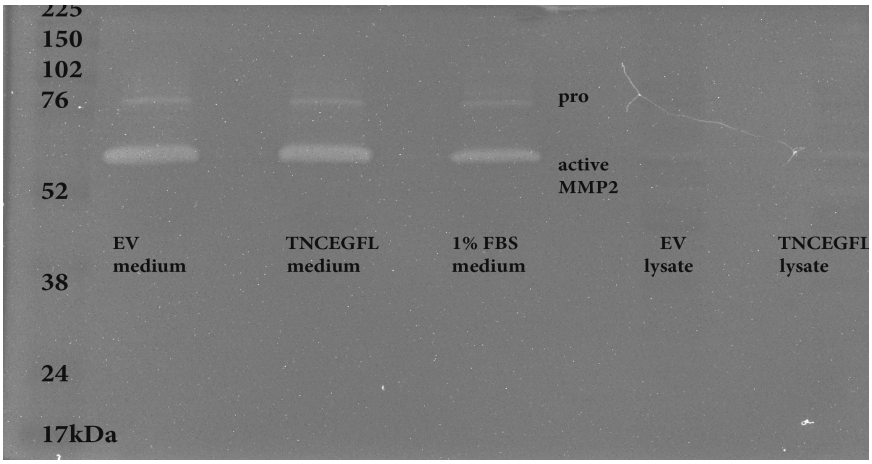

Figure 22. TNCEGFL expressing cells have unchanged MMP2 activity compared to WM983A-EV cells.

Gelatin zymogram of WM983A-EV and WM983A-TNCEGFL conditioned medium or cell lysates.

3.4 DISCUSSION

The most important step in progression from melanoma *in situ* to advanced metastatic disease is acquiring invasive ability. Advanced melanomas produce substantial amounts of TNC that are thought to form fibrillar channels allowing invasion (Kaariainen et al., 2006). Down-regulating TNC in melanoma cells leads to impaired lung colonization and metastasis formation (Fukunaga-Kalabis et al., 2010); this was also observed in TNC-deficient breast cancer cells in which TNC maintains the metastatic niche (Oskarsson et al., 2011). Therefore, increased levels of TNC secreted by melanoma cells may not only promote tumor invasion but also contribute to metastatic seeding. Despite the phenomenological descriptions, the actual cellular mechanisms by which TNC contributes to invasiveness of melanoma are not defined. Herein, we show that

one aspect driven by TNC is the enhanced migration through matrices signaled by the EGFL of this matrix molecule.

In this report we show that advanced melanoma cell lines themselves express large amounts of TNC that is incorporated into the extracellular matrix, and further respond to exogenous TNC by increasing migration speed. We observe that asymmetrical placement of TNC at the cells' front may promote directional translocation during melanoma cell invasion. As TNC is susceptible to proteolytic degradation by MMPs (Imai et al., 1994; Siri et al., 1995) and EGFL repeats can be released or 'uncovered' by this cleavage (Wallner et al., 2004), we focused in particular on the possible impact of TNCEGFL repeats on melanoma cell migration and invasion. We show that overexpressing TNCEGFL impairs TNC extracellular network organization and confers intrinsic anti-adhesive phenotype to melanoma cells, which is EGFL-dose dependent. We find that TNCEGFL-expressing cells migrate slower in 2D motility assays but move and have increased invasion potential in 3D systems. Invading TNCEGFL expressing cells have rounded cell morphology, consistent with reports that melanoma cells can shift to a less adhesive amoeboid mode of cell movement (Sahai and Marshall, 2003). This dichotomy of migration potential in 2D and 3D matrices has been noted previously with a shift in the adhesion-contractility towards a lesser overall value promoting speed through 3D matrices while diminishing the locomotion on 2D surfaces (Zaman et al., 2006). The mechanism of this shape plasticity in presence of TNCEGFL points to ROCK signaling that has been shown to allow melanoma switching between mesenchymal and amoeboidal types of cell movement (Sahai and Marshall, 2003; Sanz-Moreno and Marshall, 2009). This is consistent with signaling of the EGFL repeats via the EGFR. However, we could not definitively demonstrate such a pathway as EGFL repeats being at ultra-low affinity (Swindle et al., 2001) and melanoma cells expressing

low levels of steady state EGFR; further, the melanoma cells did not survive in the face of EGFR inhibition (data not shown). Nevertheless, Proximity Ligation Assays (PLA) (Soderberg et al., 2006) implicate a close physical association (<40nm) of TNC and EGFR in these melanoma cells (Figure 23). Still in the absence of definitive evidence, it is possible that the EGFL repeats signal via other surface receptors.

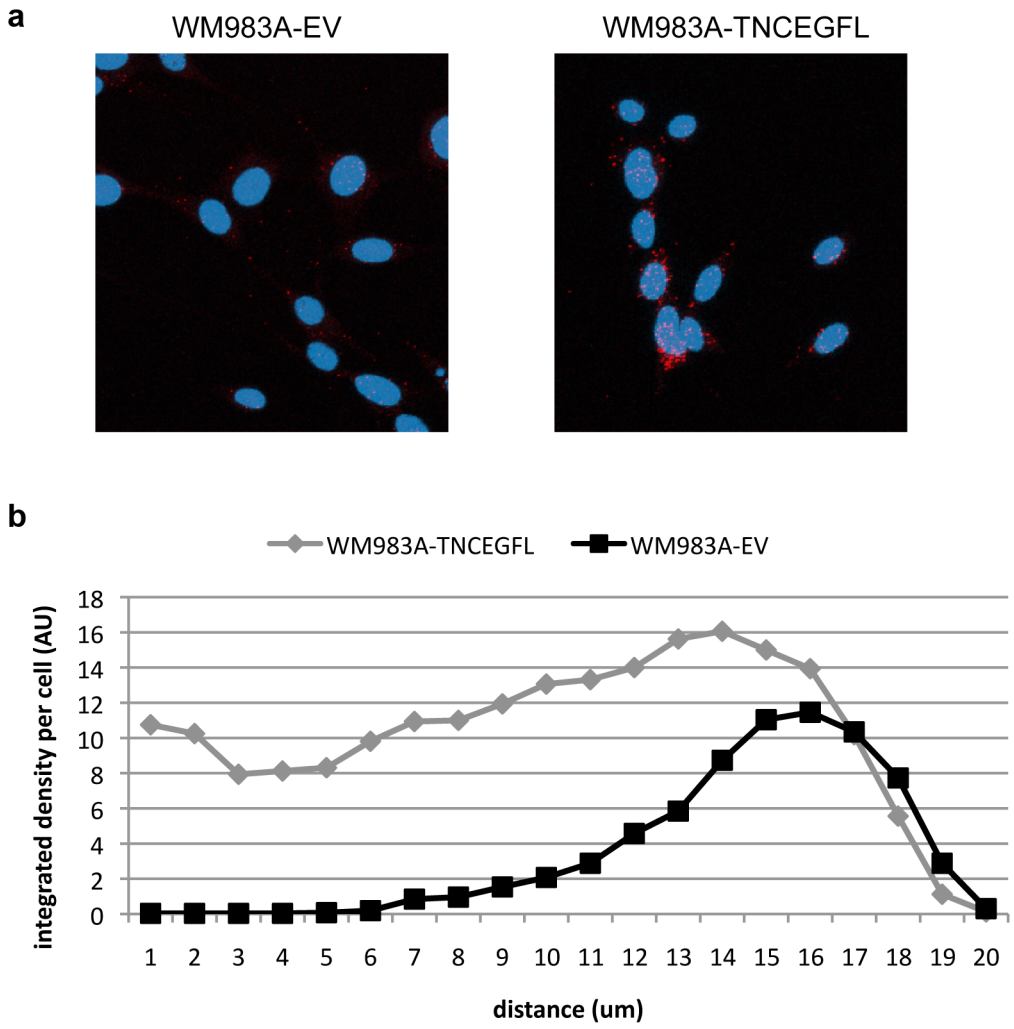

Figure 23. Proximity ligation assay for physical association of EGFR and TNC.

PLA assay was performed with primary anti EGFR antibody (Cell signaling) and anti TNC antibody that recognizes EGFL repeats (ab6393, Abcam). Close physical association of the two proteins is visualized as a red fluorescent signal. (A) Representative maximum intensity

projections from 20 planes 1 μm apart. PLA signal is red, nuclei stained with DAPI. (B) Average integrated density of the red signal per cell in each plane was calculated with Image J software Particle Analyzer. The distance of 20 represents the surface of the coverslip.

It has been described that amoeboid-like melanoma cells that have high ROCK activity are found at the invasive fronts of melanomas, while mesenchymal elongated cells comprise the body of the tumors (Sanz-Moreno et al., 2011). We find that TNCEGFL-expressing cells have increased ROCK signaling, as observed by increased phosphorylation of its targets: biphosphorylation of MLC2, that increases transcellular contractility, and phosphorylation of MYPT, that negates the inhibition of actin cytoskeleton contraction. This is validated by the loss of the anti-adhesive phenotype and rounded morphology in presence of the ROCK inhibitor Y27632 on both rigid 2D substrates and in 3D Matrigel. Furthermore, in the blebs of TNCEGFL expressing cells invading the 3D matrices, diphosphorylated MLC2 co-localizes with the actin cytoskeleton; this is characteristic of contractile amoeboid type of movement (reviewed in (Lammermann and Sixt, 2009)). Finally, we show that TNCEGFL expressing cells are more efficient in invading into a human skin organ culture, a setting that better resembles the first steps of actual melanoma invasion in patients.

Supporting our signaling model, it has been shown that recombinant TNC construct Ten70 which does not contain EGFL repeats, suppresses Rho A activation while maintaining the level of active Cdc42 thus preventing stress fiber formation (Wenk et al., 2000). Cells seeded on Ten70 form prominent filopodia, and that exact feature is lost in TNCEGFL-expressing melanoma cells. By overexpressing EGFL repeats, the balance of endogenous signaling of TNC is shifted and activation of ROCK enables amoeboid morphology. Our results are in concordance

with observation that distinct modes of cell motility have different requirements for ROCK activity (Sahai and Marshall, 2003), as TNCEGFL expressing cells perform better in 3D migration assays and have impaired migration in 2D assays compared to melanoma cells transfected with an empty vector. It is interesting to speculate that TNC, highly expressed at the invasion fronts of melanoma (Kaariainen et al., 2006) and at the front of invading melanoma cells promotes activation of ROCK and amoeboid cell morphology observed at the fronts of invasion in melanoma tumors (Sanz-Moreno et al., 2011).

Taken together, our data demonstrate that over expression of TNCEGFL repeats alters both adhesive and migratory states of melanoma cells and the composition of the extracellular matrix making it more permissive for melanoma cell invasion. The rounded morphology and enhanced blebbing of the amoeboid form of motility allows for cells to more easily penetrate smaller sized pores in matrices and thus are less dependent on proteolytic 'opening' of channels in a collagen-rich matrix such as the dermis (Friedl, 2004). Our findings also reinforce the notion that cells utilize different signaling cascades to effect migration dependent on the 2D versus 3D matrix context.

3.5 MATERIALS AND METHODS

3.5.1 Cell culture

Melanoma cell line WM35, obtained from Coriell Institute for Medical Research (Camden, NJ), was maintained in MCDB153: L15 4:1 medium mixture with addition of 5% FBS, 5μg/ml insulin and 2mM $CaCl_2$. WM983A and WM983B were obtained from Wistar

Institute (Philadelphia, PA) and cultured in DMEM: L15 3:1 mixture with addition of 10% FBS (Herlyn et al., 1991). Human epidermal keratinocytes were obtained from Invitrogen and cultured on collagen-coated dishes in Epilife medium with growth supplements (Invitrogen, Grand Island, NY). Human neonatal fibroblasts were cultured in DMEM with 10% FBS. Primary cells were used in skin organ cultures under 6th passage.

3.5.2 Generation of TNCEGFL and TNCFULLL constructs and TNCEGFL expressing melanoma cell lines

Full length TNC construct (X78565) was obtained form Dr. Harold Erickson (Duke University, Durham, NC)(Aukhil et al., 1993). The first half of the TNC sequence was amplified with introduced NotI and EcoRV cutting sites, of total length of 2355 bases, and cloned into pcDNA3.1(-) vector (Invitrogen). The primers for amplification were 5'-ATA CTC AAG CGG CCG CAT GGG GGC CAT GAC TCA-3' and 5'-CGG ATA TCT CAT ACT CTT GCC CAG GA-3'. Subsequently, TAA stop codon was introduced instead of TCA codon at the end of 14th EGFL repeat with Quick Change II Site Directed Mutagenesis Kit (Stratagene) and primers 5'-GGG AGG AGA CAC CTCTTA GCA GTC TTC TCC G-3' and 5'-CGG AGA AGA CTG CTA AGA GGT GTC TCC TCC C-3'. WM983A cells were transfected with TNCEGFL using Lipofectamine (Invitrogen) and G418 resistant clones were selected. Clone expressing the highest amount of TNCEGFL (C1) was selected for further analysis and clone with lower level of TNCEGFL expression (C3) for comparison in some assays. As a control, a monoclonal WM983A isolate expressing empty pcDNA3.1(-) vector was established. For the TNCFULL construct the full length TNC was cloned into the same vector and G418 resistant clones were

selected. The same vectors EV, TNCEGFL and TNCFULL were used for transient transfection in WM35 cell line.

3.5.3 TNC TMA immunohistochemistry

Melanoma tissue microarrays ME1004 and ME242 were purchased from Biomax (Rockville, MD) and stained with anti-TNC antibody that recognizes the EGFL repeats (ab6393, Abcam, Cambridge, MA) as previously described (Hood et al., 2010). Images were acquired with an Olympus 40X 0.75 NA objective on Olympus BX-40 microscope.

3.5.4 Immunoblotting and immunostaining

Immunoblotting and immunostaining were performed as previously described (Hood et al., 2010). Antibodies used were: anti-TNC recognizing FN repeats (MAB33581, R&D Systems), anti-TNC recognizing EGFL repeats (MAB2138, R&D Systems), anti-pMLC2 Ser-19, anti-pMLC2 Thr-18/Ser-19, anti pMYPT Thr-853 (#3675, #3674 and #4563, respectively, Cell Signaling Technology) and anti-GAPDH (G9545, Sigma-Aldrich). All secondary antibodies were from Sigma-Aldrich or Molecular Probes, Invitrogen. Actin fibers were stained with 488- or 568-Alexa Fluor phalloidin (Invitrogen) and nuclei with DAPI. Images were acquired with an Olympus 60X 1.25 NA or Olympus 20x 0.4 NA objective on Olympus BX-40 microscope.

3.5.5 Cell spreading and inverted centrifugation assays

For spreading assays cells were trypsinized and re-plated on plastic culture dishes in regular medium or in the presence of 5μM Y27632 (Calbiochem). After 2, 4, 6 and 8 hours images were acquired using Olympus IX70 microscope with a 10X 0.3 NA objective, cells were counted (n=100 per treatment) and percentage of spread cells was determined. Completely round phase-bright cells were counted as non-spread and those that lacked round shape and had membrane protrusions were counted as spread. Data was collected from three independent experiments.

Inverted centrifugation assay was performed as described (Shao et al., 2010). In this assay, after 2, 4, 6 and 8 hours, we compared stationary plates washed with PBS against plates spun inverted at 1000 rpm (150g). This was used to calculate the % of attached cells compared to not centrifuged plate controls.

3.5.6 2D migration assays and cell tracking

For wound healing assay cells were seeded in regular medium and let attach 12h and then quesced in 0.5% FBS medium for 24h. The cross wound was introduced with a yellow pipette tip, and the cross was used as a reference of position for taking images. If used, 5μM Y27632 (Calbiochem) was added at the time of introducing the wound. Images were taken at 0 and 22h post scratching using Olympus IX70 microscope with a 4X 0.13 NA objective. Area of the wound was calculated using ImageJ software and results were expressed as % of the area closed within 22h.

For imaging of single cell movement of WM35, WM983A and WM983B cells, plates were coated with 2μg/cm^2 of rat tail Collagen I (BD Biosciences, Bedford, MA) or 2μg/cm^2 of Collagen I and 2μg/cm^2 of human Tenascin C (Millipore, Temecula, CA) in PBS for 2 hours at ambient temperature and then blocked for 30 minutes with 0.1% BSA in PBS. 2x10^4 cells per well were seeded and let attach for 12 hours. Cells were labeled with Cell Tracker red CMPTX (Invitrogen, Carlsbad, CA) and after 6h in 0.5% FBS medium imaged for 8 hours every 10 minutes in TRITC and phase channels with Nikon 10X 0.5 NA objective on Nikon Ti-E inverted microscope with CO_2 stage incubator (Okolabs, Quarto, Italy). Cell migration speed and track length and displacement were analyzed with Imaris software (Bitplane, Zurich, Switzerland) based on tracking of movement of fluorescence as autoregressive motion. Experiment was repeated two times and total of more than 50 tracks per treatment were analyzed. For tracking of WM35 cell movement upon expression of TNC constructs, cells were transfected with EV, TNCFULL or TNCEGFL, and 24h later imaged for 8h every 10 minutes. For tracking of WM983A-EV and WM983A-TNCEGFL cell movement, cells were seeded on glass-bottom dishes (MatTek Corporation, Ashland, MA) an let grow for 72 h before imaging to allow deposition of the matrix and then imaged and analyzed as described above.

3.5.7 3D invasion assay

Matrigel invasion assay was performed in BD BioCoat Matrigel Invasion Chamber per manufacturer instructions (354480, BD Biosciences, Bedford, MA). Cells were let to invade for 48h or 72h as specified in the legends. The invaded cells at the bottom side of membrane were stained with DAPI and five random 10x fields were counted, with each condition in triplicate.

Experiments were repeated three times and average number of invaded cells was expressed as number of invaded cell per 10x field or relative to WM983A-EV.

3.5.8 Confocal imaging of Matrigel invading cells

Cells were seeded as for Matrigel invasion assay and let invade 48h. Matrigels were stained as described with modifications (Hooper et al., 2006). Briefly, Matrigel inserts were washed with PBS, fixed 30 minutes in 4% formaldehyde 0.25% glutaraldehyde in PBS, treated with 0.2% Triton X for 30 min on ice, and stained with 0.2μg/ml 568-Alexa-Fluor phalloidin (Molecular Probes, Invitrogen) and 2μg/ml DAPI (Sigma) in dark for 3h. After washing with PBS samples were incubated with anti-TNC or anti-ppMLC antibody for 12h at 4°C and another 2h at ambient temperature with anti-rat 488-Alexa Fluor secondary antibody (Invitrogen). Membranes were cut out with a razor blade and mounted on glass slides in PBS. Images were taken on Nikon Sweptfield Confocal Microscope (TSI inverted) using 10X and 60X 1.4 NA objectives. 3D volume representations of Z-stacks were made using Nikon Elements software.

3.5.9 Skin organ cultures and H&E staining

Skin organ cultures were established as previously described (Simpson et al., 2010) with modifications. Briefly, $5x10^5$ primary human fibroblasts were seeded in collagen gels, and after 5 days in submerged culture $1x10^6$ normal human keratinocytes were seeded on top. The next day $1x10^5$ WM983A-EV or WM983A-TNCEGFL cells were seeded in the center of the plug within the cloning rings, let attach for 8h and then the cloning rings were removed. After 3 days, the cultures were lifted to air liquid interface to allow epidermis maturation and medium was

replenished every other day for total of 20 days of culture. The samples were fixed and paraffin embedded and H&E stained as previously described (Hood et al., 2010). Experiment was repeated two times with similar results.

3.5.10 Gelatin zymography

Gelatinase activities of MMP2 and MMP9 in WM983A-EV and WM983A-TNCEGFL conditioned medium and lysates were assessed according to prior protocols (Toth and Fridman, 2001).

3.5.11 PCR array

RT^2 Profiler PCR Array of Human Extracellular Matrix and Adhesion Molecules (PAHS-013A, SABiosciences, Frederick, MD) was performed per manufacturer instructions in 96 well format with 1μg of total RNA. Experiment was repeated two times and data was analyzed with SABiosciences PCR Array analysis web-based Utility (http://sabiosciences.com/pcrarraydataanalysis.php).

3.5.12 Proximity ligation assay (PLA)

WM983A-EV and WM983A-TNCEGFL cells were grown on glass cover slips, fixed with 4% formaldehyde, treated with 0.2% Triton-X, blocked with 5% goat serum and incubated with primary rabbit anti-EGFR (#2232, Cell Signaling Technology) and mouse anti-TNC (ab6393, Abcam) that recognizes EGFL overnight at 4°C. PLA was performed according to the

manufacturer's instructions (Duolink II Red Starter kit, Olink Bioscience, Uppsala Sweden). Briefly, rabbit and mouse specific oligonucleotide conjugated secondary antibodies (PLA probes) bind to the primary antibodies. Next, probes are annealed if they are in close proximity (<4 0nm) and in the presence of fluorescently labeled onligonucleotides allow rolling circle amplification. The signal from the close physical association between the proteins of interest is visualized as red dots. Nuclei were labeled with DAPI and images were taken on Nikon Sweptfield Confocal Microscope (TSI inverted) using 40 1.2 NA objective. 20 Z plane images were taken every 1μm and the intensity and number of red signals were analyzed with Image J Particle Analyzer for at least 20 cells in each treatment, and expressed as average integrated density per cell. Experiment was repeated two times. Controls with single anti EGFR and anti TNC antibodies were performed and they gave low or no signal.

3.5.13 Statistical testing

All statistics of quantification in this study, including spreading assay, wound healing assay, Matrigel invasion assay, RT-PCR and live cell tracking experiments were performed by two- tailed Student's *t* test with a $P < 0.05$ being required to be considered significant and shown as mean ± SD or SEM (if each experiment was performed in triplicate).

3.6 ACKNOWLEDGEMENTS

We would like to thank Taiki Hakozaki for assistance with the cell attachment experiments, Diane George for technical assistance and Dr. Harold Erickson (Duke University,

Durham, NC) for the TNC construct in pNUT vector. A VA Merit Award and RO1 award to A. W. supported these studies.

4.0 EXTRACELLUALR MATRIX PROTEIN DECORIN CAN COUNTERACT TENASCIN C INDUCED MELANOMA CELL INVASION

Jelena Grahovac and Alan Wells

Department of Pathology, University of Pittsburgh and Pittsburgh VAMC, Pittsburgh PA, 15217 USA

4.1 ABSTRACT

Melanoma is the most aggressive type of skin cancer with increasing incidence rates whose progression is characterized by drastic changes in the composition of the extracellular matrix (ECM). Tenascin C in the melanoma matrix is highly up regulated and there is significant decrease in levels of the small leucine-rich proteoglycan Decorin compared to normal skin. Interestingly, both Tenascin C (TNC) and Decorin (DCN) have been shown to signal through the Epidermal Growth Factor receptor, with opposite outcomes on cell proliferation, survival and migration. We therefore examined expression of these two ECM proteins and found that they have opposite and almost mutually exclusive patterns of expression in benign nevi and primary melanoma samples. Therefore, we asked whether DCN could counteract the effects of increased TNC expression during melanoma invasion. DCN was able to reverse the influence of TNC on cytoskeletal organization and to block TNC induced increased invasion in collagen gels. Ultimately, in skin organ culture models DCN was able to ameliorate melanoma invasion even in the presence of TNC. These findings imply a role for Decorin as a preventive ECM moiety in melanoma invasion that could potentially be used for developing treatments.

4.2 INTRODUCTION

In order to develop efficient cancer therapies it is important to identify the mechanisms by which tumor cells invade into surrounding tissues. Melanoma, the most aggressive cancer of the skin with high resistance to therapy and ability to metastasize to multiple organs, is a good model for studying tumor invasion partly due to its step-wise progression. Melanoma arises from transformed melanocytes, pigmented cells of neuroectodermal origin that normally reside at the basal layers of the epidermis. The majority of melanomas have a linear progression: from benign melanocytic nevi to the radial growth phase (RGP) melanoma that divides and spreads within epidermis, to vertical growth phase (VGP) during which melanoma cells invade through the basement membrane into dermis, reaching the final step-metastatic growth phase (MGP) that metastasizes to lymph nodes, lungs, liver, bones and brain (Clark et al., 1984). While melanoma *in situ* has a high cure rate by surgical resection, invasive melanoma that has penetrated dermis has very poor prognosis and the depth of invasion in primary tumors highly correlates with patient survival (Wanebo et al., 1975). It is therefore of utmost importance to elucidate changes that precede and/or induce melanoma invasion from the epidermis into the dermis.

In addition to the changes in cell to cell adhesion, remodeling of the extracellular matrix (ECM) plays a critical role in tumor invasion as ECM proteins provide both mechanical and chemical signals to the tumor cells. In recent years, deciphering the regulation of tumor growth, invasion and metastasis by the extracellular matrix components has shed a new light on the sequence of events in cancer progression (Herlyn, 2009; Malanchi et al., 2012; Oskarsson and Massague, 2012). In melanoma, the production of ECM proteins is significantly altered compared to normal skin: components characteristic of an immature and healing dermis, such as Tenascin C, Fibronectin, certain laminins and SPARC are upregulated (Ilmonen et al., 2004;

Ledda et al., 1997; Natali et al., 1995; Pyke et al., 1994) while components characteristic of a mature matrix such as Decorin, Lumican and certain collagens are down-regulated (Hood et al., 2010). Therefore, we asked the question whether the changes in ECM could drive melanoma invasion and dissemination.

Both melanoma cells and stromal fibroblasts secrete Tenascin C (TNC) (Herlyn et al., 1991) which has been shown to promote tumor invasion (Galoian et al., 2007; Grahovac et al., 2012; Hancox et al., 2009; Sarkar et al., 2006). On the other hand, Decorin (DCN) is expressed in normal human dermis by quiescent fibroblasts (Honardoust et al., 2012; Mauviel et al., 1995), and can be present in melanoma tumor stroma at low levels, but is absent in melanoma cells themselves (Brezillon et al., 2007). Contrary to TNC, DCN has been shown to have an inhibitory role in cancer progression (Neill et al., 2012). Both TNC and DCN have been shown to bind the Epidermal Growth Factor Receptor (EGFR) (Iozzo et al., 1999b; Iyer et al., 2007a), DCN with the affinity of around 70nM (Santra et al., 2000; Santra et al., 2002) and TNC with lower affinity in the micromolar range but with high avidity due to its hexameric structure and tethering within the ECM (Swindle et al., 2001). DCN and TNC have different effects on EGFR signaling: DCN causes down-regulation of the receptor and attenuation of downstream EGFR signaling cascades (Zhu et al., 2005), while TNC causes sustained membrane-restricted signaling which promotes pro-migratory EGFR cascade (Iyer et al., 2008). Having this in mind, we explored whether DCN can counteract TNC promoting effects on melanoma invasion.

4.3 RESULTS

4.3.1 Tenascin C and Decorin have opposite patterns of expression in melanoma tissue and benign nevi

We have previously reported comparative proteomic analysis of melanoma and the adjacent uninvolved skin of the same patient in which the expression of TNC was highly up-regulated and expression of small leucine rich proteoglycans DCN and Lumican was decreased in melanoma samples (Hood et al., 2010). To investigate this further, we examined the expression of TNC and DCN in melanoma tissue array and observed that the expression of these two proteins is inversed in benign nevi and primary melanoma (Figure 24). Namely, TNC was absent in benign nevi, while the dermis was rich in DCN; on the other hand, in primary melanoma samples TNC was detectable throughout the samples with decreased or non-detectable levels of DCN. Furthermore, the expression of these two proteins seemed to be almost mutually exclusive, as regions of the same samples rich with TNC were devoid of DCN, and vice versa (arrowheads, Figure 24).

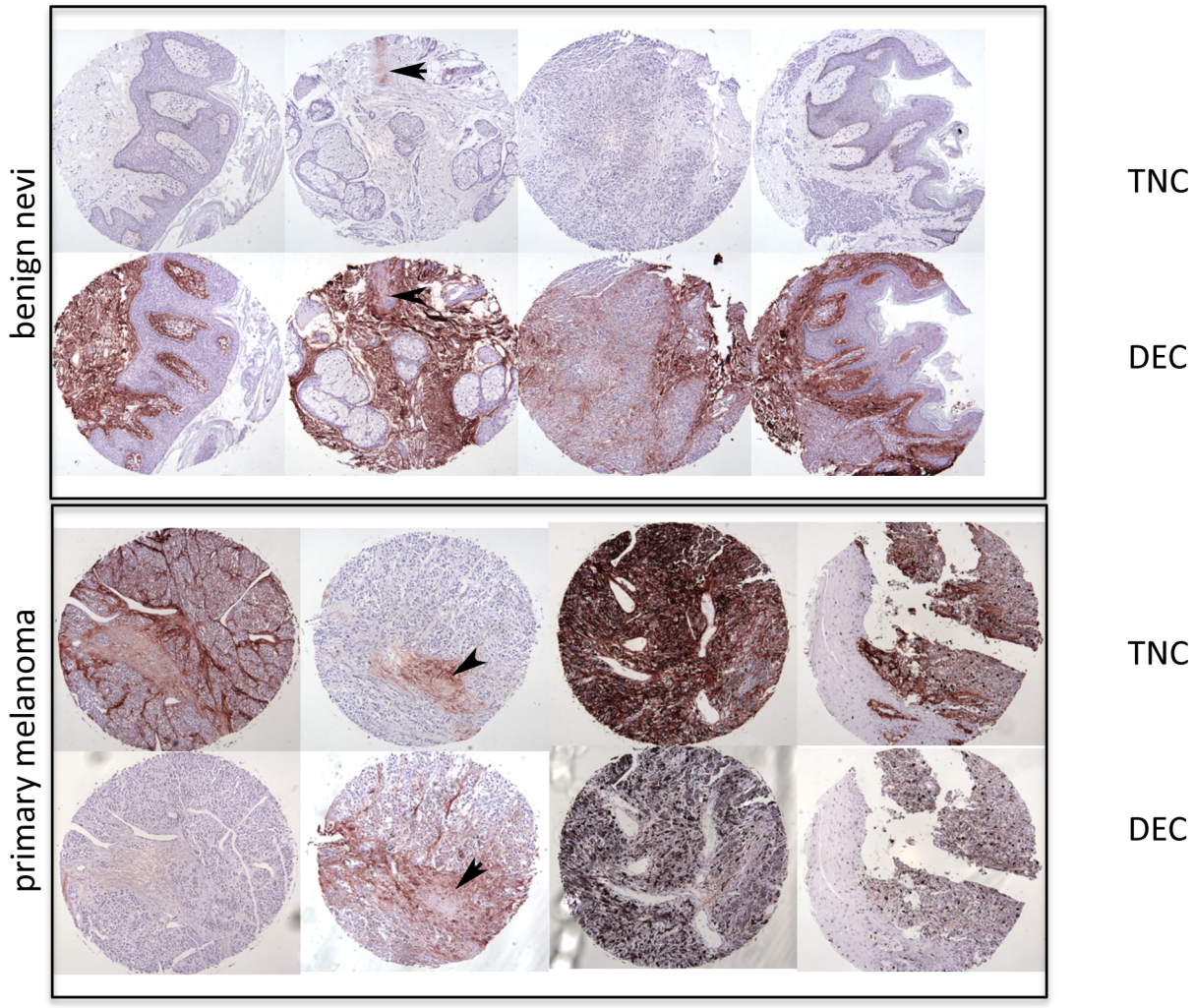

Figure 24. Expression of TNC and DCN in benign nevi and primary melanoma.

Representative images from the melanoma TMA stained for TNC and DCN (brick red). Upper panel shows benign nevi samples, and lower panel shows primary melanoma samples. Arrowheads point to the regions with inversed TNC and DCN expression in the same sample. Magnification 10X. Brown-black stain in the third and fourth lower panel samples is the endogenous melanin.

4.3.2 Tenascin C and Decorin have opposite effects on melanoma cell cytoskeleton

Both TNC and DCN have been reported to influence cytoskeletal organization by the modulation of small GTPases RhoA and Rac (De Wever et al., 2004; Tufvesson and Westergren-Thorsson, 2003), thus affecting cell migration. This implies that the presence or absence of TNC and/or DCN in the melanoma ECM would modulate cell migration and invasion. We first examined the effects of TNC and DCN on the melanoma cell cytoskeletal organization. We chose two metastatic melanoma lines with different cellular morphologies (Figure 25A): WM983B have a more mesenchymal morphology with filopodia protrusions, while WM1158 cells have a more spread morphology with membrane ruffling. Both cell types were seeded on collagen-coated surfaces (COL) with the addition of 2μg/cm^2 TNC (COLTNC) or 2μg/cm^2 DCN (COLDCN) or both (COLDCNTNC) and 24 hours post seeding cytoskeletal changes were detected by phalloidin staining (Figure 25B). Both cell lines seeded on COLTNC substratum had less spread, stretched morphology, while the cells seeded on COLDCN were spread with prominent stress fibers compared to cells seeded on collagen alone (Figure 25B). The addition of both DCN and TNC proteins counteracted the effects of one another, with cell shape resembling the one seen on collagen-coated surface alone. These findings imply that DCN could counteract the effects of TNC on cytoskeletal rearrangement, and therefore influence invasion.

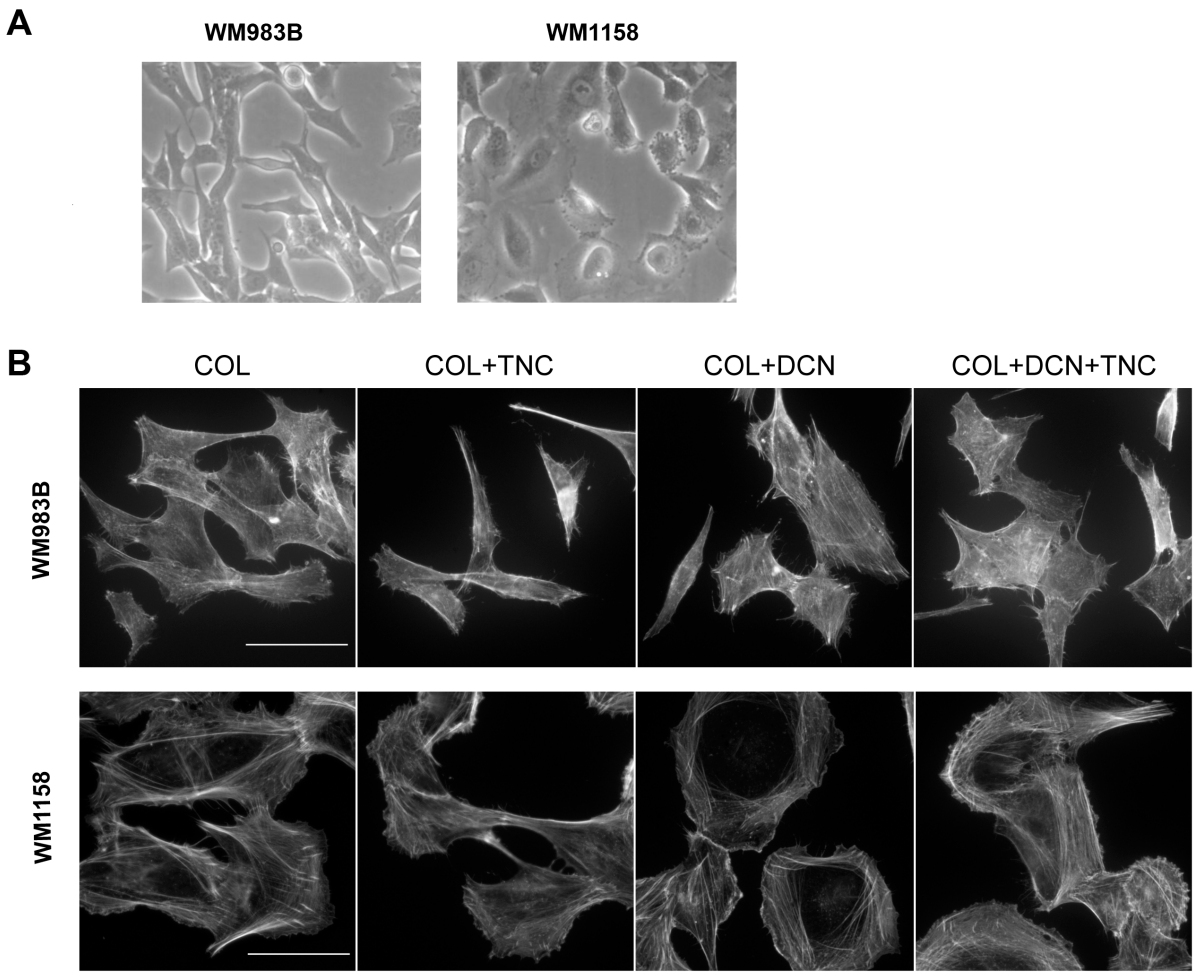

Figure 25. TNC and DCN have opposite effects on melanoma cell cytoskeletal arrangement.

(A) Bright field images of WM983B and WM1158 cells. (B) Both cell lines respond to TNC and DEC by cytoskeletal rearrangement. Phalloidin 568 (gray). Scale bar 50μm.

4.3.3 Decorin can counteract Tenascin C-promoted melanoma invasion

To test the effects of TNC and DCN on melanoma invasion we chose to examine more aggressive WM1158 cells, given that they presented higher migration speed in cell tracking

experiments and higher invasion potential in both Matrigel and collagen invasion assays (data not shown). WM1158 cells showed prominent invasion into 3mg/ml Collagen I gels, with both collective invasion and individually detaching invading cells (Figure 26A). The addition of 4μg/ml of DCN into collagen gels decreased the collective invasion of WM1158 cells compared to the invasion into simple collagen gel (Figure 26C), to average 185μm depth compared to 240μm depth of invasion in collagen alone. The addition of 4μg/ml of TNC to collagen gels significantly increased the extent of the WM1158 cell invasion (to average of 285μm depth). Moreover, the addition of TNC to collagen gels increased the number of cells that detached from the initial mass seeded on top of the gel (Figure 26B, detached cells (green); continuous tumor mass (yellow)), as quantified by Imaris software (Figure 26C). The addition of both DCN and TNC together dramatically decreased the collective invasion of WM1158 cells into collagen gels as well as the detachment of cells from the initial mass.

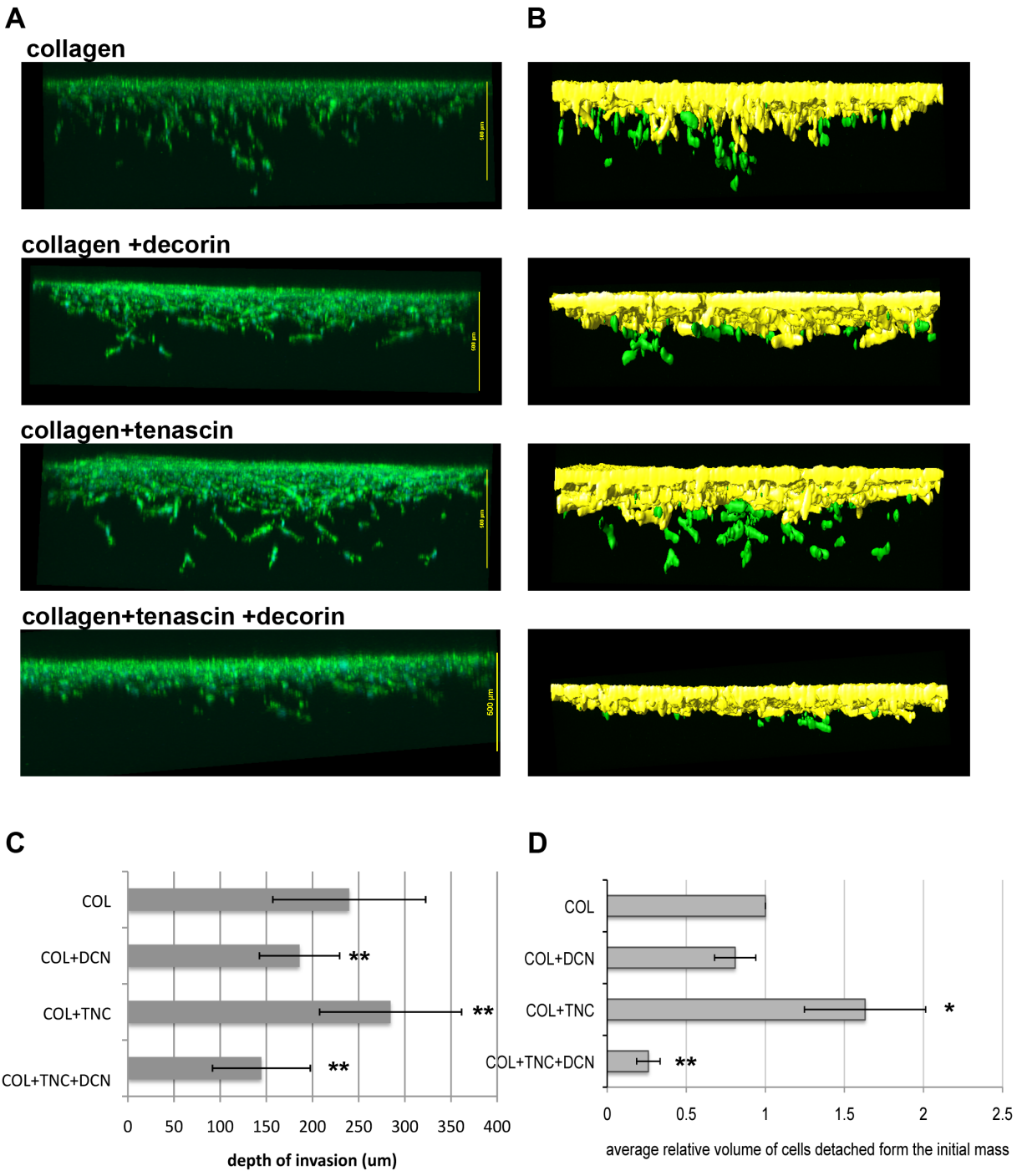

Figure 26. WM1158 cell invasion in 3D collagen gels enriched with TNC or DCN.

(A) Confocal Z stack representation of WM1158 cells invading into collagen gels enriched with DCN, TNC or both. Phalloidin 488 (green), scale bar 500µm. (B) The same stacks

*represented with Imaris software surfaces function: yellow represents continuous mass with detail level of 3μm, green represents cells and clusters of cells detached from the continuous mass 3 or more micrometers away. (C) Quantification of the depth of the melanoma cell invasion (D) Quantification of the volume of detached cell mass. Results are presented as average ± SD n=3, * p < 0.05, **p<0.01.*

To validate these results in more complex melanoma microenvironmental context, we tested the invasion of WM1158 cells in skin organ cultures (SOCs) (Figure 27). Embedding neonatal fibroblasts into 3mg/ml collagen gels formed the dermal compartment onto which a layer of normal human keratinocytes was seeded to form epidermis. WM1158 cells were seeded 2 days after the seeding of keratinocytes to allow formation of the basement membrane between the epidermis and the dermis. WM1158 cells invaded into the dermal compartment of SOCs within 20-day time frame, both collectively and as detached cell clusters (Figure 27, upper left). The addition of 4μg/ml DCN into the dermal compartment prevented melanoma cells from invading into the dermis, and the growth was confined to the epidermis. The addition of TNC at the same concentration induced profound melanoma invasion into dermis, with multicellular streaming-like pattern. These anti and pro- invasive effects of DCN and TNC, respectively, were dose-dependent a 1:1 DCN: TNC ratio in the dermis induced an increased growth of the WM1158 mass in the epidermis, but a barely observable invasion into the dermis, while a 1:2 DCN: TNC ratio induced an invasion into the dermis, although to the lesser extent than TNC alone. This implies that DCN can counteract pro-invasive TNC signals in a dose-dependent manner.

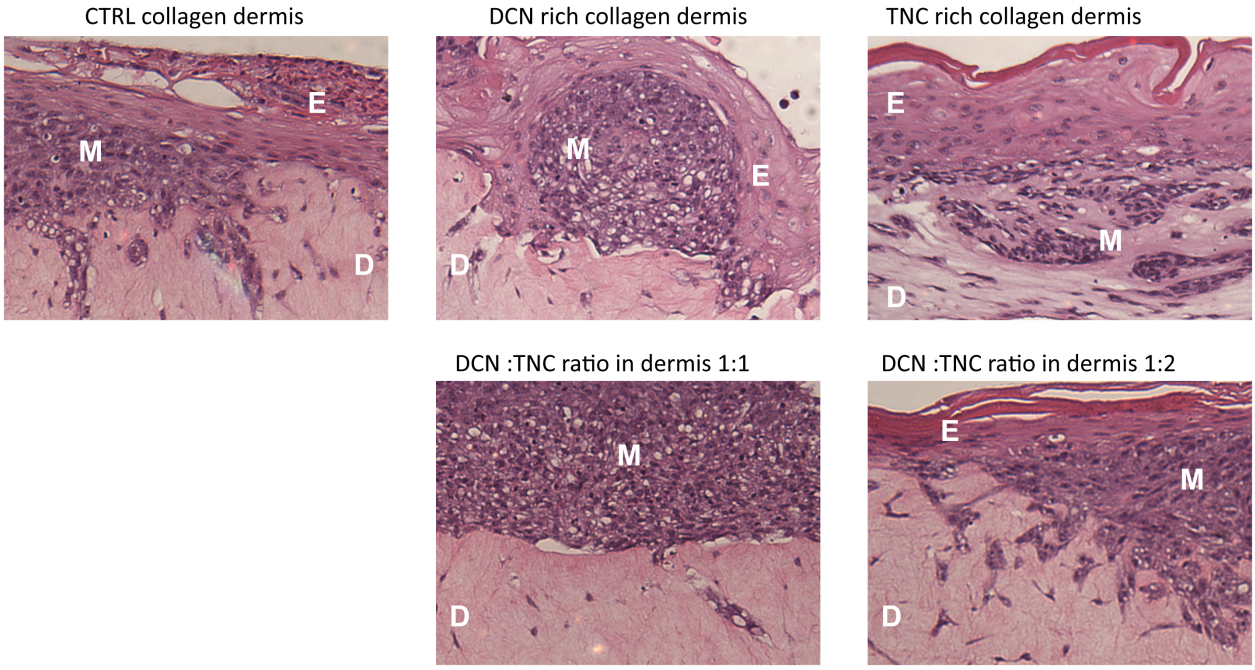

Figure 27. WM1158 cell invasion in skin organ cultures in presence of TNC and DCN.

Representative images of H&E stained skin organ cultures seeded with WM1158 and melanoma cells after 20 days of culture. E-epidermis, D-dermis, M-melanoma. These results are representative of two independent experiments.

4.4 DISCUSSION

Molecular events that direct the progression from melanoma *in situ* to advanced melanoma and the microenvironmental influences on melanoma progression are two critical aspects the understanding of which would greatly contribute to development of new treatment strategies. The composition of the extracellular matrix in melanoma is significantly changed

compared to normal skin (Hood et al., 2010; Naba et al., 2012; Quatresooz et al., 2011) and these changes could drive melanoma invasion. Here we the examined expression of two ECM proteins Tenascin C and Decorin in the panel of melanoma samples and found that their expression is opposite and almost mutually exclusive in benign nevi and primary melanoma samples. The presence of TNC and DCN in the ECM presented to melanoma cells had an opposite influence on the cytoskeletal organization and had a profound effect on melanoma cell invasion in 3D collagen gels. Tenascin C promoted while Decorin limited WM1158 cell invasion. While DCN decreased the depth of invasion in collagen gels, it did not limit WM1158 melanoma cell detachment form the initial mass. Interestingly, DCN showed a dramatic effect on the cells induced to detach by TNC, and inhibited melanoma cell invasion into collagen gels even more in the presence of TNC then when presented alone. Ultimately, in skin organ cultures the presence of Decorin in the dermal equivalent was able to prevent melanoma invasion from the epidermis into dermis, and even in the presence of pro-invasive TNC it was able to ameliorate the invasion potential of melanoma cells. The mechanistic explanation of this effect, which was beyond this initial exploration, could be grounded in the fact that both TNC and DCN can bind and signal through EGFR with opposite outcomes. Select EGFL repeats of TNC have been shown to bind to the EGF binding pocket of EGFR (Iyer et al., 2007a), while DCN binding site in EGFR partially overlaps but is distinct from the EGF binding epitope (Santra et al., 2002). We have previously shown that EGFL repeats of TNC promote melanoma cell invasiveness by increasing the ROCK activity and myosin-light chain phosphorylation in migrating cells, which leads to a shift in mode of motility from mesenchymal to amoeboid and allows greater flexibility in 3D microenvironment (Grahovac et al., 2012). Decorin could simply prevent this effect by competing for EGFR given that it has higher affinity for the receptor (Santra et al., 2000), or

could signal inhibition of migration through other receptors such as c-Met, PDGFR or IGF-1R (Neill et al., 2012), all of which can independently contribute to melanoma invasiveness (Wu et al., 2012). Decorin has also been shown to inhibit melanoma migration by cellular acidification (Stock et al., 2011). As a natural moiety present in the skin, Decorin is an attractive candidate for the development of anti-melanoma therapy both as a natural kinase antagonist and as an enhancer of targeted gene delivery due to its collagen binding affinity (Choi et al., 2010). Further studies of the exact mechanistics of Decorin interference with Tenascin C are underway.

4.5 MATERIALS AND METHODS

4.5.1 Cell culture

Melanoma cell lines WM983B and WM1158 were obtained from the Wistar Institute (Philadelphia, PA) and cultured in DMEM: L15 3:1 mixture with the addition of 10% FBS (Herlyn et al., 1991). Human epidermal keratinocytes were obtained from Invitrogen and cultured on collagen-coated dishes in Epilife medium with growth supplements (Invitrogen, Grand Island, NY). Human neonatal fibroblasts were cultured in DMEM with 10% FBS. Primary cells were used in skin organ cultures under 6^{th} passage.

4.5.2 Melanoma tissue microarray immunohistochemistry

Melanoma tissue microarrays ME1004, ME1004a and ME242 were purchased from Biomax (Rockville, MD) and stained with anti-TNC antibody (ab6393, Abcam, Cambridge,

MA) or anti-DCN antibody (AF143, R&D Systems, Minneapolis, MN). Antigens were retrieved in 1% pepsin in 10mM HCl for TNC staining or heat-induced in citrate buffer pH6 (Dako, Carpinteria, CA) for DCN staining. Endogenous peroxidase was blocked with 3% H_2O_2, and sections were incubated in 5% goat or rabbit serum to decrease background staining. Sections were incubated with primary antibodies for 2h in a humified chamber at ambient temperature, washed and incubated with biotinilated secondary goat anti-mouse antibody or rabbit anti-goat antibody (Jackson ImmunoResearch, West Grove, PA). Vectastatin ABC kit (PK-6100), ImmPACT NovaRed (SK-4805) and Meyer's hematoxylin counter stain were all from Vector Laboratories (Burlingame, CA). Samples were dehydrated and mounted with Permount solution (Fisher Scientific, Pittsburgh, PA). Images were acquired with a 10X 0.3 NA objective on Olympus BX-40 microscope with SPOT imaging software (Sterling Heights, MI).

4.5.3 Immunostaining

Glass coverslips were coated with 2µg/cm2 Collagen I (BD Biosciences, Bedford, MA), Collagen + 2µg/cm2 Tenascin C (Millipore, Temecula, CA), Collagen + 2µg/cm2 Decorin (R&D Systems, Minneapolis, MN) in PBS for 12 hours at ambient temperature and then blocked for 30 minutes with 0.1% BSA in PBS. Cells were seeded on coverslips and let attach 12h, and fixed with 4% formaldehyde for 115 min at ambient temperature. After washing with PBS, cells were treated for 5 min with 0.2% Triton-X, and stained with 568-Alexa-Fluor phalloidin (Molecular Probes, Invitrogen) and 2µg/ml DAPI (Sigma) for 40 minutes at ambient temperature. Images were acquired with an Olympus 60X 1.25 NA objective on the Olympus BX-40 microscope.

4.5.4 Confocal imaging of invasion into collagen gels

Accellular collagen gels were made by mixing rat tail Collagen I (BD Biosciences, Bedford, MA) in $NaHCO_3$-based buffer to a final concentration of 3mg/ml, as previously described (Simpson et al., 2010). TNC (Millipore, Temecula, CA), DCN (R&D systems, Minneapolis, MN) or both were added at a concentration of 4 μg/ml prior to the gel neutralization with 0.2M NaOH. 50μl gels were casted in optical clear cell culture inserts (353095, BD Falcon, Franklin Lakes, NJ). $5x10^4$ WM1158 cells were seeded on top of the gels in 1% FBS medium and 10% FBS medium was added to the bottom of the insert to induce invasion. Gels were fixed after 72h and stained as described with modifications (Hooper et al. 2006). Briefly, collagen inserts were washed with PBS, fixed 30 minutes in 4% formaldehyde-0.25% glutaraldehyde in PBS, treated with 0.2% Triton X for 30 min on ice, and stained with 0.2μg/ml 488-Alexa-Fluor phalloidin (Molecular Probes, Invitrogen) and 2μg/ml DAPI (Sigma) in dark for 3h. Gels were imaged directly in the inserts in PBS on the Nikon Sweptfield Confocal Microscope (TSI inverted) using 10X and 60X 1.4 NA objectives. 3D volume representations of Z-stacks were made using Nikon Elements software and surfaces of the invading cells were modeled with Imaris software based on the absolute intensity of phalloidin staining with 3μm surface area detail level (Bitplane, Zurich, Switzerland). Quantification of the depth of invasion was performed with the length measurement tool of Nikon Elements software by measuring 60 random positions per sample from the surface of seeded cells to the bottom most detected intensity. Experiments were repeated three times.

4.5.5 Skin organ cultures and H&E staining

Skin organ cultures were established as previously described (Grahovac et al., 2012; Simpson et al., 2010), with modifications. Briefly, $15x10^4$ primary human fibroblasts were seeded in 1.5 ml 2mg/ml collagen gels alone or with the addition of 4μg/ml of TNC, DCN or both, in 24 well plates. After 5 days in submerged culture, $25x10^4$ normal human keratinocytes were seeded on top of contracted gels. Keratinocytes were allowed to adhere and 48h later $10x10^4$ WM1158 cells were seeded in the center of the plug within the 4,7mm R cloning rings (Bel Art, 14-512-78, Thermo Fisher Scientific, Pittsburgh, PA), let attach for 8h and then the cloning rings were removed. After 3 days, the cultures were lifted to the air liquid interface to allow epidermis maturation and the medium was replenished every other day for total of 20 days of culture. The samples were fixed and paraffin embedded and H&E stained as previously described (Hood et al., 2010). The experiment was repeated two times with similar results.

4.5.6 Statistical testing

Statistical analysis in this study was performed by two-tailed Student's *t* test with a $p < 0.05$ being required to be considered significant and values were shown as mean ± SD.

5.0 DISCUSSION

Despite the enormous efforts in developing new drug strategies to treat advanced melanoma, the number of melanoma related deaths rises yearly. Melanoma is one of the most aggressive and treatment-resistant human cancers. Given that there is a mathematical relationship between the primary tumor thickness and the survival prognosis (Balch et al., 2009) it appears that the invasive capacity that melanoma cells acquire at the primary tumor site greatly contributes to the disease outcome. Once the melanoma cells have penetrated the basement membrane and reached the dermis, they are very hard to combat. Therefore, an understanding of the events that lead to the progression from the radial epidermal melanoma spreading to the vertical invasion is crucial in order to design better treatment tactics. Many studies have concentrated on molecular changes that melanoma cells undergo during progression, and some of the recent therapies that target specific changes, like Vemurafenib - BRAF inhibitor that blocks V600E mutated BRAF, proved to be efficient. Nevertheless, the constant obstacle that is common for any type of cancer treatment is the acquisition of resistance to specific therapy and metastatic dormancy. It is postulated that the signals from the outside of the tumor cell shape the fate of disseminated tumor cells to progress or to pause in the state of dormancy (Ossowski and Aguirre-Ghiso, 2010). Moreover, since tumor microenvironment may also facilitate the development of multidrug resistance (Correia and Bissell, 2012), it is important to incorporate the knowledge on both tumor cells and their respective microenvironments in order to develop

the treatments of malignancies as complex organs rather than mutated cells. Targeting the microenvironment would, presumably, irrespective of the tumor cell heterogeneity, impede their survival and dissemination. In this work we investigated changes in the extracellular matrix of primary melanoma tumors to get a better understanding of how signaling from the extracellular space impacts melanoma cell invasion.

5.1 SKIN ORGAN CULTURES AS A MODEL SYSTEM FOR STUDYING MELANOMA INVASION

Given the microenvironmental complexity of primary melanoma, studies of melanoma cell behavior and drug response have to be undertaken in the models that resemble the natural occurrence most closely. Skin organ cultures are the most advanced *in vitro* system for this purpose, since they allow the incorporation and/or modification of the major cell types of the skin: keratinocytes, melanocytes, fibroblasts and melanoma cells.

In this work we have first shown that melanoma cells incorporated into SOCs modify the extracellular matrix in the way that resembles melanoma microenvironment in human melanoma samples (Hood et al., 2010). Proteomic analysis of laser micro-dissected SOCs detected increased amounts of Tenascin C, Fibronectin and Thrombospondin-1 in melanoma seeded samples, matricellular proteins known to be involved in modulation of cell-matrix interactions (Fukunaga-Kalabis et al., 2008). Furthermore, we were able to detect a difference in the amounts of abundant intracellular proteins involved in cytoskeletal organization such as α-actinin-4 and plectin. The changes we detected in SOCs closely matched the changes detected by the proteomic analysis of the melanoma tissue sample and the uninvolved skin of a melanoma

patient. This proteomic approach shows promise in tracking protein changes in a high-throughput manner in SOCs, compared to traditional immunostaining. For example, the response of the stroma to genetically manipulated melanoma cells and vice versa can be tracked by this approach or effects of therapy application on melanoma matrix composition.

Next, we reasoned that by modifying the dermal compartment of SOCs, the influence of particular microenvironmental components on melanoma cell behavior could be followed. Based on the proteomic data from the patient sample, where significant upregulation of TNC and down-regulation of DCN were detected, we included extra Tenascin C into dermal matrices of SOCs and observed an increased invasion of melanoma cells, or included Decorin and observed an inhibition of invasion. Decorin could also counteract invasion-promoting TNC in this setting. This proves that the composition of the ECM strongly impacts the ability of melanoma cells to disseminate from the primary site.

5.2 HETEROGENEITY OF CANCER CELL MIGRATION PHENOTYPES IN THE MICROENVIRONMENTAL CONTEXT

The influence of the extracellular matrix on cancer invasion has long been recognized (Liotta, 1986). ECM protein TNC has been shown to promote cancer invasion by both MMP-dependent and independent mechanisms (Hancox et al., 2009). TNC induces the expression of MMPs 1, 3, 9 and 13 (Hancox et al., 2009; Tremble et al., 1994) and the activation of MMP2, and there is a positive feedback loop between the induction of MMPs by TNC and its cleavage (Dang et al., 2004). Interestingly, cleavage sites for all the MMPs tested so far are outside of the EGFL repeats domain in the TNC molecule (Siri et al., 1995), leaving them intact in the face of

increased ECM remodeling. As the work from our group has previously shown that distinct EGFL repeats of TNC can promote pro-migratory EGFR signaling cascade (Iyer et al., 2008) we postulated that the increased TNC expression in melanoma allows increased migratory capabilities of cancer cells. Melanoma cells themselves secrete TNC (Herlyn et al., 1991), and we observed that the TNC production increases with an increase in severity of the stage from which the melanoma cells were derived and that the invasiveness in 3D matrices highly correlates with the amounts of TNC being deposited in the matrix (Grahovac et al., 2012). Imaging cells during their migration in three dimensions revealed that TNC is being deposited at the front of the invading cells.

Given that TNC is a multidomain protein, signaling pathways that would promote invasive behavior are not obvious. We therefore over-expressed TNC EGFL repeats with the assembly domain in melanoma cells, and showed that they have profound effect on cell adhesion. Decreased adhesion was not due to changes in integrin expression, but due to increased activation of Rho–associated kinase (ROCK), which induced cytoskeletal reorganization and cell rounding due to contraction. As a result of decreased adhesiveness TNCEGFL-expressing cells moved slower on 2D substrates, but nevertheless moved faster and invaded deeper into 3D matrices, despite there being no increase in MMP activities. The persistence of cell invasion with low adhesion, high intracellular contractility and independence of MMP activity is a characteristic of amoeboid type of movement (Lammermann and Sixt, 2009; Sahai and Marshall, 2003; Wolf et al., 2003). To our knowledge, this is the first signal from the extracellular matrix protein that has been shown to promote mesenchymal to amoeboidal migration switch.

The plasticity of the cell movement allows efficient migration in complex microenvironments and allows more effective cancer dissemination (Friedl and Wolf, 2003). It is

possible that a single cell during its invasion process can oscillate between mesenchymal and amoeboid modes of invasion, which are dictated by the microenvironmental signals, and cell mechanical properties. The initial invadopod-rich phenotype, which is needed for collagen invasion, can be switched to intracellular contractility-driven push through the space that has been released by the matrix-degrading enzymes. This phenotype could be time sensitive, e.g. change every couple of minutes/hours and highly dependent on the encountered ECM. While intracellular signaling pathways that control cell cytoskeleton during migration have been extensively studied, little is known about the signals from the outside of the cell that dictate the phenotypic switches in the migrational mode. Collagen fibril orientation has been shown to dictate the mesenchymal mode of migration (Provenzano et al., 2008), and we now show that EGFL repeats of TNC can induce cytoskeletal changes in melanoma cells that lead to a shift towards amoeboid movement. The expression of TNC not only modulates the structural composition of the ECM, but also permits greater migrational plasticity. We speculate that invadopod protrusions that can localize MMPs in the front of migrating cells (Yamaguchi, 2012) could cleave TNC (which we observed being deposited in the front) and TNCEGFL repeats could signal contraction and rounding of the cell body that then pushes forward. It is possible that after proteolytic cleavage, TNC fragments may have distinct signaling activity compared to the full-length TNC protein. Proposed mechanism by which TNC promotes melanoma cell invasion is depicted in Figure 28. These are further avenues of research that await exploration. Furthermore, it would be interesting to investigate whether TNC expression changes the stiffness of the ECM, as increased stiffness promotes transformation of epithelial cells (reviewed in (Kumar and Weaver, 2009)).

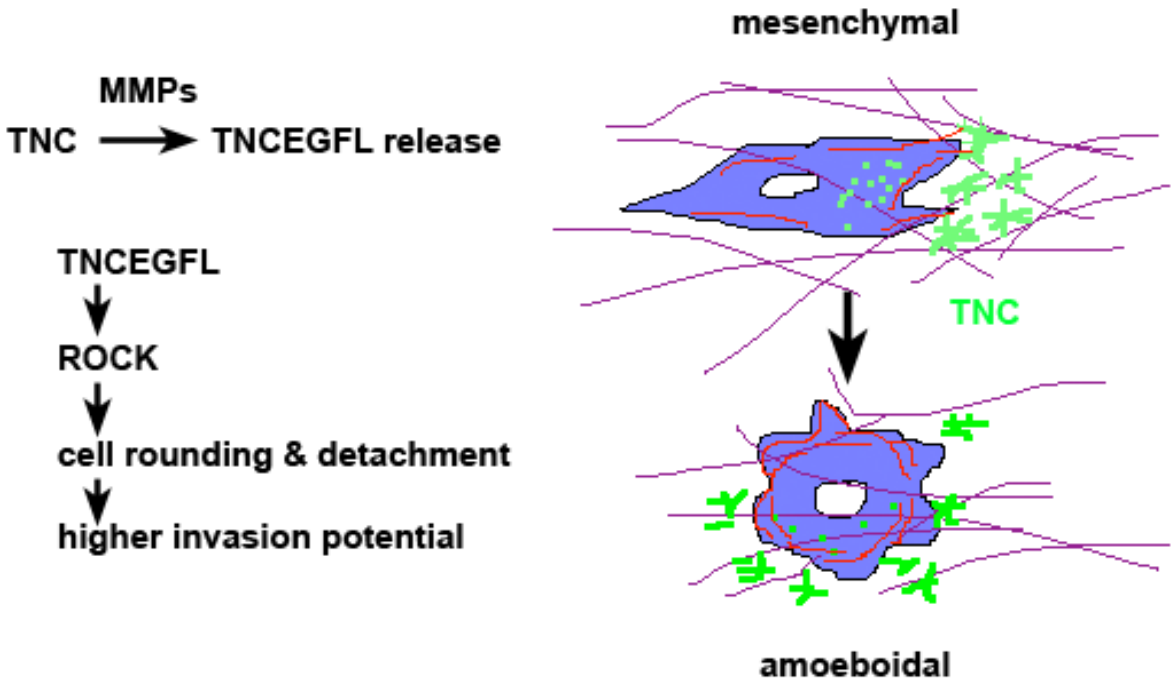

Figure 28. Schematic representation of the proposed mechanism by which TNC promotes melanoma cell invasiveness.

Having in mind plasticity of melanoma cell migration it would be interesting to investigate whether combinational therapy of MMP and ROCK inhibitors targeting both phenotypic modes could abolish melanoma cell migration.

5.3 DECORIN AS AN ANTI-INVASIVE MOIETY

We have found that TNC and DCN have inversed expression in melanoma and benign nevi samples. In melanoma TNC is up-regulated and DCN down-regulated, in contrast to benign nevi which have barely detectable TNC levels and prominent amounts of DCN. The expression of these two proteins is at least in part regulated by the same growth factor: TGFβ1 secreted by melanoma cells down-regulates DCN expression (Mauviel et al., 1995) and up-regulates TNC expression (Berking et al., 2001). These two proteins also have a common receptor – EGFR (Iozzo et al., 1999b; Iyer et al., 2007a), the signaling of which they dictate in opposite manner: DCN induces internalization and attenuation of EGFR (Zhu et al., 2005) while TNC promotes membrane-bound EGF pro-migratory cascades (Iyer et al., 2008).

Decorin possesses intrinsic potent anti-tumorigenic properties. It has a promiscuous binding repertoire consisting of ECM proteins, cell receptors and growth factors, and is considered to be a "guardian from the matrix" (Neill et al., 2012). Although previous studies did not find significant correlation between levels of DCN expression and Breslow tumor thickness or Clark level of melanoma (Brezillon et al., 2007; Gambichler et al., 2008) we found that primary melanoma samples contain decreased DCN amounts compared to benign nevi of the skin. Furthermore, we showed that DCN has a remarkable negative impact on melanoma cell invasion, in both simple collagen dermal equivalents and dermal equivalents enriched with

Tenascin C. Since DCN can inhibit TNC-induced melanoma invasion, we speculate that this inhibitory effect is signaled by inhibition of the EGFR signaling in response to TNC (Figure 29).

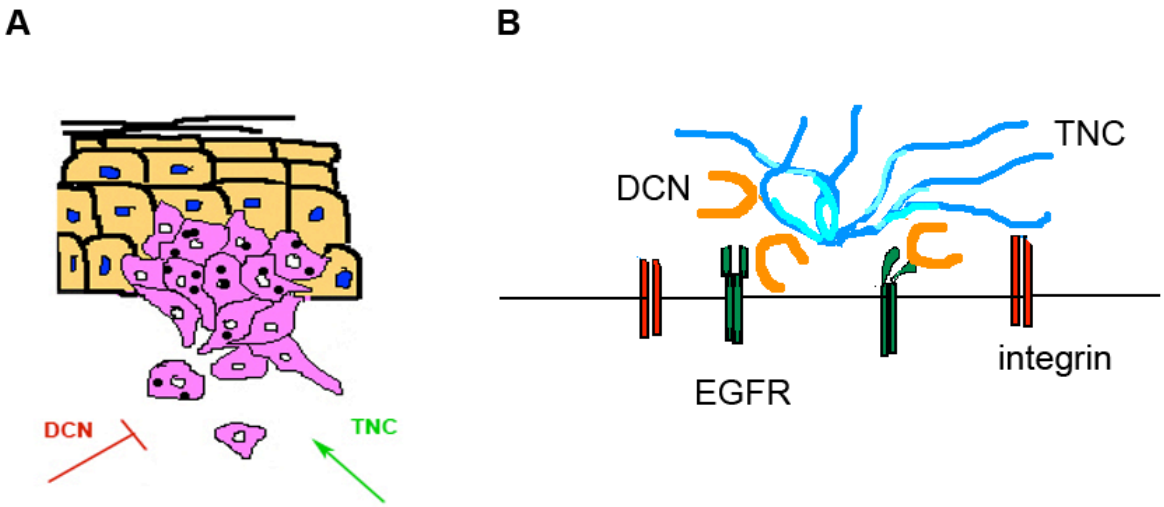

Figure 29. Decorin can counteract pro-invasive effects of TNC on melanoma cells.

(A) Addition of DCN to dermal matrices ameliorates effects of TNC on melanoma invasion. (B) Possible mechanism by which DCN can counteract TNC.

EGFR gene undergoes frequent amplification in advanced melanoma (Koprowski et al., 1985; Udart et al., 2001) and the gain of chromosome 7 copy number (on which EGFR gene resides) occurs later in the melanoma progression (Bastian et al., 1998). Despite the experimental evidence that EGFR can promote melanoma progression there is little clinical evidence that supports single agent anti EGFR therapy (Tsao et al., 2012). However, EGFR axis activation or over expression is a cause for resistance to Vemurafenib, one of the most effective drugs for treatment of melanoma that inhibits the oncopotein BRAF(V600E) (Prahallad et al., 2012). Therefore, the inhibition of EGFR in combinational therapy may be a candidate for future clinical investigations. Decorin could in this case contribute even more profoundly than chemical

EGFR inhibitors as it targets multiple kinase receptors involved in cancer promotion in addition to EGFR (Csordas et al., 2000; Iozzo and Sanderson, 2011). DCN gene delivery has already been shown to retard the growth of human tumors in immunocompromised animals (Reed et al., 2002) and due to its collagen binding capacity can even overcome the extracellular matrix barrier that is a major obstacle for successful adenoviral gene therapy (Choi et al., 2010). Therefore, Decorin is an excellent candidate for combinational therapy both as anti-tumor moiety itself, and as an enhancer of the distribution of targeted gene delivery.

5.4 FUTURE DIRECTIONS

This work has opened several new avenues of research. First, given the extent of knowledge on the composition of the melanoma microenvironment, systems for studying melanoma progression should be heterotypic and designed to mimic heterogeneity of both melanoma cells as well as the supporting stroma. Skin organ cultures could be further adapted to incorporate other cell types found in primary melanomas; such are endothelial cells and macrophages, as these were shown to have a significant role in cancer cell invasion. This model could also be customized to test the drugs that target tumor microenvironment. Second, we have shown that matrikine signaling can influence the mode of melanoma cell migration during the invasion. This plasticity of cell movement should be taken into account when considering melanoma treatment, as the two modes of cancer cell migration have different mechanistics and only the inhibition of both would potentially give results, e.g. a combination of MMP inhibitors and ROCK inhibitors. Finally, the ability of another ECM protein present in normal skin, to

counteract TNC should not be taken lightly. An exploration of the exact signaling mechanisms that DCN elicits to block melanoma cell invasion even in the presence of proinvasive TNC could shed light on potential regulatory nodes in cell pro-migratory molecular network that could be exploited for further drug development.

APPENDIX A

COMPLETE LIST OF PEPTIDES IDENTIFIED IN MELANOMA AND SKIN TISSUE SAMPLES AND SOCS

Appendix can be downloaded from http://pubs.acs.org/doi/full/10.1021/pr100164x

APPENDIX B

B.1 ABBREVIATIONS

ACN-4 – α-actinin-4
ATP – adenosine thriphosphate
bFGF – basic fibroblast growth factor
BRAF – B rapidly accelerated fibrosarcoma kinase
CAF – cancer-associated fibroblast
Cdc42 – cell division cycle protein 42
CGH – comparative genomic hybridization
CK - cytokeratin
COL - Collagen
CTLA-4 - cytotoxic T lymphocyte antigen-4
DAPI - 4',6-diamidino-2-phenylindole
DCN - Decorin
E-cadherin - epithelial cadherin
ECM – extracellular matrix
EGF- epidermal growth factor
EGFR – epidermal growth factor receptor
FBS – fetal bovine serum
FDA -Food and Drug Administration
FFPE – formalin-fixed paraffin-embedded
FN - Fibronectin
FNIII – Fibronectin III like
GAPDH – glyceraldehide-3-phosphate dehydrogenase
GTP – guanosine thriphosphate
IGF-1R – insulin-like growth factor 1 receptor
LTQ – linear trap quadrupole
Met receptor – mesenchymal epithelial transition receptor
MGP - metastatic growth phase
MLC – myosin light chain
MMP – matrix metallo-protease/proteinase
MS – mass spectrometry
MYPT – myosin phosphatase targeting protein
NA – numerical aperture
N-cadherin - neural cadherin
PDGF – platelet-derived growth factor
PLA – proximity ligation assay
Rac – Ras-related C3 botulinum toxin substrate

Ras – Rat sarcoma oncogene
Rho – Ras homolog
RGP - radial growth phase
ROCK – Rho associated kinase
SAGE – serial analysis of gene expression
SD – standard deviation
SEM – standard error mean
SOC – skin organ culture
SPARC – secreted protein acidic rich in cysteine
TGF-β – tumor growth factor β
TLR4 – toll like receptor 4
TMA – tissue micro array
TNC – Tenascin C
TNFα – tumor necrosis factor α
TSP-1 – Thrombospondin-1
VGP - vertical growth phase

BIBLIOGRAPHY

Adams, J. C., and Schwartz, M. A. (2000). Stimulation of fascin spikes by thrombospondin-1 is mediated by the GTPases Rac and Cdc42. J Cell Biol *150*, 807-822.

Albelda, S. M., Mette, S. A., Elder, D. E., Stewart, R., Damjanovich, L., Herlyn, M., and Buck, C. A. (1990). Integrin distribution in malignant melanoma: association of the beta 3 subunit with tumor progression. Cancer Res *50*, 6757-6764.

Allen, M., and Louise Jones, J. (2011). Jekyll and Hyde: the role of the microenvironment on the progression of cancer. J Pathol *223*, 162-176.

Amano, M., Fukata, Y., and Kaibuchi, K. (2000). Regulation and functions of Rho-associated kinase. Exp Cell Res *261*, 44-51.

Aukhil, I., Joshi, P., Yan, Y., and Erickson, H. P. (1993). Cell- and heparin-binding domains of the hexabrachion arm identified by tenascin expression proteins. J Biol Chem *268*, 2542-2553.

Balch, C. M., Gershenwald, J. E., Soong, S. J., Thompson, J. F., Atkins, M. B., Byrd, D. R., Buzaid, A. C., Cochran, A. J., Coit, D. G., Ding, S.*, et al.* (2009). Final version of 2009 AJCC melanoma staging and classification. J Clin Oncol *27*, 6199-6206.

Balsamo, M., Scordamaglia, F., Pietra, G., Manzini, C., Cantoni, C., Boitano, M., Queirolo, P., Vermi, W., Facchetti, F., Moretta, A.*, et al.* (2009). Melanoma-associated fibroblasts modulate NK cell phenotype and antitumor cytotoxicity. Proc Natl Acad Sci U S A *106*, 20847-20852.

Baruthio, F., Quadroni, M., Ruegg, C., and Mariotti, A. (2008). Proteomic analysis of membrane rafts of melanoma cells identifies protein patterns characteristic of the tumor progression stage. Proteomics *8*, 4733-4747.

Bastian, B. C., LeBoit, P. E., Hamm, H., Brocker, E. B., and Pinkel, D. (1998). Chromosomal gains and losses in primary cutaneous melanomas detected by comparative genomic hybridization. Cancer Res *58*, 2170-2175.

Bausch, D., Mino-Kenudson, M., Fernandez-Del Castillo, C., Warshaw, A. L., Kelly, K. A., and Thayer, S. P. (2009). Plectin-1 is a Biomarker of Malignant Pancreatic Intraductal Papillary Mucinous Neoplasms. J Gastrointest Surg.

Becker, J. K., Goldberg, L. H., and Tschen, J. A. (1989). Differential diagnosis of malignant melanoma. Am Fam Physician *39*, 203-214.

Bell, E., Sher, S., Hull, B., Merrill, C., Rosen, S., Chamson, A., Asselineau, D., Dubertret, L., Coulomb, B., Lapiere, C.*, et al.* (1983). The reconstitution of living skin. J Invest Dermatol *81*, 2s-10s.

Bergamaschi, A., Tagliabue, E., Sorlie, T., Naume, B., Triulzi, T., Orlandi, R., Russnes, H. G., Nesland, J. M., Tammi, R., Auvinen, P.*, et al.* (2008). Extracellular matrix signature identifies breast cancer subgroups with different clinical outcome. J Pathol *214*, 357-367.

Berking, C., and Herlyn, M. (2001). Human skin reconstruct models: a new application for studies of melanocyte and melanoma biology. Histol Histopathol *16*, 669-674.

Berking, C., Takemoto, R., Schaider, H., Showe, L., Satyamoorthy, K., Robbins, P., and Herlyn, M. (2001). Transforming growth factor-beta1 increases survival of human melanoma through stroma remodeling. Cancer Res *61*, 8306-8316.

Betz, C., Papadopoulos, T., Buchwald, J., Dammrich, J., and Muller-Hermelink, H. K. (1995). Surfactant protein gene expression in metastatic and micrometastatic pulmonary adenocarcinomas and other non-small cell lung carcinomas: detection by reverse transcriptase-polymerase chain reaction. Cancer Res *55*, 4283-4286.

Betz, P., Nerlich, A., Tubel, J., Penning, R., and Eisenmenger, W. (1993). Localization of tenascin in human skin wounds--an immunohistochemical study. Int J Legal Med *105*, 325-328.

Bianco, P., Fisher, L. W., Young, M. F., Termine, J. D., and Robey, P. G. (1990). Expression and localization of the two small proteoglycans biglycan and decorin in developing human skeletal and non-skeletal tissues. J Histochem Cytochem *38*, 1549-1563.

Bissell, M. J., and Hines, W. C. (2011). Why don't we get more cancer? A proposed role of the microenvironment in restraining cancer progression. Nat Med *17*, 320-329.

Bornstein, P. (2001). Thrombospondins as matricellular modulators of cell function. J Clin Invest *107*, 929-934.

Bornstein, P. (2009). Thrombospondins function as regulators of angiogenesis. J Cell Commun Signal.

Brezillon, S., Venteo, L., Ramont, L., D'Onofrio, M. F., Perreau, C., Pluot, M., Maquart, F. X., and Wegrowski, Y. (2007). Expression of lumican, a small leucine-rich proteoglycan with antitumour activity, in human malignant melanoma. Clin Exp Dermatol *32*, 405-416.

Caron, J., Mange, A., Guillot, B., and Solassol, J. (2009). Highly sensitive detection of melanoma based on serum proteomic profiling. J Cancer Res Clin Oncol *135*, 1257-1264.

Charras, G. T., Hu, C. K., Coughlin, M., and Mitchison, T. J. (2006). Reassembly of contractile actin cortex in cell blebs. J Cell Biol *175*, 477-490.

Chiquet-Ehrismann, R., and Chiquet, M. (2003). Tenascins: regulation and putative functions during pathological stress. J Pathol *200*, 488-499.

Chiquet-Ehrismann, R., Kalla, P., Pearson, C. A., Beck, K., and Chiquet, M. (1988). Tenascin interferes with fibronectin action. Cell *53*, 383-390.

Choi, I. K., Lee, Y. S., Yoo, J. Y., Yoon, A. R., Kim, H., Kim, D. S., Seidler, D. G., Kim, J. H., and Yun, C. O. (2010). Effect of decorin on overcoming the extracellular matrix barrier for oncolytic virotherapy. Gene Ther *17*, 190-201.

Chopra, R. K., Pearson, C. H., Pringle, G. A., Fackre, D. S., and Scott, P. G. (1985). Dermatan sulphate is located on serine-4 of bovine skin proteodermatan sulphate. Demonstration that most molecules possess only one glycosaminoglycan chain and comparison of amino acid sequences around glycosylation sites in different proteoglycans. Biochem J *232*, 277-279.

Chung, C. Y., Murphy-Ullrich, J. E., and Erickson, H. P. (1996). Mitogenesis, cell migration, and loss of focal adhesions induced by tenascin-C interacting with its cell surface receptor, annexin II. Mol Biol Cell *7*, 883-892.

Clark, E. A., Golub, T. R., Lander, E. S., and Hynes, R. O. (2000). Genomic analysis of metastasis reveals an essential role for RhoC. Nature *406*, 532-535.

Clark, W. H., Jr., Elder, D. E., Guerry, D. t., Epstein, M. N., Greene, M. H., and Van Horn, M. (1984). A study of tumor progression: the precursor lesions of superficial spreading and nodular melanoma. Hum Pathol *15*, 1147-1165.

Colotta, F., Allavena, P., Sica, A., Garlanda, C., and Mantovani, A. (2009). Cancer-related inflammation, the seventh hallmark of cancer: links to genetic instability. Carcinogenesis *30*, 1073-1081.

Correia, A. L., and Bissell, M. J. (2012). The tumor microenvironment is a dominant force in multidrug resistance. Drug Resist Updat *15*, 39-49.

Coussens, L. M., Tinkle, C. L., Hanahan, D., and Werb, Z. (2000). MMP-9 supplied by bone marrow-derived cells contributes to skin carcinogenesis. Cell *103*, 481-490.

Csordas, G., Santra, M., Reed, C. C., Eichstetter, I., McQuillan, D. J., Gross, D., Nugent, M. A., Hajnoczky, G., and Iozzo, R. V. (2000). Sustained down-regulation of the epidermal growth factor receptor by decorin. A mechanism for controlling tumor growth in vivo. J Biol Chem *275*, 32879-32887.

Cukierman, E., Pankov, R., Stevens, D. R., and Yamada, K. M. (2001). Taking cell-matrix adhesions to the third dimension. Science *294*, 1708-1712.

Dang, D., Yang, Y., Li, X., Atakilit, A., Regezi, J., Eisele, D., Ellis, D., and Ramos, D. M. (2004). Matrix metalloproteinases and TGFbeta1 modulate oral tumor cell matrix. Biochem Biophys Res Commun *316*, 937-942.

Danielson, K. G., Baribault, H., Holmes, D. F., Graham, H., Kadler, K. E., and Iozzo, R. V. (1997). Targeted disruption of decorin leads to abnormal collagen fibril morphology and skin fragility. J Cell Biol *136*, 729-743.

Davis, G. E., Bayless, K. J., Davis, M. J., and Meininger, G. A. (2000). Regulation of tissue injury responses by the exposure of matricryptic sites within extracellular matrix molecules. Am J Pathol *156*, 1489-1498.

De Wever, O., Nguyen, Q. D., Van Hoorde, L., Bracke, M., Bruyneel, E., Gespach, C., and Mareel, M. (2004). Tenascin-C and SF/HGF produced by myofibroblasts in vitro provide convergent pro-invasive signals to human colon cancer cells through RhoA and Rac. FASEB J *18*, 1016-1018.

DiMilla, P. A., Barbee, K., and Lauffenburger, D. A. (1991). Mathematical model for the effects of adhesion and mechanics on cell migration speed. Biophys J *60*, 15-37.

DiMilla, P. A., Stone, J. A., Quinn, J. A., Albelda, S. M., and Lauffenburger, D. A. (1993). Maximal migration of human smooth muscle cells on fibronectin and type IV collagen occurs at an intermediate attachment strength. J Cell Biol *122*, 729-737.

Dvorak, H. F. (1986). Tumors: wounds that do not heal. Similarities between tumor stroma generation and wound healing. N Engl J Med *315*, 1650-1659.

Dyduch, G., Okon, K., and Pescarini, E. (2011). Mast cells in melanocytic skin lesions. An i mmunohistochemical and quantitative study. Pol J Pathol *62*, 139-144.

Egeblad, M., and Werb, Z. (2002). New functions for the matrix metalloproteinases in cancer progression. Nat Rev Cancer *2*, 161-174.

Elias, G., Hasskamp, J., and Sharma, B. (2010a). Cytokines and Growth Factors Expressed by Human Cutaneous Melanoma. Cancers *2*, 794-808.

Elias, G., Hasskapm, J., and Sharma, B. (2010b). Bology of Human Cutaneous Melanoma. Cancers *2*, 165-189.

Elias, J. E., and Gygi, S. P. (2007). Target-decoy search strategy for increased confidence in large-scale protein identifications by mass spectrometry. Nat Methods *4*, 207-214.

Erickson, H. P., and Bourdon, M. A. (1989). Tenascin: an extracellular matrix protein prominent in specialized embryonic tissues and tumors. Annu Rev Cell Biol *5*, 71-92.

Eves, P., Katerinaki, E., Simpson, C., Layton, C., Dawson, R., Evans, G., and Mac Neil, S. (2003). Melanoma invasion in reconstructed human skin is influenced by skin cells--investigation of the role of proteolytic enzymes. Clin Exp Metastasis *20*, 685-700.

Eves, P., Layton, C., Hedley, S., Dawson, R. A., Wagner, M., Morandini, R., Ghanem, G., and Mac Neil, S. (2000). Characterization of an in vitro model of human melanoma invasion based on reconstructed human skin. Br J Dermatol *142*, 210-222.

Felding-Habermann, B., Mueller, B. M., Romerdahl, C. A., and Cheresh, D. A. (1992). Involvement of integrin alpha V gene expression in human melanoma tumorigenicity. J Clin Invest *89*, 2018-2022.

Filsell, W., Rudman, S., Jenkins, G., and Green, M. R. (1999). Coordinate upregulation of tenascin C expression with degree of photodamage in human skin. Br J Dermatol *140*, 592-599.

Forgber, M., Trefzer, U., Sterry, W., and Walden, P. (2009). Proteome serological determination of tumor-associated antigens in melanoma. PLoS One *4*, e5199.

Friedl, P. (2004). Prespecification and plasticity: shifting mechanisms of cell migration. Curr Opin Cell Biol *16*, 14-23.

Friedl, P., and Gilmour, D. (2009). Collective cell migration in morphogenesis, regeneration and cancer. Nat Rev Mol Cell Biol *10*, 445-457.

Friedl, P., and Wolf, K. (2003). Tumour-cell invasion and migration: diversity and escape mechanisms. Nat Rev Cancer *3*, 362-374.

Friedl, P., and Wolf, K. (2010). Plasticity of cell migration: a multiscale tuning model. J Cell Biol *188*, 11-19.

Friedl, P., Zanker, K. S., and Brocker, E. B. (1998). Cell migration strategies in 3-D extracellular matrix: differences in morphology, cell matrix interactions, and integrin function. Microsc Res Tech *43*, 369-378.

Fritz, G., Just, I., and Kaina, B. (1999). Rho GTPases are over-expressed in human tumors. Int J Cancer *81*, 682-687.

Fukunaga-Kalabis, M., Martinez, G., Nguyen, T. K., Kim, D., Santiago-Walker, A., Roesch, A., and Herlyn, M. (2010). Tenascin-C promotes melanoma progression by maintaining the ABCB5-positive side population. Oncogene *29*, 6115-6124.

Fukunaga-Kalabis, M., Santiago-Walker, A., and Herlyn, M. (2008). Matricellular proteins produced by melanocytes and melanomas: in search for functions. Cancer Microenviron *1*, 93-102.

Gaggioli, C., and Sahai, E. (2007). Melanoma invasion - current knowledge and future directions. Pigment Cell Res *20*, 161-172.

Galoian, K. A., Garamszegi, N., Garamszegi, S. P., and Scully, S. P. (2007). Molecular mechanism of tenascin-C action on matrix metalloproteinase-1 invasive potential. Exp Biol Med (Maywood) *232*, 515-522.

Gambichler, T., Kreuter, A., Grothe, S., Altmeyer, P., Brockmeyer, N. H., and Rotterdam, S. (2008). Versican overexpression in cutaneous malignant melanoma. Eur J Med Res *13*, 500-504.

Ghosh, M. M., Boyce, S., Layton, C., Freedlander, E., and Mac Neil, S. (1997). A comparison of methodologies for the preparation of human epidermal-dermal composites. Ann Plast Surg *39*, 390-404.

Giancotti, F. G., and Ruoslahti, E. (1999). Integrin signaling. Science *285*, 1028-1032.
Giannelli, G., Falk-Marzillier, J., Schiraldi, O., Stetler-Stevenson, W. G., and Quaranta, V. (1997). Induction of cell migration by matrix metalloprotease-2 cleavage of laminin-5. Science *277*, 225-228.
Goldoni, S., Humphries, A., Nystrom, A., Sattar, S., Owens, R. T., McQuillan, D. J., Ireton, K., and Iozzo, R. V. (2009). Decorin is a novel antagonistic ligand of the Met receptor. J Cell Biol *185*, 743-754.
Grahovac, J., Becker, D., and Wells, A. (2012). Melanoma Cell Invasiveness Is Promoted at Least in Part by the Epidermal Growth Factor-Like Repeats of Tenascin-C. J Invest Dermatol.doi: 10.1038/jid.2012.263. [Epub ahead of print]
Haass, N. K., Smalley, K. S., and Herlyn, M. (2004). The role of altered cell-cell communication in melanoma progression. J Mol Histol *35*, 309-318.
Haass, N. K., Smalley, K. S., Li, L., and Herlyn, M. (2005). Adhesion, migration and communication in melanocytes and melanoma. Pigment Cell Res *18*, 150-159.
Hanahan, D., and Weinberg, R. A. (2000). The hallmarks of cancer. Cell *100*, 57-70.
Hanamura, N., Yoshida, T., Matsumoto, E., Kawarada, Y., and Sakakura, T. (1997). Expression of fibronectin and tenascin-C mRNA by myofibroblasts, vascular cells and epithelial cells in human colon adenomas and carcinomas. Int J Cancer *73*, 10-15.
Hancox, R. A., Allen, M. D., Holliday, D. L., Edwards, D. R., Pennington, C. J., Guttery, D. S., Shaw, J. A., Walker, R. A., Pringle, J. H., and Jones, J. L. (2009). Tumour-associated tenascin-C isoforms promote breast cancer cell invasion and growth by matrix metalloproteinase-dependent and independent mechanisms. Breast Cancer Res *11*, R24.
Hendrix, M. J., Seftor, E. A., Kirschmann, D. A., Quaranta, V., and Seftor, R. E. (2003). Remodeling of the microenvironment by aggressive melanoma tumor cells. Ann N Y Acad Sci *995*, 151-161.
Herlyn, M. (2009). Driving in the melanoma landscape. Exp Dermatol *18*, 506-508.
Herlyn, M., Ferrone, S., Ronai, Z., Finerty, J., Pelroy, R., and Mohla, S. (2001). Melanoma biology and progression. Cancer Res *61*, 4642-4643.
Herlyn, M., Graeven, U., Speicher, D., Sela, B. A., Bennicelli, J. L., Kath, R., and Guerry, D. t. (1991). Characterization of tenascin secreted by human melanoma cells. Cancer Res *51*, 4853-4858.
Hildebrand, A., Romaris, M., Rasmussen, L. M., Heinegard, D., Twardzik, D. R., Border, W. A., and Ruoslahti, E. (1994). Interaction of the small interstitial proteoglycans biglycan, decorin and fibromodulin with transforming growth factor beta. Biochem J *302 (Pt 2)*, 527-534.
Honardoust, D., Varkey, M., Marcoux, Y., Shankowsky, H. A., and Tredget, E. E. (2012). Reduced decorin, fibromodulin, and transforming growth factor-beta3 in deep dermis leads to hypertrophic scarring. J Burn Care Res *33*, 218-227.
Hood, B. L., Grahovac, J., Flint, M. S., Sun, M., Charro, N., Becker, D., Wells, A., and Conrads, T. P. (2010). Proteomic analysis of laser microdissected melanoma cells from skin organ cultures. J Proteome Res *9*, 3656-3663.
Hooper, S., Marshall, J. F., and Sahai, E. (2006). Tumor cell migration in three dimensions. Methods Enzymol *406*, 625-643.
Hsu, M. Y., Meier, F., and Herlyn, M. (2002). Melanoma development and progression: a conspiracy between tumor and host. Differentiation *70*, 522-536.

Hsu, M. Y., Meier, F. E., Nesbit, M., Hsu, J. Y., Van Belle, P., Elder, D. E., and Herlyn, M. (2000). E-cadherin expression in melanoma cells restores keratinocyte-mediated growth control and down-regulates expression of invasion-related adhesion receptors. Am J Pathol *156*, 1515-1525.

Hsu, M. Y., Shih, D. T., Meier, F. E., Van Belle, P., Hsu, J. Y., Elder, D. E., Buck, C. A., and Herlyn, M. (1998). Adenoviral gene transfer of beta3 integrin subunit induces conversion from radial to vertical growth phase in primary human melanoma. Am J Pathol *153*, 1435-1442.

Hu, M., and Polyak, K. (2008a). Microenvironmental regulation of cancer development. Curr Opin Genet Dev *18*, 27-34.

Hu, M., and Polyak, K. (2008b). Molecular characterisation of the tumour microenvironment in breast cancer. Eur J Cancer *44*, 2760-2765.

Huang, Q., Chen, W., Wang, L., Lin, W., Lin, J., and Lin, X. (2008). Identification of transgelin as a potential novel biomarker for gastric adenocarcinoma based on proteomics technology. J Cancer Res Clin Oncol *134*, 1219-1227.

Huang, W., Chiquet-Ehrismann, R., Moyano, J. V., Garcia-Pardo, A., and Orend, G. (2001). Interference of tenascin-C with syndecan-4 binding to fibronectin blocks cell adhesion and stimulates tumor cell proliferation. Cancer Res *61*, 8586-8594.

Hussein, M. R., Elsers, D. A., Fadel, S. A., and Omar, A. E. (2006). Immunohistological characterisation of tumour infiltrating lymphocytes in melanocytic skin lesions. J Clin Pathol *59*, 316-324.

Hynes, R. O. (2009). The extracellular matrix: not just pretty fibrils. Science *326*, 1216-1219.

Hynes, R. O. (2012). The evolution of metazoan extracellular matrix. J Cell Biol *196*, 671-679.

Ilmonen, S., Jahkola, T., Turunen, J. P., Muhonen, T., and Asko-Seljavaara, S. (2004). Tenascin-C in primary malignant melanoma of the skin. Histopathology *45*, 405-411.

Imai, K., Kusakabe, M., Sakakura, T., Nakanishi, I., and Okada, Y. (1994). Susceptibility of tenascin to degradation by matrix metalloproteinases and serine proteinases. FEBS Lett *352*, 216-218.

Iozzo, R. V., Buraschi, S., Genua, M., Xu, S. Q., Solomides, C. C., Peiper, S. C., Gomella, L. G., Owens, R. C., and Morrione, A. (2011). Decorin antagonizes IGF receptor I (IGF-IR) function by interfering with IGF-IR activity and attenuating downstream signaling. J Biol Chem *286*, 34712-34721.

Iozzo, R. V., Chakrani, F., Perrotti, D., McQuillan, D. J., Skorski, T., Calabretta, B., and Eichstetter, I. (1999a). Cooperative action of germ-line mutations in decorin and p53 accelerates lymphoma tumorigenesis. Proc Natl Acad Sci U S A *96*, 3092-3097.

Iozzo, R. V., Moscatello, D. K., McQuillan, D. J., and Eichstetter, I. (1999b). Decorin is a biological ligand for the epidermal growth factor receptor. J Biol Chem *274*, 4489-4492.

Iozzo, R. V., and Sanderson, R. D. (2011). Proteoglycans in cancer biology, tumour microenvironment and angiogenesis. J Cell Mol Med *15*, 1013-1031.

Iyer, A. K., Tran, K. T., Borysenko, C. W., Cascio, M., Camacho, C. J., Blair, H. C., Bahar, I., and Wells, A. (2007). Tenascin cytotactin epidermal growth factor-like repeat binds epidermal growth factor receptor with low affinity. J Cell Physiol *211*, 748-758.

Iyer, A. K., Tran, K. T., Griffith, L., and Wells, A. (2008). Cell surface restriction of EGFR by a tenascin cytotactin-encoded EGF-like repeat is preferential for motility-related signaling. J Cell Physiol *214*, 504-512.

Jarvelainen, H., Sainio, A., Koulu, M., Wight, T. N., and Penttinen, R. (2009). Extracellular matrix molecules: potential targets in pharmacotherapy. Pharmacol Rev *61*, 198-223.

Javaherian, A., Vaccariello, M., Fusenig, N. E., and Garlick, J. A. (1998). Normal keratinocytes suppress early stages of neoplastic progression in stratified epithelium. Cancer Res *58*, 2200-2208.

Jones, F. S., and Jones, P. L. (2000a). The tenascin family of ECM glycoproteins: structure, function, and regulation during embryonic development and tissue remodeling. Dev Dyn *218*, 235-259.

Jones, P. L., and Jones, F. S. (2000b). Tenascin-C in development and disease: gene regulation and cell function. Matrix Biol *19*, 581-596.

Kaariainen, E., Nummela, P., Soikkeli, J., Yin, M., Lukk, M., Jahkola, T., Virolainen, S., Ora, A., Ukkonen, E., Saksela, O., and Holtta, E. (2006). Switch to an invasive growth phase in melanoma is associated with tenascin-C, fibronectin, and procollagen-I forming specific channel structures for invasion. J Pathol *210*, 181-191.

Kassis, J., Lauffenburger, D. A., Turner, T., and Wells, A. (2001). Tumor invasion as dysregulated cell motility. Semin Cancer Biol *11*, 105-117.

Keene, D. R., San Antonio, J. D., Mayne, R., McQuillan, D. J., Sarris, G., Santoro, S. A., and Iozzo, R. V. (2000). Decorin binds near the C terminus of type I collagen. J Biol Chem *275*, 21801-21804.

Keller, H., and Eggli, P. (1998). Protrusive activity, cytoplasmic compartmentalization, and restriction rings in locomoting blebbing Walker carcinosarcoma cells are related to detachment of cortical actin from the plasma membrane. Cell Motil Cytoskeleton *41*, 181-193.

Kessenbrock, K., Plaks, V., and Werb, Z. (2010). Matrix metalloproteinases: regulators of the tumor microenvironment. Cell *141*, 52-67.

Koprowski, H., Herlyn, M., Balaban, G., Parmiter, A., Ross, A., and Nowell, P. (1985). Expression of the receptor for epidermal growth factor correlates with increased dosage of chromosome 7 in malignant melanoma. Somat Cell Mol Genet *11*, 297-302.

Kumar, S., and Weaver, V. M. (2009). Mechanics, malignancy, and metastasis: the force journey of a tumor cell. Cancer Metastasis Rev *28*, 113-127.

Lammermann, T., and Sixt, M. (2009). Mechanical modes of 'amoeboid' cell migration. Curr Opin Cell Biol *21*, 636-644.

Latijnhouwers, M., Bergers, M., Ponec, M., Dijkman, H., Andriessen, M., and Schalkwijk, J. (1997). Human epidermal keratinocytes are a source of tenascin-C during wound healing. J Invest Dermatol *108*, 776-783.

Latijnhouwers, M. A., Bergers, M., Van Bergen, B. H., Spruijt, K. I., Andriessen, M. P., and Schalkwijk, J. (1996). Tenascin expression during wound healing in human skin. J Pathol *178*, 30-35.

Lauffenburger, D. A., and Horwitz, A. F. (1996). Cell migration: a physically integrated molecular process. Cell *84*, 359-369.

Ledda, F., Bravo, A. I., Adris, S., Bover, L., Mordoh, J., and Podhajcer, O. L. (1997). The expression of the secreted protein acidic and rich in cysteine (SPARC) is associated with the neoplastic progression of human melanoma. J Invest Dermatol *108*, 210-214.

Lee, K. Y., Liu, Y. H., Ho, C. C., Pei, R. J., Yeh, K. T., Cheng, C. C., and Lai, Y. S. (2004). An early evaluation of malignant tendency with plectin expression in human colorectal adenoma and adenocarcinoma. J Med *35*, 141-149.

Li, G., Satyamoorthy, K., Meier, F., Berking, C., Bogenrieder, T., and Herlyn, M. (2003). Function and regulation of melanoma-stromal fibroblast interactions: when seeds meet soil. Oncogene *22*, 3162-3171.

Li, L., Dragulev, B., Zigrino, P., Mauch, C., and Fox, J. W. (2009). The invasive potential of human melanoma cell lines correlates with their ability to alter fibroblast gene expression in vitro and the stromal microenvironment in vivo. Int J Cancer *125*, 1796-1804.

Lightner, V. A., Gumkowski, F., Bigner, D. D., and Erickson, H. P. (1989). Tenascin/hexabrachion in human skin: biochemical identification and localization by light and electron microscopy. J Cell Biol *108*, 2483-2493.

Liotta, L. A. (1986). Tumor invasion and metastases--role of the extracellular matrix: Rhoads Memorial Award lecture. Cancer Res *46*, 1-7.

Liu, H., Sadygov, R. G., and Yates, J. R., 3rd (2004). A model for random sampling and estimation of relative protein abundance in shotgun proteomics. Anal Chem *76*, 4193-4201.

Liu, K., and Shih, N. (2007). The Role of Enolase in Tissue Invasion and Metastasis of Pathogens and Tumor Cells. Journal of Cancer Molecules *3*, 45-48.

Mackie, E. J., Tucker, R. P., Halfter, W., Chiquet-Ehrismann, R., and Epperlein, H. H. (1988). The distribution of tenascin coincides with pathways of neural crest cell migration. Development *102*, 237-250.

Malanchi, I., Santamaria-Martinez, A., Susanto, E., Peng, H., Lehr, H. A., Delaloye, J. F., and Huelsken, J. (2012). Interactions between cancer stem cells and their niche govern metastatic colonization. Nature *481*, 85-89.

Maniotis, A. J., Folberg, R., Hess, A., Seftor, E. A., Gardner, L. M., Pe'er, J., Trent, J. M., Meltzer, P. S., and Hendrix, M. J. (1999). Vascular channel formation by human melanoma cells in vivo and in vitro: vasculogenic mimicry. Am J Pathol *155*, 739-752.

Maquart, F. X., Simeon, A., Pasco, S., and Monboisse, J. C. (1999). [Regulation of cell activity by the extracellular matrix: the concept of matrikines]. J Soc Biol *193*, 423-428.

Margulis, A., Zhang, W., and Garlick, J. A. (2005). In vitro fabrication of engineered human skin. Methods Mol Biol *289*, 61-70.

Marionnet, C., Pierrard, C., Vioux-Chagnoleau, C., Sok, J., Asselineau, D., and Bernerd, F. (2006). Interactions between fibroblasts and keratinocytes in morphogenesis of dermal epidermal junction in a model of reconstructed skin. J Invest Dermatol *126*, 971-979.

Mauviel, A., Santra, M., Chen, Y. Q., Uitto, J., and Iozzo, R. V. (1995). Transcriptional regulation of decorin gene expression. Induction by quiescence and repression by tumor necrosis factor-alpha. J Biol Chem *270*, 11692-11700.

Meier, F., Nesbit, M., Hsu, M. Y., Martin, B., Van Belle, P., Elder, D. E., Schaumburg-Lever, G., Garbe, C., Walz, T. M., Donatien, P.*, et al.* (2000). Human melanoma progression in skin reconstructs : biological significance of bFGF. Am J Pathol *156*, 193-200.

Merline, R., Moreth, K., Beckmann, J., Nastase, M. V., Zeng-Brouwers, J., Tralhao, J. G., Lemarchand, P., Pfeilschifter, J., Schaefer, R. M., Iozzo, R. V., and Schaefer, L. (2011). Signaling by the matrix proteoglycan decorin controls inflammation and cancer through PDCD4 and MicroRNA-21. Sci Signal *4*, ra75.

Midwood, K., Sacre, S., Piccinini, A. M., Inglis, J., Trebaul, A., Chan, E., Drexler, S., Sofat, N., Kashiwagi, M., Orend, G.*, et al.* (2009). Tenascin-C is an endogenous activator of Toll-like receptor 4 that is essential for maintaining inflammation in arthritic joint disease. Nat Med *15*, 774-780.

Midwood, K. S., Hussenet, T., Langlois, B., and Orend, G. (2011). Advances in tenascin-C biology. Cell Mol Life Sci *68*, 3175-3199.

Midwood, K. S., and Orend, G. (2009). The role of tenascin-C in tissue injury and tumorigenesis. J Cell Commun Signal *3*, 287-310.

Miki, H., Suetsugu, S., and Takenawa, T. (1998). WAVE, a novel WASP-family protein involved in actin reorganization induced by Rac. EMBO J *17*, 6932-6941.

Montgomery, A. M., Reisfeld, R. A., and Cheresh, D. A. (1994). Integrin alpha v beta 3 rescues melanoma cells from apoptosis in three-dimensional dermal collagen. Proc Natl Acad Sci U S A *91*, 8856-8860.

Murphy-Ullrich, J. E. (2001). The de-adhesive activity of matricellular proteins: is intermediate cell adhesion an adaptive state? J Clin Invest *107*, 785-790.

Murphy-Ullrich, J. E., and Hook, M. (1989). Thrombospondin modulates focal adhesions in endothelial cells. J Cell Biol *109*, 1309-1319.

Murphy-Ullrich, J. E., Lightner, V. A., Aukhil, I., Yan, Y. Z., Erickson, H. P., and Hook, M. (1991). Focal adhesion integrity is downregulated by the alternatively spliced domain of human tenascin. J Cell Biol *115*, 1127-1136.

Naba, A., Clauser, K. R., Hoersch, S., Liu, H., Carr, S. A., and Hynes, R. O. (2012). The matrisome: in silico definition and in vivo characterization by proteomics of normal and t umor extracellular matrices. Mol Cell Proteomics *11*, M111 014647.

Nardin, A., Wong, W. C., Tow, C., Molina, T. J., Tissier, F., Audebourg, A., Garcette, M., Caignard, A., Avril, M. F., Abastado, J. P., and Prevost-Blondel, A. (2011). Dacarbazine promotes stromal remodeling and lymphocyte infiltration in cutaneous melanoma lesions. J Invest Dermatol *131*, 1896-1905.

Natali, P. G., Hamby, C. V., Felding-Habermann, B., Liang, B., Nicotra, M. R., Di Filippo, F., Giannarelli, D., Temponi, M., and Ferrone, S. (1997). Clinical significance of alpha(v)beta3 integrin and intercellular adhesion molecule-1 expression in cutaneous malignant melanoma lesions. Cancer Res *57*, 1554-1560.

Natali, P. G., Nicotra, M. R., Bartolazzi, A., Cavaliere, R., and Bigotti, A. (1993). Integrin expression in cutaneous malignant melanoma: association of the alpha 3/beta 1 heterodimer with tumor progression. Int J Cancer *54*, 68-72.

Natali, P. G., Nicotra, M. R., Di Filippo, F., and Bigotti, A. (1995). Expression of fibronectin, fibronectin isoforms and integrin receptors in melanocytic lesions. Br J Cancer *71*, 1243-1247.

Nawarak, J., Huang-Liu, R., Kao, S. H., Liao, H. H., Sinchaikul, S., Chen, S. T., and Cheng, S. L. (2009). Proteomics analysis of A375 human malignant melanoma cells in response to arbutin treatment. Biochim Biophys Acta *1794*, 159-167.

Neil, S. M., Eves, P., Richardson, B., Molife, R., Lorigan, P., Wagner, M., Layton, C., Morandini, R., and Ghanem, G. (2000). Oestrogenic steroids and melanoma cell interaction with adjacent skin cells influence invasion of melanoma cells in vitro. Pigment Cell Res *13 Suppl 8*, 68-72.

Neill, T., Schaefer, L., and Iozzo, R. V. (2012). Decorin: a guardian from the matrix. Am J Pathol *181*, 380-387.

Nishio, T., Kawaguchi, S., Yamamoto, M., Iseda, T., Kawasaki, T., and Hase, T. (2005). Tenascin-C regulates proliferation and migration of cultured astrocytes in a scratch wound assay. Neuroscience *132*, 87-102.

Nobes, C. D., and Hall, A. (1995). Rho, rac, and cdc42 GTPases regulate the assembly of multimolecular focal complexes associated with actin stress fibers, lamellipodia, and filopodia. Cell *81*, 53-62.

Nystrom, M. L., Thomas, G. J., Stone, M., Mackenzie, I. C., Hart, I. R., and Marshall, J. F. (2005). Development of a quantitative method to analyse tumour cell invasion in organotypic culture. J Pathol *205*, 468-475.

Olumi, A. F., Grossfeld, G. D., Hayward, S. W., Carroll, P. R., Tlsty, T. D., and Cunha, G. R. (1999). Carcinoma-associated fibroblasts direct tumor progression of initiated human prostatic epithelium. Cancer Res *59*, 5002-5011.

Orend, G. (2005). Potential oncogenic action of tenascin-C in tumorigenesis. Int J Biochem Cell Biol *37*, 1066-1083.

Orend, G., and Chiquet-Ehrismann, R. (2000). Adhesion modulation by antiadhesive molecules of the extracellular matrix. Exp Cell Res *261*, 104-110.

Orend, G., and Chiquet-Ehrismann, R. (2006). Tenascin-C induced signaling in cancer. Cancer Lett *244*, 143-163.

Oskarsson, T., Acharyya, S., Zhang, X. H., Vanharanta, S., Tavazoie, S. F., Morris, P. G., Downey, R. J., Manova-Todorova, K., Brogi, E., and Massague, J. (2011). Breast cancer cells produce tenascin C as a metastatic niche component to colonize the lungs. Nat Med *17*, 867-874.

Oskarsson, T., and Massague, J. (2012). Extracellular matrix players in metastatic niches. EMBO J *31*, 254-256.

Ossowski, L., and Aguirre-Ghiso, J. A. (2010). Dormancy of metastatic melanoma. Pigment Cell Melanoma Res *23*, 41-56.

Palecek, S. P., Loftus, J. C., Ginsberg, M. H., Lauffenburger, D. A., and Horwitz, A. F. (1997). Integrin-ligand binding properties govern cell migration speed through cell-substratum adhesiveness. Nature *385*, 537-540.

Pankova, K., Rosel, D., Novotny, M., and Brabek, J. (2010). The molecular mechanisms of transition between mesenchymal and amoeboid invasiveness in tumor cells. Cell Mol Life Sci *67*, 63-71.

Paron, I., Berchtold, S., Voros, J., Shamarla, M., Erkan, M., Hofler, H., and Esposito, I. (2011). Tenascin-C enhances pancreatic cancer cell growth and motility and affects cell adhesion through activation of the integrin pathway. PLoS One *6*, e21684.

Pas, J., Wyszko, E., Rolle, K., Rychlewski, L., Nowak, S., Zukiel, R., and Barciszewski, J. (2006). Analysis of structure and function of tenascin-C. Int J Biochem Cell Biol *38*, 1594-1602.

Patel, V., Hood, B. L., Molinolo, A. A., Lee, N. H., Conrads, T. P., Braisted, J. C., Krizman, D. B., Veenstra, T. D., and Gutkind, J. S. (2008). Proteomic analysis of laser-captured paraffin-embedded tissues: a molecular portrait of head and neck cancer progression. Clin Cancer Res *14*, 1002-1014.

Paulitschke, V., Kunstfeld, R., Mohr, T., Slany, A., Micksche, M., Drach, J., Zielinski, C., Pehamberger, H., and Gerner, C. (2009). Entering a new era of rational biomarker discovery for early detection of melanoma metastases: secretome analysis of associated stroma cells. J Proteome Res *8*, 2501-2510.

Perlis, C., and Herlyn, M. (2004). Recent advances in melanoma biology. Oncologist *9*, 182-187.

Pezzolo, A., Parodi, F., Marimpietri, D., Raffaghello, L., Cocco, C., Pistorio, A., Mosconi, M., Gambini, C., Cilli, M., Deaglio, S., *et al.* (2011). Oct-4+/Tenascin C+ neuroblastoma cells serve as progenitors of tumor-derived endothelial cells. Cell Res *21*, 1470-1486.

Prahallad, A., Sun, C., Huang, S., Di Nicolantonio, F., Salazar, R., Zecchin, D., Beijersbergen, R. L., Bardelli, A., and Bernards, R. (2012). Unresponsiveness of colon cancer to BRAF(V600E) inhibition through feedback activation of EGFR. Nature *483*, 100-103.

Prieto, A. L., Andersson-Fisone, C., and Crossin, K. L. (1992). Characterization of multiple adhesive and counteradhesive domains in the extracellular matrix protein cytotactin. J Cell Biol *119*, 663-678.

Provenzano, P. P., Inman, D. R., Eliceiri, K. W., Trier, S. M., and Keely, P. J. (2008). Contact guidance mediated three-dimensional cell migration is regulated by Rho/ROCK-dependent matrix reorganization. Biophys J *95*, 5374-5384.

Pyke, C., Romer, J., Kallunki, P., Lund, L. R., Ralfkiaer, E., Dano, K., and Tryggvason, K. (1994). The gamma 2 chain of kalinin/laminin 5 is preferentially expressed in invading malignant cells in human cancers. Am J Pathol *145*, 782-791.

Quatresooz, P., Reginster, M. A., and Pierard, G. E. (2011). 'Malignant melanoma microecosystem': Immunohistopathological insights into the stromal cell phenotype. Exp Ther Med *2*, 379-384.

Ramos, D. M., Chen, B., Regezi, J., Zardi, L., and Pytela, R. (1998). Tenascin-C matrix assembly in oral squamous cell carcinoma. Int J Cancer *75*, 680-687.

Reed, C. C., Gauldie, J., and Iozzo, R. V. (2002). Suppression of tumorigenicity by adenovirus-mediated gene transfer of decorin. Oncogene *21*, 3688-3695.

Reed, C. C., and Iozzo, R. V. (2002). The role of decorin in collagen fibrillogenesis and skin homeostasis. Glycoconj J *19*, 249-255.

Regnier, M., Schweizer, J., Michel, S., Bailly, C., and Prunieras, M. (1986). Expression of high molecular weight (67K) keratin in human keratinocytes cultured on dead de-epidermized dermis. Exp Cell Res *165*, 63-72.

Ren, X. D., Wang, R., Li, Q., Kahek, L. A., Kaibuchi, K., and Clark, R. A. (2004). Disruption of Rho signal transduction upon cell detachment. J Cell Sci *117*, 3511-3518.

Ridley, A. J., and Hall, A. (1992). The small GTP-binding protein rho regulates the assembly of focal adhesions and actin stress fibers in response to growth factors. Cell *70*, 389-399.

Ridley, A. J., Paterson, H. F., Johnston, C. L., Diekmann, D., and Hall, A. (1992). The small GTP-binding protein rac regulates growth factor-induced membrane ruffling. Cell *70*, 401-410.

Riker, A. I., Enkemann, S. A., Fodstad, O., Liu, S., Ren, S., Morris, C., Xi, Y., Howell, P., Metge, B., Samant, R. S., *et al.* (2008). The gene expression profiles of primary and metastatic melanoma yields a transition point of tumor progression and metastasis. BMC Med Genomics *1*, 13.

Rodeck, U., Melber, K., Kath, R., Menssen, H. D., Varello, M., Atkinson, B., and Herlyn, M. (1991). Constitutive expression of multiple growth factor genes by melanoma cells but not normal melanocytes. J Invest Dermatol *97*, 20-26.

Rofstad, E. K., and Graff, B. A. (2001). Thrombospondin-1-mediated metastasis suppression by the primary tumor in human melanoma xenografts. J Invest Dermatol *117*, 1042-1049.

Rohatgi, R., Ma, L., Miki, H., Lopez, M., Kirchhausen, T., Takenawa, T., and Kirschner, M. W. (1999). The interaction between N-WASP and the Arp2/3 complex links Cdc42-dependent signals to actin assembly. Cell *97*, 221-231.

Sahai, E., and Marshall, C. J. (2003). Differing modes of tumour cell invasion have distinct requirements for Rho/ROCK signalling and extracellular proteolysis. Nat Cell Biol *5*, 711-719.

Saito, Y., Imazeki, H., Miura, S., Yoshimura, T., Okutsu, H., Harada, Y., Ohwaki, T., Nagao, O., Kamiya, S., Hayashi, R.*, et al.* (2007). A peptide derived from tenascin-C induces beta1 integrin activation through syndecan-4. J Biol Chem *282*, 34929-34937.

Sander, E. E., ten Klooster, J. P., van Delft, S., van der Kammen, R. A., and Collard, J. G. (1999). Rac downregulates Rho activity: reciprocal balance between both GTPases determines cellular morphology and migratory behavior. J Cell Biol *147*, 1009-1022.

Santiago-Walker, A., Li, L., Haass, N. K., and Herlyn, M. (2009). Melanocytes: from morphology to application. Skin Pharmacol Physiol *22*, 114-121.

Santra, M., Eichstetter, I., and Iozzo, R. V. (2000). An anti-oncogenic role for decorin. Down-regulation of ErbB2 leads to growth suppression and cytodifferentiation of mammary carcinoma cells. J Biol Chem *275*, 35153-35161.

Santra, M., Reed, C. C., and Iozzo, R. V. (2002). Decorin binds to a narrow region of the epidermal growth factor (EGF) receptor, partially overlapping but distinct from the EGF-binding epitope. J Biol Chem *277*, 35671-35681.

Sanz-Moreno, V., Gadea, G., Ahn, J., Paterson, H., Marra, P., Pinner, S., Sahai, E., and Marshall, C. J. (2008). Rac activation and inactivation control plasticity of tumor cell movement. Cell *135*, 510-523.

Sanz-Moreno, V., Gaggioli, C., Yeo, M., Albrengues, J., Wallberg, F., Viros, A., Hooper, S., Mitter, R., Feral, C. C., Cook, M.*, et al.* (2011). ROCK and JAK1 Signaling Cooperate to Control Actomyosin Contractility in Tumor Cells and Stroma. Cancer Cell *20*, 229-245.

Sanz-Moreno, V., and Marshall, C. J. (2009). Rho-GTPase signaling drives melanoma cell plasticity. Cell Cycle *8*, 1484-1487.

Sanz-Moreno, V., and Marshall, C. J. (2010). The plasticity of cytoskeletal dynamics underlying neoplastic cell migration. Curr Opin Cell Biol *22*, 690-696.

Sarkar, S., Nuttall, R. K., Liu, S., Edwards, D. R., and Yong, V. W. (2006). Tenascin-C stimulates glioma cell invasion through matrix metalloproteinase-12. Cancer Res *66*, 11771-11780.

Satyamoorthy, K., Muyrers, J., Meier, F., Patel, D., and Herlyn, M. (2001). Mel-CAM-specific genetic suppressor elements inhibit melanoma growth and invasion through loss of gap junctional communication. Oncogene *20*, 4676-4684.

Seftor, E. A., Brown, K. M., Chin, L., Kirschmann, D. A., Wheaton, W. W., Protopopov, A., Feng, B., Balagurunathan, Y., Trent, J. M., Nickoloff, B. J.*, et al.* (2005). Epigenetic transdifferentiation of normal melanocytes by a metastatic melanoma microenvironment. Cancer Res *65*, 10164-10169.

Seyger, M. M., van Pelt, J. P., van den Born, J., Latijnhouwers, M. A., and de Jong, E. M. (1997). Epicutaneous application of leukotriene B4 induces patterns of tenascin and a heparan sulfate proteoglycan epitope that are typical for psoriatic lesions. Arch Dermatol Res *289*, 331-336.

Shao, H., Wang, J. H., Pollak, M. R., and Wells, A. (2010). alpha-actinin-4 is essential for maintaining the spreading, motility and contractility of fibroblasts. PLoS One *5*, e13921.

Shao, H., Wu, C., and Wells, A. (2009). Phosphorylation of alpha-actinin-4 upon epidermal growth factor (EGF) exposure regulates its interaction with actin. J Biol Chem.

Sid, B., Sartelet, H., Bellon, G., El Btaouri, H., Rath, G., Delorme, N., Haye, B., and Martiny, L. (2004). Thrombospondin 1: a multifunctional protein implicated in the regulation of tumor growth. Crit Rev Oncol Hematol *49*, 245-258.

Siegel, R., Naishadham, D., and Jemal, A. (2012). Cancer statistics, 2012. CA Cancer J Clin *62*, 10-29.

Simpson, C. L., Kojima, S., and Getsios, S. (2010). RNA interference in keratinocytes and an organotypic model of human epidermis. Methods Mol Biol *585*, 127-146.

Siri, A., Knauper, V., Veirana, N., Caocci, F., Murphy, G., and Zardi, L. (1995). Different susceptibility of small and large human tenascin-C isoforms to degradation by matrix metalloproteinases. J Biol Chem *270*, 8650-8654.

Sjoblom, B., Salmazo, A., and Djinovic-Carugo, K. (2008). Alpha-actinin structure and regulation. Cell Mol Life Sci *65*, 2688-2701.

Smola, H., Stark, H. J., Thiekotter, G., Mirancea, N., Krieg, T., and Fusenig, N. E. (1998). Dynamics of basement membrane formation by keratinocyte-fibroblast interactions in organotypic skin culture. Exp Cell Res *239*, 399-410.

Soderberg, O., Gullberg, M., Jarvius, M., Ridderstrale, K., Leuchowius, K. J., Jarvius, J., Wester, K., Hydbring, P., Bahram, F., Larsson, L. G., and Landegren, U. (2006). Direct observation of individual endogenous protein complexes in situ by proximity ligation. Nat Methods *3*, 995-1000.

Spring, J., Beck, K., and Chiquet-Ehrismann, R. (1989). Two contrary functions of tenascin: dissection of the active sites by recombinant tenascin fragments. Cell *59*, 325-334.

Sriramarao, P., Mendler, M., and Bourdon, M. A. (1993). Endothelial cell attachment and spreading on human tenascin is mediated by alpha 2 beta 1 and alpha v beta 3 integrins. J Cell Sci *105 (Pt 4)*, 1001-1012.

Stark, H. J., Szabowski, A., Fusenig, N. E., and Maas-Szabowski, N. (2004). Organotypic cocultures as skin equivalents: A complex and sophisticated in vitro system. Biol Proced Online *6*, 55-60.

Stock, C., Jungmann, O., and Seidler, D. G. (2011). Decorin and chondroitin-6 sulfate inhibit B16V melanoma cell migration and invasion by cellular acidification. J Cell Physiol *226*, 2641-2650.

Svitkina, T. M., Verkhovsky, A. B., and Borisy, G. G. (1996). Plectin sidearms mediate interaction of intermediate filaments with microtubules and other components of the cytoskeleton. J Cell Biol *135*, 991-1007.

Swindle, C. S., Tran, K. T., Johnson, T. D., Banerjee, P., Mayes, A. M., Griffith, L., and Wells, A. (2001). Epidermal growth factor (EGF)-like repeats of human tenascin-C as ligands for EGF receptor. J Cell Biol *154*, 459-468.

Tanaka, K., Hiraiwa, N., Hashimoto, H., Yamazaki, Y., and Kusakabe, M. (2004). Tenascin-C regulates angiogenesis in tumor through the regulation of vascular endothelial growth factor expression. Int J Cancer *108*, 31-40.

Torisu, H., Ono, M., Kiryu, H., Furue, M., Ohmoto, Y., Nakayama, J., Nishioka, Y., Sone, S., and Kuwano, M. (2000). Macrophage infiltration correlates with tumor stage and angiogenesis in human malignant melanoma: possible involvement of TNFalpha and IL-1alpha. Int J Cancer *85*, 182-188.

Toth, M., and Fridman, R. (2001). Assessment of Gelatinases (MMP-2 and MMP-9 by Gelatin Zymography. Methods Mol Med *57*, 163-174.

Tran, K. T., Griffith, L., and Wells, A. (2004). Extracellular matrix signaling through growth factor receptors during wound healing. Wound Repair Regen *12*, 262-268.

Tran, K. T., Lamb, P., and Deng, J. S. (2005). Matrikines and matricryptins: Implications for cutaneous cancers and skin repair. J Dermatol Sci *40*, 11-20.

Tremble, P., Chiquet-Ehrismann, R., and Werb, Z. (1994). The extracellular matrix ligands fibronectin and tenascin collaborate in regulating collagenase gene expression in fibroblasts. Mol Biol Cell *5*, 439-453.

Tsao, H., Chin, L., Garraway, L. A., and Fisher, D. E. (2012). Melanoma: from mutations to medicine. Genes Dev *26*, 1131-1155.

Tufvesson, E., and Westergren-Thorsson, G. (2003). Biglycan and decorin induce morphological and cytoskeletal changes involving signalling by the small GTPases RhoA and Rac1 resulting in lung fibroblast migration. J Cell Sci *116*, 4857-4864.

Tuominen, H., and Kallioinen, M. (1994). Increased tenascin expression in melanocytic tumors. J Cutan Pathol *21*, 424-429.

Udart, M., Utikal, J., Krahn, G. M., and Peter, R. U. (2001). Chromosome 7 aneusomy. A marker for metastatic melanoma? Expression of the epidermal growth factor receptor gene and chromosome 7 aneusomy in nevi, primary malignant melanomas and metastases. Neoplasia *3*, 245-254.

Ulrich, T. A., de Juan Pardo, E. M., and Kumar, S. (2009). The mechanical rigidity of the extracellular matrix regulates the structure, motility, and proliferation of glioma cells. Cancer Res *69*, 4167-4174.

Valyi-Nagy, I. T., Murphy, G. F., Mancianti, M. L., Whitaker, D., and Herlyn, M. (1990). Phenotypes and interactions of human melanocytes and keratinocytes in an epidermal reconstruction model. Lab Invest *62*, 314-324.

Van Belle, P. A., Elenitsas, R., Satyamoorthy, K., Wolfe, J. T., Guerry, D. t., Schuchter, L., Van Belle, T. J., Albelda, S., Tahin, P., Herlyn, M., and Elder, D. E. (1999). Progression-related expression of beta3 integrin in melanomas and nevi. Hum Pathol *30*, 562-567.

van der Flier, A., and Sonnenberg, A. (2001). Function and interactions of integrins. Cell Tissue Res *305*, 285-298.

Wallner, K., Li, C., Shah, P. K., Wu, K. J., Schwartz, S. M., and Sharifi, B. G. (2004). EGF-Like domain of tenascin-C is proapoptotic for cultured smooth muscle cells. Arterioscler Thromb Vasc Biol *24*, 1416-1421.

Wanebo, H. J., Woodruff, J., and Fortner, J. G. (1975). Malignant melanoma of the extremities: a clinicopathologic study using levels of invasion (microstage). Cancer *35*, 666-676.

Warburg, O., Geissler, A. W., and Lorenz, S. (1970). [Genesis of tumor metabolism by vitamin B1 deficiency (thiamine deficiency)]. Z Naturforsch B *25*, 332-333.

Watanabe, K., Takahashi, H., Habu, Y., Kamiya-Kubushiro, N., Kamiya, S., Nakamura, H., Yajima, H., Ishii, T., Katayama, T., Miyazaki, K., and Fukai, F. (2000). Interaction with heparin and matrix metalloproteinase 2 cleavage expose a cryptic anti-adhesive site of fibronectin. Biochemistry *39*, 7138-7144.

Wells, A. (2000). Tumor invasion: role of growth factor-induced cell motility. Adv Cancer Res *78*, 31-101.

Wenk, M. B., Midwood, K. S., and Schwarzbauer, J. E. (2000). Tenascin-C suppresses Rho activation. J Cell Biol *150*, 913-920.

Wiche, G. (1989). Plectin: general overview and appraisal of its potential role as a subunit protein of the cytomatrix. Crit Rev Biochem Mol Biol *24*, 41-67.

Wilkinson, S., Paterson, H. F., and Marshall, C. J. (2005). Cdc42-MRCK and Rho-ROCK signalling cooperate in myosin phosphorylation and cell invasion. Nat Cell Biol *7*, 255-261.

Wilm, M., Shevchenko, A., Houthaeve, T., Breit, S., Schweigerer, L., Fotsis, T., and Mann, M. (1996). Femtomole sequencing of proteins from polyacrylamide gels by nano-electrospray mass spectrometry. Nature *379*, 466-469.

Wolf, K., and Friedl, P. (2011). Extracellular matrix determinants of proteolytic and non-proteolytic cell migration. Trends Cell Biol *21*, 736-744.

Wolf, K., Mazo, I., Leung, H., Engelke, K., von Andrian, U. H., Deryugina, E. I., Strongin, A. Y., Brocker, E. B., and Friedl, P. (2003). Compensation mechanism in tumor cell migration: mesenchymal-amoeboid transition after blocking of pericellular proteolysis. J Cell Biol *160*, 267-277.

Wu, X., Zhou, J., Rogers, A. M., Janne, P. A., Benedettini, E., Loda, M., and Hodi, F. S. (2012). c-Met, epidermal growth factor receptor, and insulin-like growth factor-1 receptor are important for growth in uveal melanoma and independently contribute to migration and metastatic potential. Melanoma Res *22*, 123-132.

Wyckoff, J. B., Pinner, S. E., Gschmeissner, S., Condeelis, J. S., and Sahai, E. (2006). ROCK- and myosin-dependent matrix deformation enables protease-independent tumor-cell invasion in vivo. Curr Biol *16*, 1515-1523.

Yamaguchi, H. (2012). Pathological roles of invadopodia in cancer invasion and metastasis. Eur J Cell Biol *91*, 902-907.

Yamazaki, D., Kurisu, S., and Takenawa, T. (2009). Involvement of Rac and Rho signaling in cancer cell motility in 3D substrates. Oncogene *28*, 1570-1583.

Yokoyama, K., Erickson, H. P., Ikeda, Y., and Takada, Y. (2000). Identification of amino acid sequences in fibrinogen gamma -chain and tenascin C C-terminal domains critical for binding to integrin alpha vbeta 3. J Biol Chem *275*, 16891-16898.

Yoshida, T., Matsumoto, E., Hanamura, N., Kalembeyi, I., Katsuta, K., Ishihara, A., and Sakakura, T. (1997). Co-expression of tenascin and fibronectin in epithelial and stromal cells of benign lesions and ductal carcinomas in the human breast. J Pathol *182*, 421-428.

Zaman, M. H., Trapani, L. M., Sieminski, A. L., Mackellar, D., Gong, H., Kamm, R. D., Wells, A., Lauffenburger, D. A., and Matsudaira, P. (2006). Migration of tumor cells in 3D matrices is governed by matrix stiffness along with cell-matrix adhesion and proteolysis. Proc Natl Acad Sci U S A *103*, 10889-10894.

Zhang, G., Ezura, Y., Chervoneva, I., Robinson, P. S., Beason, D. P., Carine, E. T., Soslowsky, L. J., Iozzo, R. V., and Birk, D. E. (2006). Decorin regulates assembly of collagen fibrils and acquisition of biomechanical properties during tendon development. J Cell Biochem *98*, 1436-1449.

Zhang, Y., Ye, Y., Shen, D., Jiang, K., Zhang, H., Sun, W., Zhang, J., Xu, F., Cui, Z., and Wang, S. (2009). Identification of transgelin-2 as a biomarker of colorectal cancer by laser capture microdissection and quantitative proteome analysis. Cancer Sci.

Zhu, J. X., Goldoni, S., Bix, G., Owens, R. T., McQuillan, D. J., Reed, C. C., and Iozzo, R. V. (2005). Decorin evokes protracted internalization and degradation of the epidermal growth factor receptor via caveolar endocytosis. J Biol Chem *280*, 32468-32479.